9. CALWAVE PROPOSED CENTRAL COAST WEC TEST SITE AT VANDENBERG AIR FORCE BASE (VAFB)

9.1. Site Description

The California Wave Energy Test Center (CalWave) Feasibility Study evaluated offshore test sites along the California coast for establishment of a national wave energy testing facility (Williams et al. 2015). The project originally considered two candidate areas, one offshore of Humboldt Bay, which is described in Chapter 9, and another Central Coast site offshore of Vandenberg Air Force Base (VAFB). The project down selected to VAFB due to its accessibility to shore-side support infrastructure and supply chain, among other reasons. At VAFB, there are currently five siting at sea alternatives (locations) and three shore site alternatives. Two offshore sites, and one shore site, are most favorable and are considered in the Conceptual Design Scenario. The "South Base" shore location is considered as the Notional Shore Site design case. Therefore, in this catalogue, the wave statistics will be presented at both offshore alternatives. As shown in Figure 86, the two Vandenberg siting options each consist of four berths centered at approximately 34.521 N, 120.689 W for the 'South' site and 34.4851 N, 120.6024 W for the 'South by Southeast' site in the Outer Continental Shelf (outside state waters). See the CalWave report (Williams et al. 2015) for additional figures of the site. The seafloor footprint would be constrained to an area of about four square nautical miles. There are also two infrastructure scenarios that will be considered in 2016: (a) using an existing offshore oil and gas platform and on shore infrastructure, or (b) construction of new submarine power cables. If the CalWave Test Center continues to be funded, it is assumed that testing could begin in 2021.

The Central Coast site is located near Vandenberg Air Force Base and the City of Lompoc, California. At the South site, the water depth is approximately 71-109 m (38.8-59.6 fathoms), and at the South by Southeast site, the water depth is approximately 66-102 m (36.1-55.8 fathoms). The bathymetry in general is gently sloping near the potential 'South' and 'South by Southeast' berths, and then drops off to deeper water to the southeast. The sea bed is predominantly sandy, with rocky outcroppings. Figure 87 shows the bathymetry surrounding the test site. The wave climate at the test site varies seasonally, with calmer seas in the summer compared to more energetic seas in the winter. The wave environment at Vandenberg is characterized by an annual average power flux of about 39.9 kW/m at the South site and 31.4 kW/m at the South by Southeast site, including a number of events with significant wave heights exceeding 5 m each winter.

The CalWave Team plans to offer a wide range of technical and testing infrastructure included and optional support services for WEC developers. Vandenberg has full scale wave energy resources, and is planned to be appropriate for mature technologies, at Technical Readiness Level (TRL) 7-9 WECs, which are approaching full-scale, grid-connected operation. The BOEM lease blocks being considered would enable use of up to four berths in the South and South-by-Southeast alternatives, and will allow a broad range of test conditions for the

purpose of populating a WEC power matrix. Cables would land at the South Base site near Vandenberg Dock. Once WECs are proven, commercial site alternatives are available in the vicinity to power offshore oil platforms that are presently using diesel generators.

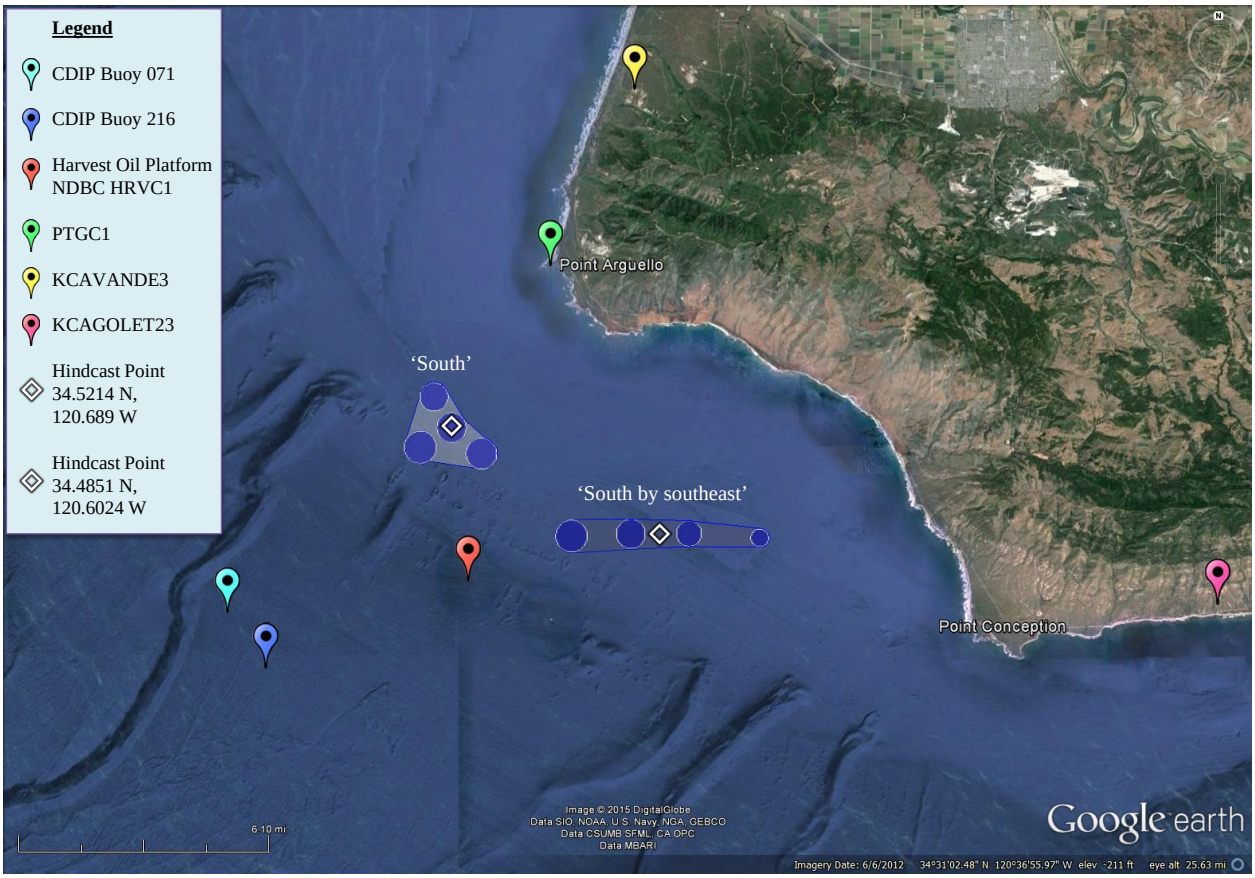

Figure 86: Two of the potential Vandenberg test site areas, 'South', and 'South by Southeast' (SSE), are located on the coast of California near the city of Lompoc and Vandenberg Air Force Base. The South site is approximately 6-9 km off-shore in 71-109 m depth water (38.8-59.6 fathoms) and the South by Southeast site is approximately 6-11 km off-shore in 66-102 m depth water (36.1-55.8 fathoms). No berthing infrastructure exists at this time, however four potential berths at each site are signified by the blue circles. Two Coastal Data Information Program (CDIP) ocean buoys, and several National Weather Service (NWS) meteorological stations are close to the test site. The points of reference for the hindcast simulation data presented in this chapter are shown. Image modified from Google Earth (2015).

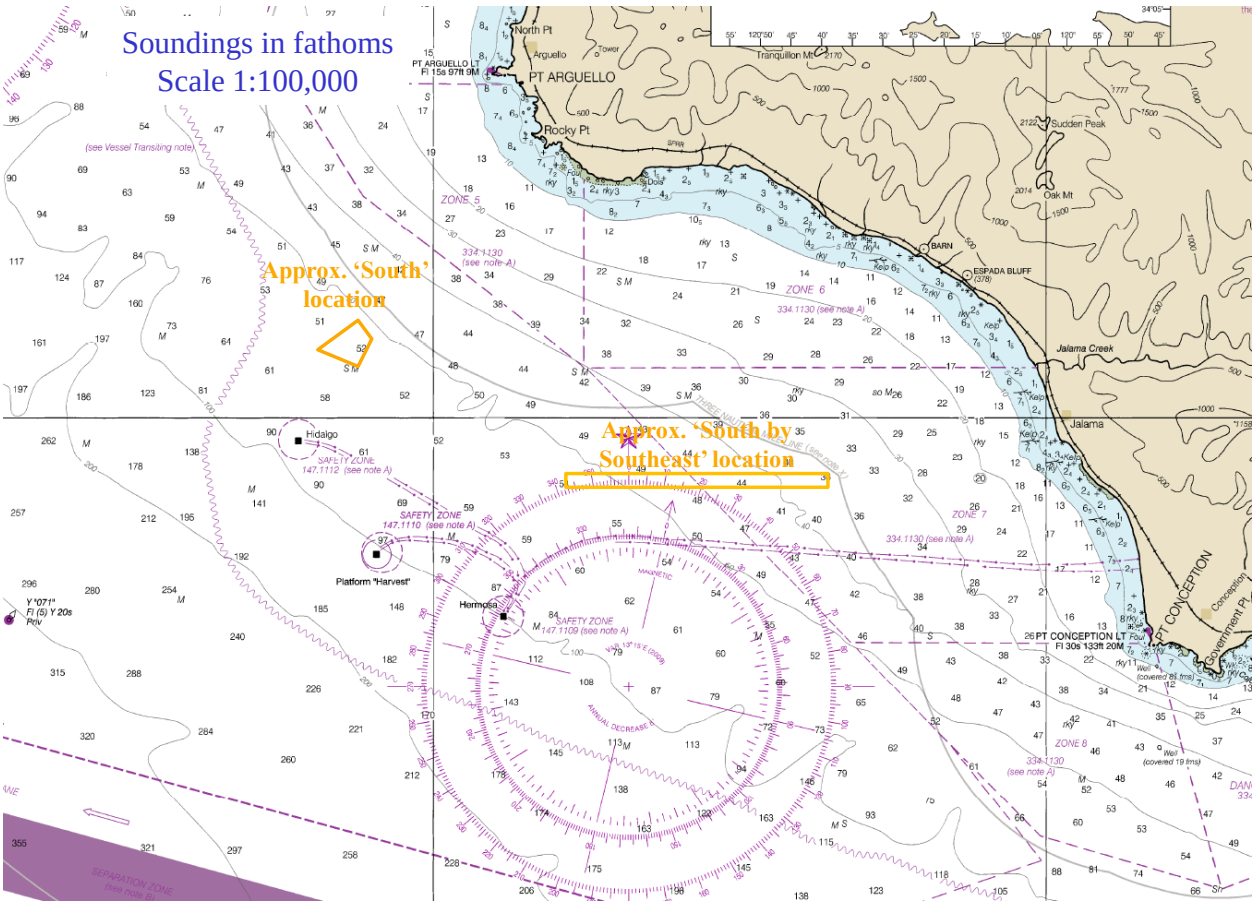

Figure 87: Nautical chart of the Vandenberg area offshore of Point Arguello and Point Conception shows the general bathymetry around the proposed test site. Soundings in fathoms (1 fathom = 1.8288 m). Image modified from nautical chart #18721 (Office of Coast Survey 2015).

9.2. WEC Testing Infrastructure

9.2.1. Mooring Berths

Four deep water berths are planned at either the South or South by Southeast locations. CalWave will be designed for WEC developers to provide key equipment optimized for their device, including the mooring and anchoring, umbilical, and power conditioning equipment. Alternatives for future expansion are available for deeper sites and shallow/mid-depth sites.

9.2.2. Electrical Grid Connection

The Conceptual Design includes four (4) "home run" cables from sea to shore, rated at 10 MW at 25 kV, plus a spare cable for a total of five (5) cables. Cables will land on VAFB at the notional "South Base" location and connect to a Department of Defense (DOD) grid

that is supplied by PG&E. Initially CalWave will connect with the Vandenberg distribution local grid at 12 kV, with an upgrade path to 70 kV.

9.2.3. Facilitating Harbor

Port Hueneme is the only deep water harbor between Los Angeles and the San Francisco Bay area, and is about 70 nm (∼130 km) from Vandenberg Dock and supports the offshore oil and gas industry. This facility can host very large vessels, and houses large cranes, dockside storage facilities and marine operations services for the oil and gas industry. Cal Poly Pier in Port San Luis and Port San Luis Boatyard are both approximately 24 nm (∼44 km) from Vandenberg Dock. Ellwood Pier is about 37 nm (∼69 km), Santa Barbara Harbor is about 54 nm (∼100 km), and Casitas Pier in Carpentaria is about 58 nm (∼107 km) from Vandenberg Dock. The Cojo Anchorage, on the sheltered side of Point Conception, is routinely used as a staging location by the offshore industry. More information and figures can be found in the CalWave report (Williams et al. 2015).

9.2.4. On-Shore Office Space

CalWave has focused on a notional shore station facility at the 'South Base' location, which would be appropriate for either the South or South by Southeast test site alternatives. This shore station facility is adjacent to Vandenberg Dock on Vandenberg AFB, and is planned to have two modular buildings, with on-site space for WEC developers. The Shore Station includes an area for modular power conditioning equipment to be provided by WEC developers. The Vandenberg Dock area, which is located at the former U.S. Coast Guard Surf Station, next to the shore station, is a potential location for office functions, on a not-to-interfere basis. This potential shore station would host key personnel and WEC developer staff during test operations.

9.2.5. Service Vessel and Engineering Boatyard Access

Capable shore side infrastructure is readily available near the project area due to a long history of oil services construction and operations in the area. Facilities include heavy lift floating cranes (offshore rated) and dockside cranes, and a variety of work boats and other vessels including large work vessels and cable lay equipment, remotely operated vehicles, and automated underwater vehicles. More detailed information is in Williams et al. 2015.

9.2.6. Travel and Communication Infrastructure

There are several airports in the area. The Santa Barbara Municipal Airport (SBA) is 38.2 miles southeast of Lompoc, and the Los Angeles International Airport (LAX) is 126.7 miles southeast of Lompoc. The Santa Maria Pub/Capt G Allan Hancock Field Airport (SMX) is 18 miles north of Lompoc. There are several Federal Communication Commission (FCC) registered cell towers located in and around Lompoc, CA, and cell phones may be used on VAFB, although coverage varies by location on-base.

9.2.7. Met-Ocean Monitoring Equipment

Real-time meteorological and wave data are collected by two met-ocean buoys and four meteorological stations. Instrument and data specifications for this monitoring equipment are summarized in Table 7. Buoy data is accessible online at the CDIP and NDBC databases. CDIP071 (NDBC 46218) is located approximately 15 km southwest of the test site, and CDIP216 (NDBC 46257) was recently deployed nearby. There is a water level observation network on the Harvest Oil Platform, just south of the site. There are several meteorological stations onshore.

Figure 88: (a) Waverider buoy CDIP071 / NDBC46218 located about 15 km southwest of test site (National Data Buoy Center 2015). (b) C-MAN Station PTGC1 located about 10 km north of test site (National Data Buoy Center 2015).

Table 7: Wave monitoring equipment in close proximity to the VAFB proposed test site.

Instrument Name (Nickname)	**CDIP071 / NDBC46218 - ("Harvest, CA")**		**CDIP216 / NDBC46257 ("Harvest Southeast, CA)**		**HRVC1 - 9411406 - Harvest Oil Platform, CA**
Type	Waverider Buoy		Waverider Buoy		Water Level Observation Network
Measured parameters	-std. met. data -spectral wave density data -spectral wave direction data		-std. met. data -spectral wave density data -spectral wave direction data		-barometric pressure -air temp
Variables reported, including derived variables (Sampling interval)	*Std. Met.:* WVHT DPD APD MWD WTMP (30 min)	-Spectral Wave Density -Spectral Wave Direction (30 min)	*Std. Met.:* WVHT DPD APD MWD WTMP (30 min)	-Spectral Wave Density -Spectral Wave Direction (30 min)	PRES ATMP (6 min sampling period)
Location	∼15 km southwest of site		∼15 km southwest of site		Just south of the site
Coordinates	34.454 N 120.782 W (34°27'14.4" N 120°46'55.2" W)		34.439 N 120.766 W (34°26'20.4" N 120°45'57.6" W)		34.469 N 120.682 W (34°28'9" N 120°40'55" W)
Depth	548.6 m		576.1 m		-air temp height: 30 m above site elevation -barometer elev: 26.1 m mean sea level
Data Start	3/19/1998 (additional short deployment in Dec 1995 - Mar 1996)		7/9/2015		3/1/2013
Data End	present		present		present
Period of Record	∼17.5 yrs		< 1 yr		∼2.5 yrs
Owner / Contact Person	NOAA – "Information Submitted by Scripps" http://cdip.ucsd.edu/themes/s?pb=1&u2=s:071:st:1&d2=p9		NOAA – "Information Submitted by Scripps" http://cdip.ucsd.edu/?nav=historic&sub=data&stn=216&stream=p1&xitem=info		NOAA's National Ocean Service http://www.ndbc.noaa.gov/station_history.php?station=hrvc1

Instrument Name (Nickname)	**PTGC1**		**KCAVANDE3**	**KCAGOLET23**
Type	C-MAN station (MARS payload)		Met station	Met station
Measured parameters	-std. met. data -continuous winds		Meteorological data	Meteorological data
Variables reported, including derived variables (Sampling interval)	*Std Met.:* WD WSPD GST BAR ATMP DEWP (1 hr sampling period)	*Contin. Winds:* WDIR WSPD GDR GST GTIME (10 min sampling period)	AirTemp DewPoint Pressure WDIR WSPD Humidity Precip (5 min)	AirTemp DewPoint Pressure WDIR WSPD Humidity Precip Solar Radiation UV Index (5 min)
Location	$\sim$ 10 km north of the site, on shoreline		SpaceX Launch Complex 4 Office	Goleta, CA
Coordinates	34.577 N 120.648 W (34°34'36" N 120°38'54" W)		34.637 N 120.613 W (34°38'13.2" N, 120°36'46.8" W)	34.461 N 120.371 W (34°27'39.6" N 120°22'15.6" W)
Depth	-site: 32.3 m above sea level -air temp: 9.1 m above site -anemometer: 9.4 m above site -barometer: 33.5 m above sea level		Elevation: 305 ft	Elevation: 98 ft
Data Start	-std met: 4/23/1984 -contin winds: 4/26/1997		1/19/2012	6/19/2015
Data End	present		present	present
Period of Record	std met: $\sim$31.5 yrs contin winds: $\sim$18.5 yrs		$\sim$3.5 yrs	$<$ 1 yr
Owner / Contact Person	National Data Buoy Center http://www.ndbc.noaa.gov/station_history.php?station=ptgc1		National Weather Service; data download wunderground.com	National Weather Service; data download wunderground.com

9.2.8. Environmental Monitoring

Environmental conditions have not been assessed at the Vandenberg Site, although a summary of potential environmental studies that may be needed are in Williams et al. 2015. When CalWave receives the next phase of funding, they will further characterize the site.

9.2.9. Permitting

No permits have been obtained as of 2015. CalWave has leveraged the lessons-learned from PG&E's WaveConnect Program and has investigated most aspects of the permitting process at this stage. A high level screening analysis to identify critical issues in the process has been ongoing. The information found so far from this process can be found in Williams et al. 2015.

9.3. Data used

Humboldt State University (part of the CalWave team) produced a 10 year hindcast dataset for the various siting alternative locations offshore of Vandenberg Air Force Base (Williams et al. 2015). This dataset was used to calculate parameters of interest for the characterization at the two locations presented for the CalWave central coast site. The hindcast data at the grid points shown in Figure 86 were analyzed.

In addition to the hindcast data set, historical data from buoy CDIP071 / NDBC 46218 was used to calculate estimates of extreme events and representative spectra. As with the other sites, CFSR wind data and OSCAR current data were used. See Figures 86 and 89 for data locations.

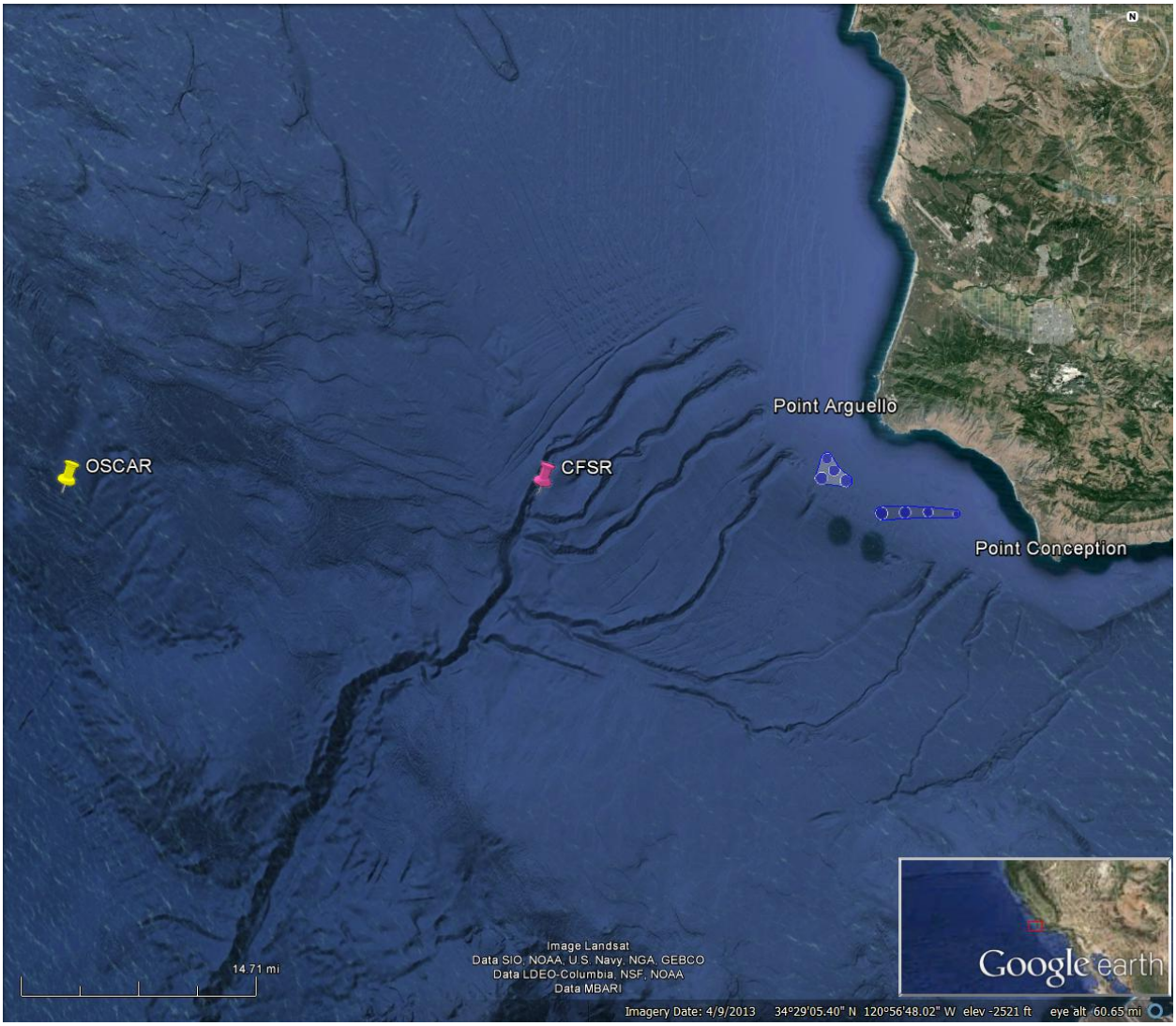

Figure 89: The catalogue test site locations in relation to OSCAR surface current and CSFR wind data points (Google Earth 2015).

9.4. Results

The following sections provide information on the joint probability of sea states, the variability of the IEC TS parameters, cumulative distributions, weather windows, extreme sea states, and representative spectra. This is supplemented by wave roses as well as wind and surface current data in Appendix G. The wind and surface current data provide additional information to help developers plan installation and operations & maintenance activities.

9.4.1. Sea States: Frequency of Occurrence and Contribution to Wave Energy

Joint probability distributions of the significant wave height, H_{m0}, and energy period, T_e, are shown in Figures 90 and 91. Figure 90 (top) shows the frequency of occurrence of each binned sea state and Figure 90 (bottom) shows the percentage contribution to the total wave energy for the South location. The same information is shown for the SSE location in 91. Figure 90 and Figure 91 (top) indicate that the majority of sea states are within the range 1.5 m $< H_{m0} <$ 3.5 m and 6 s $< T_e <$ 13 s; but a wide range of sea states are experienced at the Vandenberg site, including extreme sea states caused by severe storms where H_{m0} exceeded 6 m. The site is well suited for testing WECs at various scales, including full-scale WECs, and testing the operation of WECs under normal sea states. This would also be a desirable site for commercial deployment. Although the occurrence of an extreme sea state for survival testing of a full scale WEC is unlikely during a normal test period, the Vandenberg site wave climate offers opportunities for survival testing of scaled model WECs.

As mentioned in the methodology (Section 2.2), previous studies show that sea states with the highest occurrence do not necessarily correspond to those with the highest contribution to total wave energy, as is the case in Figures 90 and 91. The total wave energy in an average year at the South location is about 352,980 kWh/m, which corresponds to an average annual omnidirectional wave power of 39.9 kW/m. The total average wave energy in an average year at the SSE location is about 277,660 kWh/m, which corresponds to an average annual omnidirectional wave power of 31.4 kW/m. The most frequently occurring sea state is within the range 2 m $< H_{m0} <$ 2.5 m and 10 s $< T_e <$ 11 s for both the South and SSE locations, while the sea state that contributes most to energy is within the range 3 m $< H_{m0} <$ 3.5 m and 12 s $< T_e <$ 13 s for the South location and within the range 2.5 m $< H_{m0} <$ 3 m and 11 s $< T_e <$ 12 s for the SSE location. Several sea states occur at a similar frequency, and sea states within 2 m $< H_{m0} <$ 4 m and 10 s $< T_e <$ 13 s contribute a similar amount to energy.

Frequencies of occurrence and contributions to energy of less than 0.01% are not shown in the figure for clarity. For example, the sea state within 0.5 m $< H_{m0} <$ 1 m and 4 s $< T_e <$ 5 s has an occurrence of 0.04% for the South location. The contribution to total energy, however, is only 0.002% and, therefore, does not appear in Figure 90 (bottom). Similarly, the sea state within 7.5 m $< H_{m0} <$ 8 m and 16 s $< T_e <$ 17 s has an occurrence of 0.003%, but the contribution to total energy is 0.05%.

Curves showing the mean, 5^{th} and 95^{th} percentiles of wave steepness, H_{m0}/γ, are also shown in Figures 90 and 91. The mean wave steepness is 0.0150 ($\approx$1/67) at the South location,

and 0.0142 (≈1/70) at the SSE location. The 95^{th} percentile is 0.0323 (≈1/31) at the South and 0.0312 (≈1/32) at the SSE location.

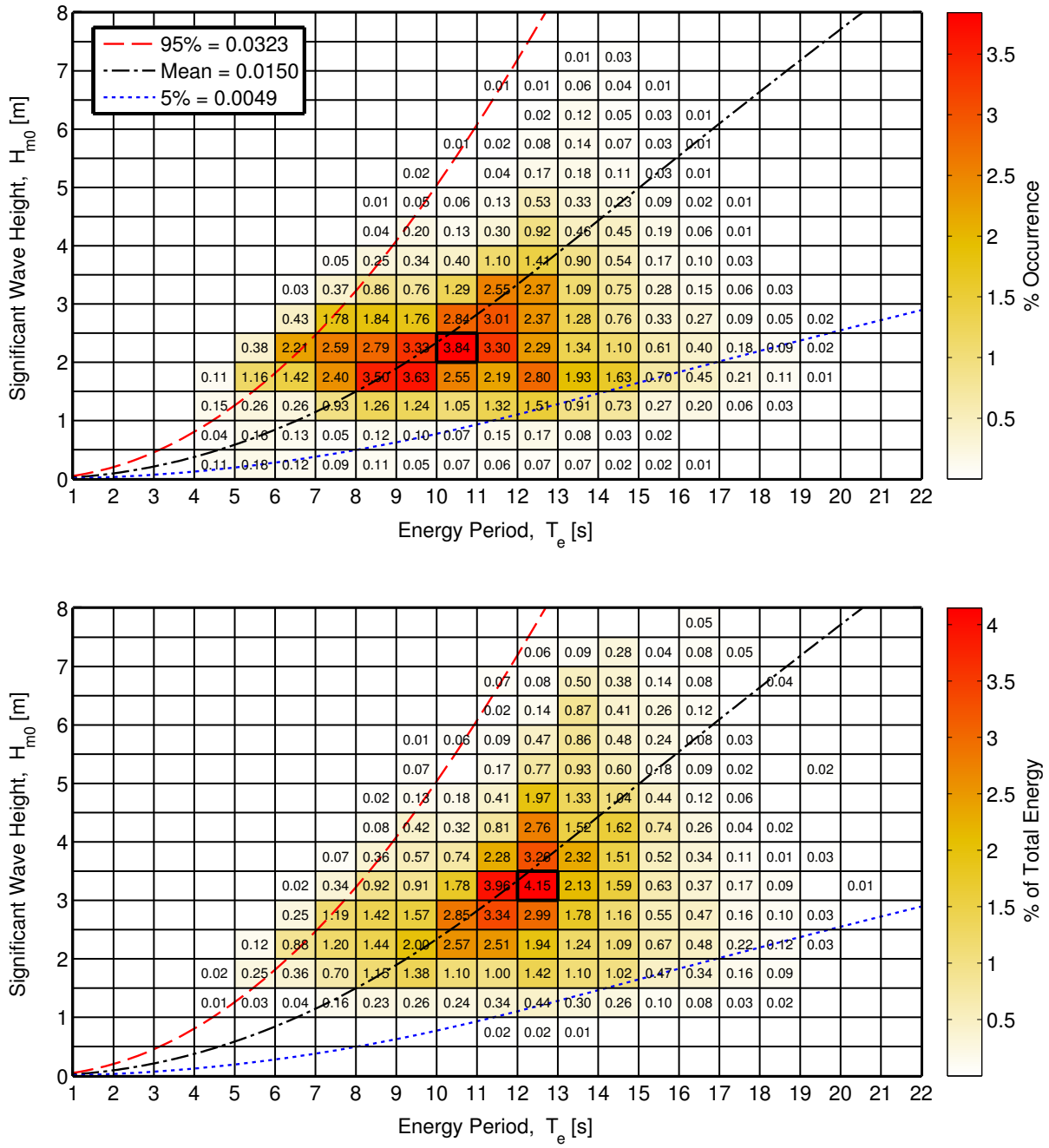

Figure 90: Joint probability distribution of sea states for the South Vandenberg site. The top figure is frequency of occurrence and the bottom figure is percentage of total energy, where total energy in an average year is 352,980 kWh/m.

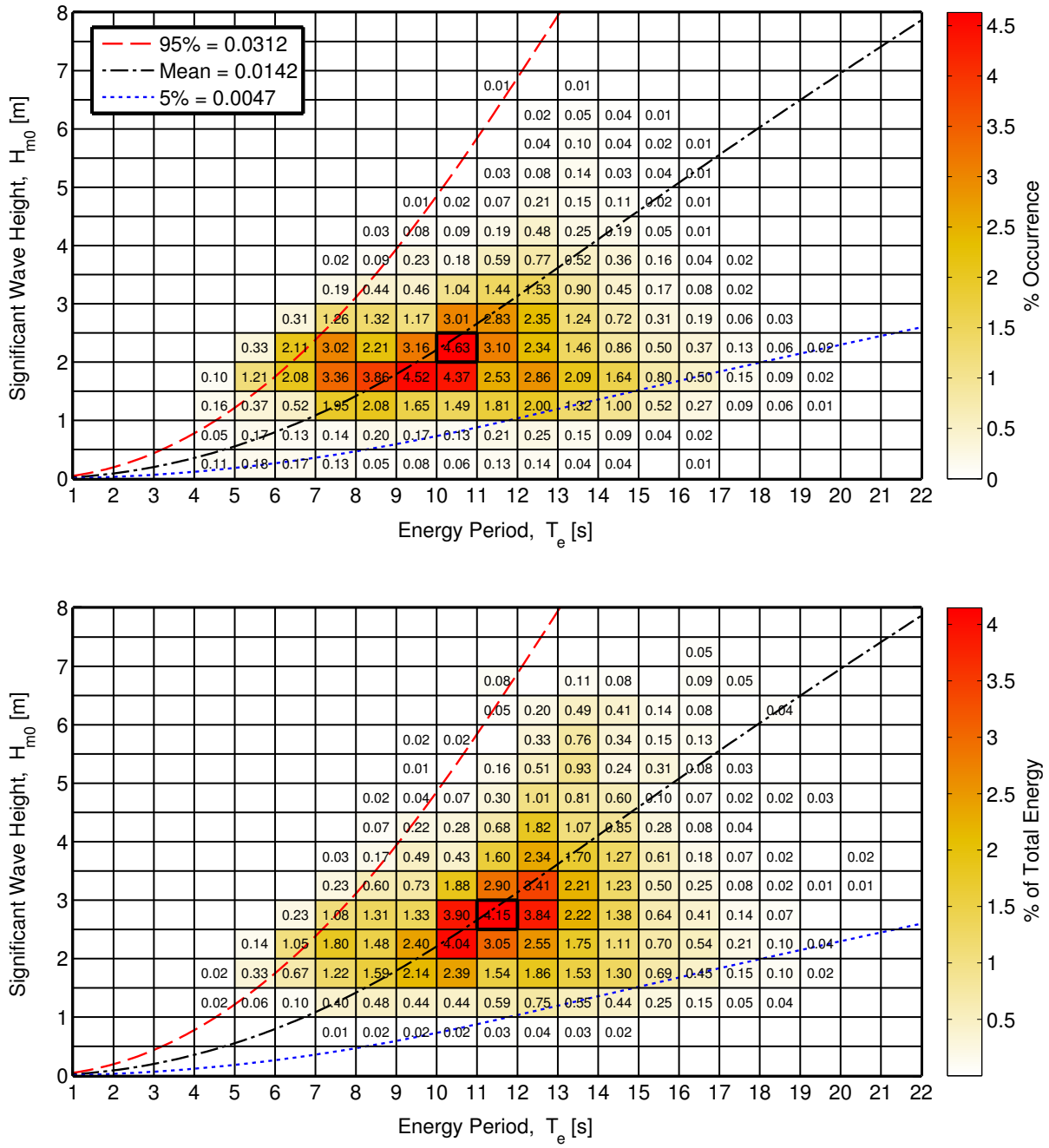

Figure 91: Joint probability distribution of sea states for the SSE Vandenberg site. The top figure is frequency of occurrence and the bottom figure is percentage of total energy, where total energy in an average year is 277,660 kWh/m.

9.4.2. IEC TS Parameters

The monthly means of the six IEC TS parameters, along with the 5^{th} and 95^{th} percentiles, are shown in Figures 92 and 93. The months, March - February, are labeled with the first letter (e.g., March is M). The values in the figure are summarized in Tables 37 and 38 in

Appendix G.

Monthly means of the significant wave height, H_{m0}, and the omnidirectional wave power density, J, show the greatest seasonal variability compared to the other parameters. Values are largest and vary the most during the winter months. The same trend is observed for the monthly mean energy period, T_e, but its variation is less pronounced. These observations are consistent with the relationship between wave power density, significant wave height and energy period, where wave power density, J, is proportional to the energy period, T_e, and the square of the significant wave height, H_{m0}.

The direction of maximum directionally resolved wave power is very consistent in the winter from west/northwest, and during the rest of the year has frequent shifts to the south, signified by the drop in the 5^{th} percentile. Seasonal variations of the remaining parameters, ϵ_0 and d_θ, are much less than J, H_{m0}, T_e, and θ_J, and are barely discernable. Monthly means for spectral width, ϵ_0, remain nearly constant at ~ 0.24. Similarly, monthly means for the directionality coefficient, d_θ, remain nearly constant at ~ 0.98. In summary, the waves at both the South and SSE locations at the Vandenberg site, from the perspective of monthly means, have a fairly consistent spectral width, are predominantly from the west/northwest, and exhibit a wave power that has a very narrow directional spread.

Wave roses of wave power and significant wave height, presented in Appendix G, Figures 156 - 159, also show the predominant direction of the wave energy at the Vandenberg site, which is west/northwest, with frequent shifts to the south. Figure G shows two dominant wave direction sectors, northwest (at 300°) and west/northwest (WNW) at 285°. At the South location, along the predominant wave direction, 300°, the omnidirectional wave power density is at or below 35 kW/m about 25% of the time, but greater than 35 kW/m nearly 15% of the time. Along the WNW direction (285°), wave power density is at or below 35 kW/m about 12% of the time, and greater than 35 kW/m about 17% of the time. At the SSE location, along the predominant wave direction, 300°, the omnidirectional wave power density is at or below 35 kW/m about 31% of the time, and greater than 35 kW/m about 6% of the time. Along the WNW direction (285°), wave power density is at or below 35 kW/m about 17% of the time, and greater than 35 kW/m about 16% of the time.

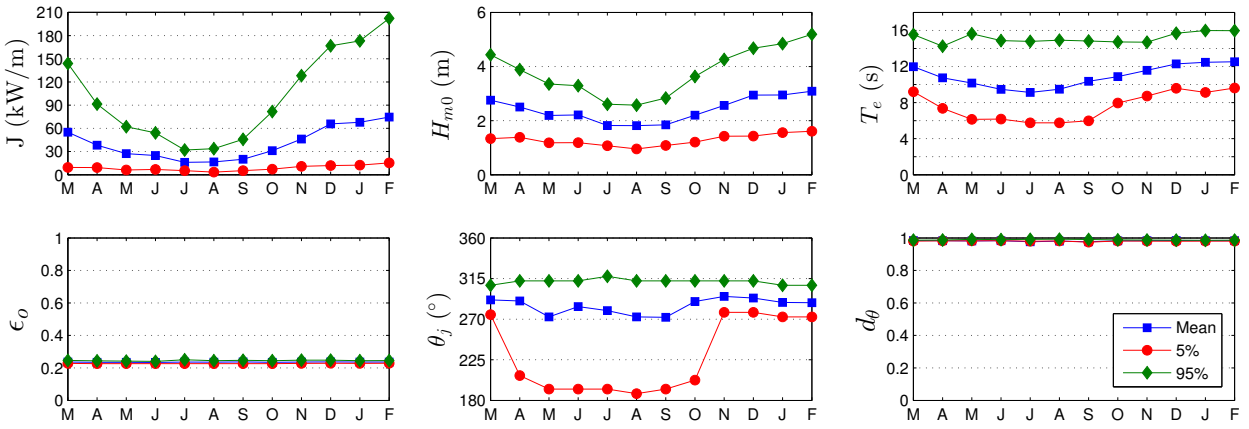

Figure 92: The average, 5^{th} and 95^{th} percentiles of the six parameters at the South Vandenberg site.

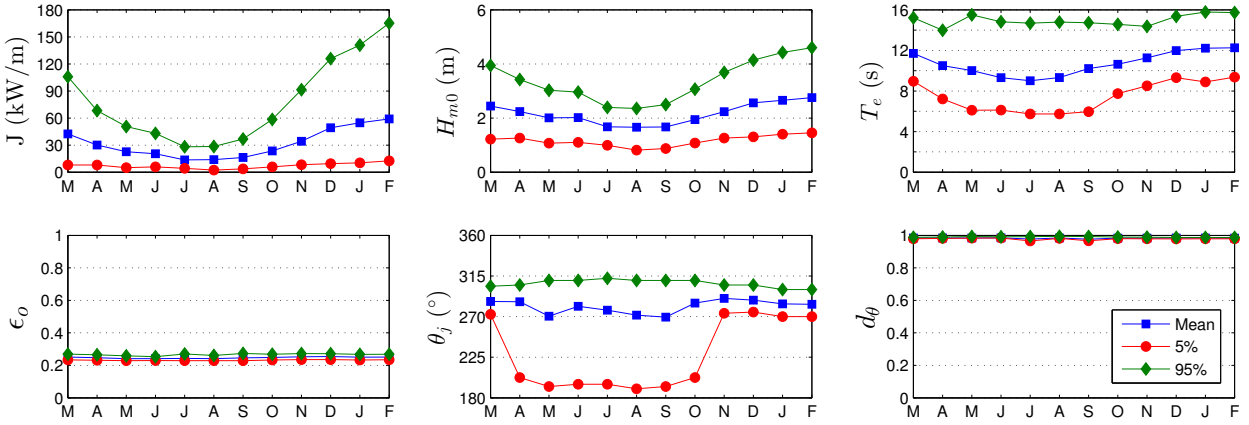

Figure 93: The average, 5^{th} and 95^{th} percentiles of the six parameters at the SSE Vandenberg site.

Monthly means, however, smear the significant variability of the six IEC parameters over small time intervals as shown in plots of the parameters at 1-hour intervals in Figures 94 and 95 for a representative year. While seasonal patterns described for Figures 92 and 93 are still evident, these plots show how sea states can vary abruptly at small time scales with sudden changes, e.g., jumps in the wave power as a result of a storm.

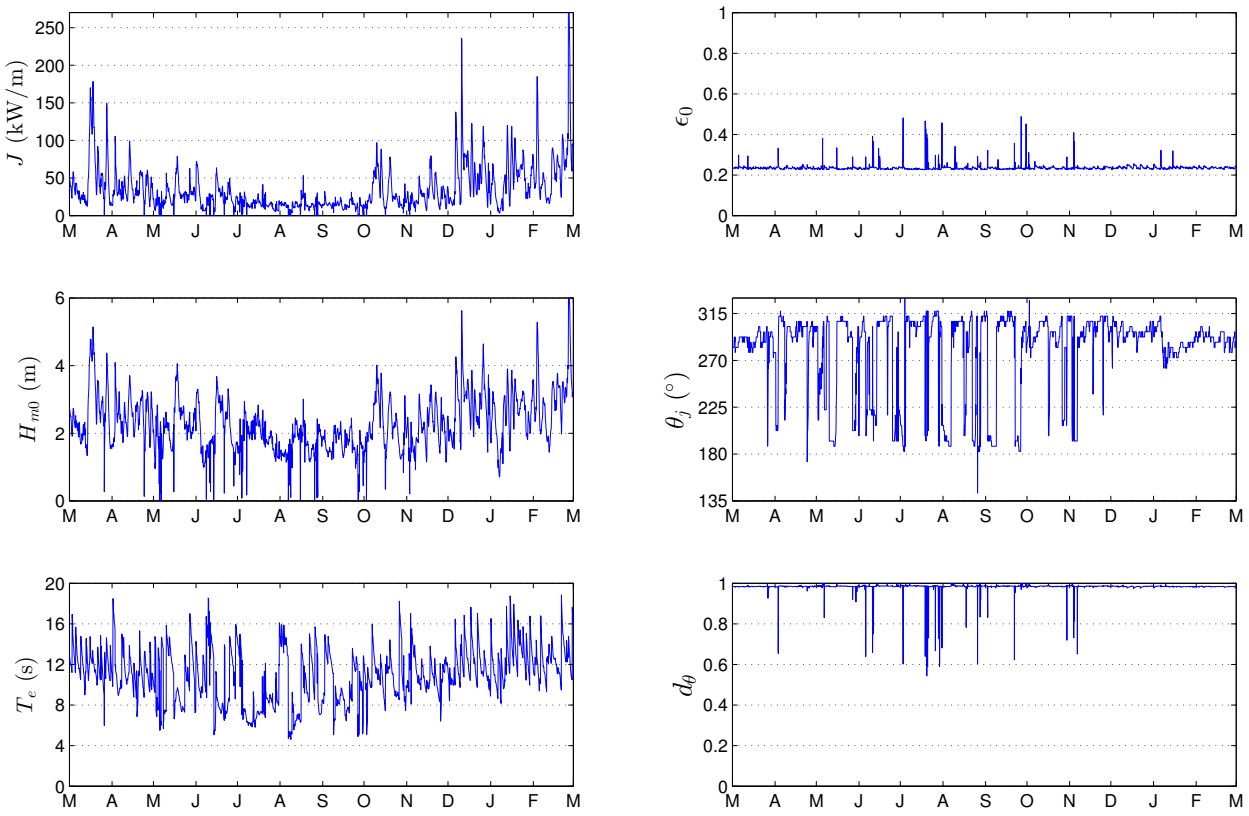

Figure 94: The six parameters of interest over a one-year period, March 2003 – February 2004 at the South Vandenberg site.

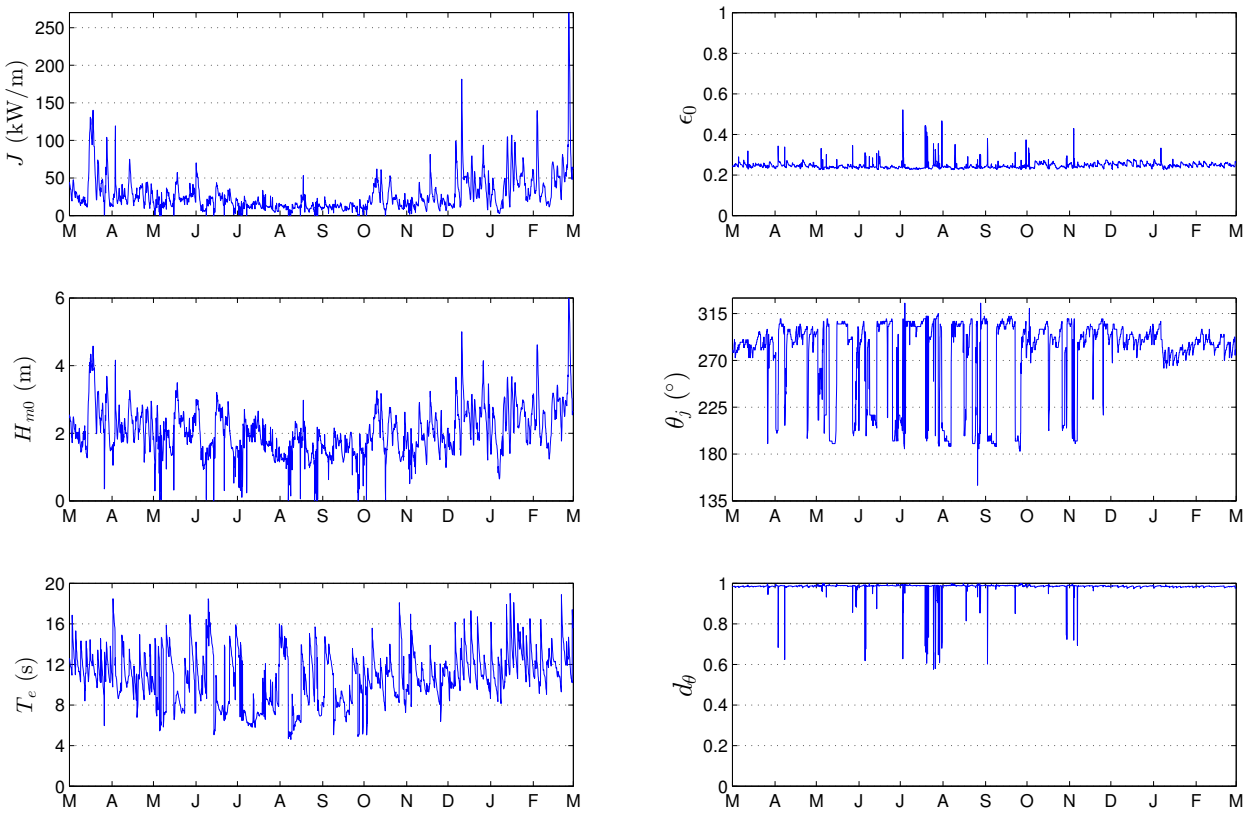

Figure 95: The six parameters of interest over a one-year period, March 2003 – February 2004 at the SSE Vandenberg site.

9.4.3. Cumulative Distributions

Annual and seasonal cumulative distributions (a.k.a., cumulative frequency distributions) are shown in Figures 96 and 97 for the South and SSE sites, respectively. Note that spring is defined as March – May, summer as June – August, fall as September – November, and winter as December – February. The cumulative distributions are another way to visualize and describe the frequency of occurrence of individual parameters, such as H_{m0} and T_e. A developer could use cumulative distributions to estimate how often they can access the site to install or perform operations and maintenance based on their specific device, service vessels, and diving operation constraints. For example, if significant wave heights need to be less than or equal to 1 m for installation and recovery, according to Figure 96, this condition occurs about 2% of the time on average within a given year. If significant wave heights need to be less than or equal to 2 m for emergency maintenance, according to Figure 96, this condition occurs about 37% of time on average within a given year. Cumulative distributions, however, do not account for the duration of a desirable sea state, or weather window, which is needed to plan deployment and servicing of a WEC device at a test site. This limitation is addressed with the construction of weather window plots in the next section.

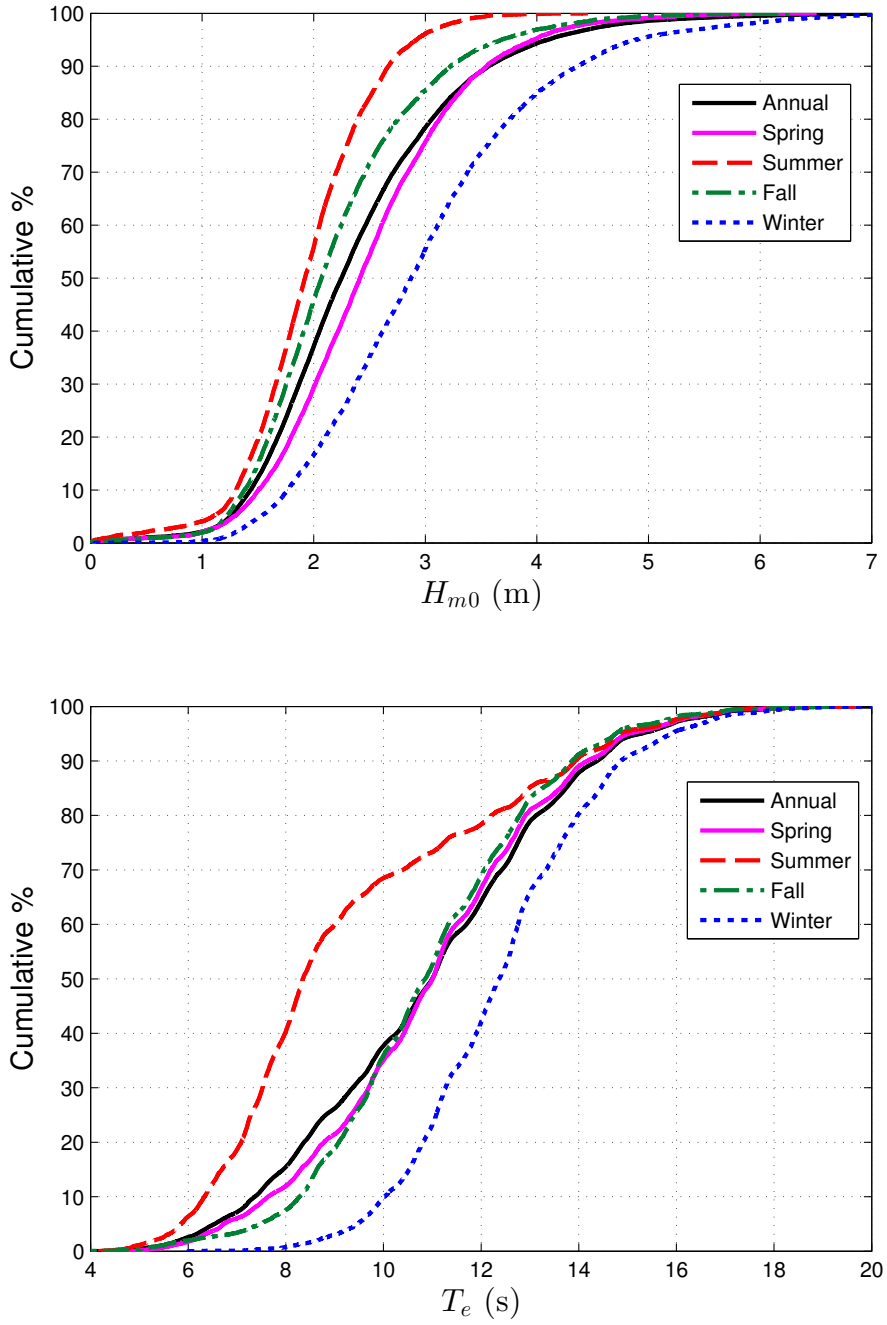

Figure 96: Annual and seasonal cumulative distributions of the significant wave height (top) and energy period (bottom) at the South Vandenberg site.

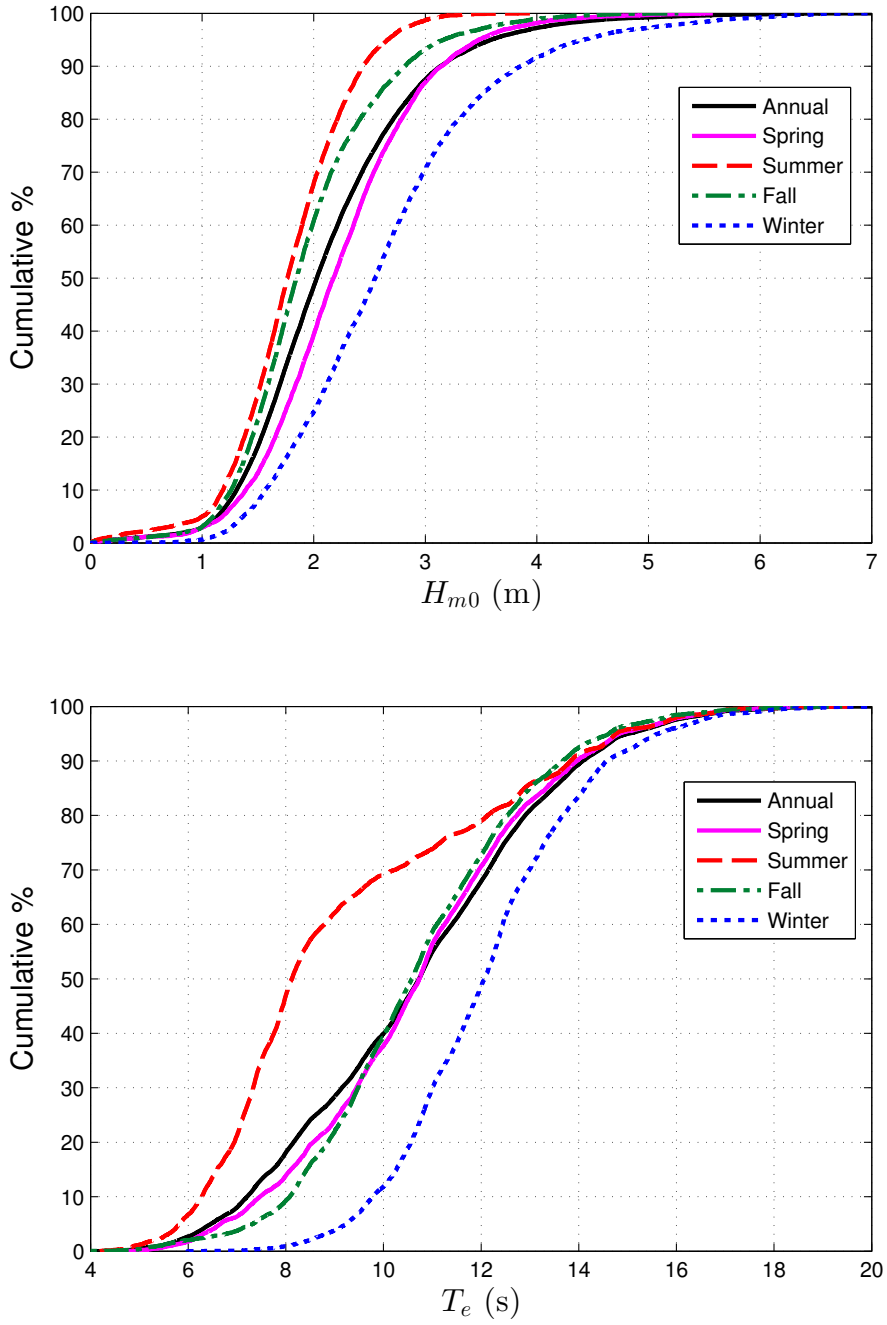

Figure 97: Annual and seasonal cumulative distributions of the significant wave height (top) and energy period (bottom) at the SSE Vandenberg site.

9.4.4. Weather Windows

Figures 98 and 101 show the number of weather windows at the South and SSE Vandenberg sites, when significant wave heights are at or below some threshold value for a given duration, for an average winter, spring, summer and fall. In these plots, each occurrence lasts a duration that is some multiple of 6-hours. The minimum weather window is, therefore,

6-hours in duration, and the maximum is 96-hours (4 days). The significant wave height threshold is the upper bound in each bin and indicates the maximum significant wave height experienced during the weather window. Note that the table is cumulative, so, for example, an occurrence of $H_{m0} \leq 1.5$ m for at least 78 consecutive hours in the fall is included in the count for 72 consecutive hours as well. In addition, one 12-hour window counts would count as two 6-hour windows. It is clear that there are more occurrences of lower significant wave heights during the summer than winter, which corresponds to increased opportunities for deployment or operations and maintenance.

Weather window plots provide useful information at test sites when planning schedules for deploying and servicing WEC test devices. For example, if significant wave heights need to be less than or equal to 1 m for at least 12 consecutive hours to service a WEC test device at the South Vandenberg site with a given service vessel, there would be, on average, two weather windows in the summer, but none in the winter. When wind speed is also considered, Figures 99 and 102 shows the average number of weather windows with the additional restriction of wind speed, $U < 15$ mph. The local winds (which are not necessarily driving the waves) are used in these weather windows, and are given in Appendix G.4. That wind data was not available from the hindcast, so data from CFSR was used (see Section 2.3, Appendix G.4). For shorter durations (6- and 12-hour windows), daylight is necessary. Windows with $U < 15$ mph and only during daylight hours are shown in Figures 100 and 103. Daylight was estimated as 5am – 10pm Local Standard Time (LST).

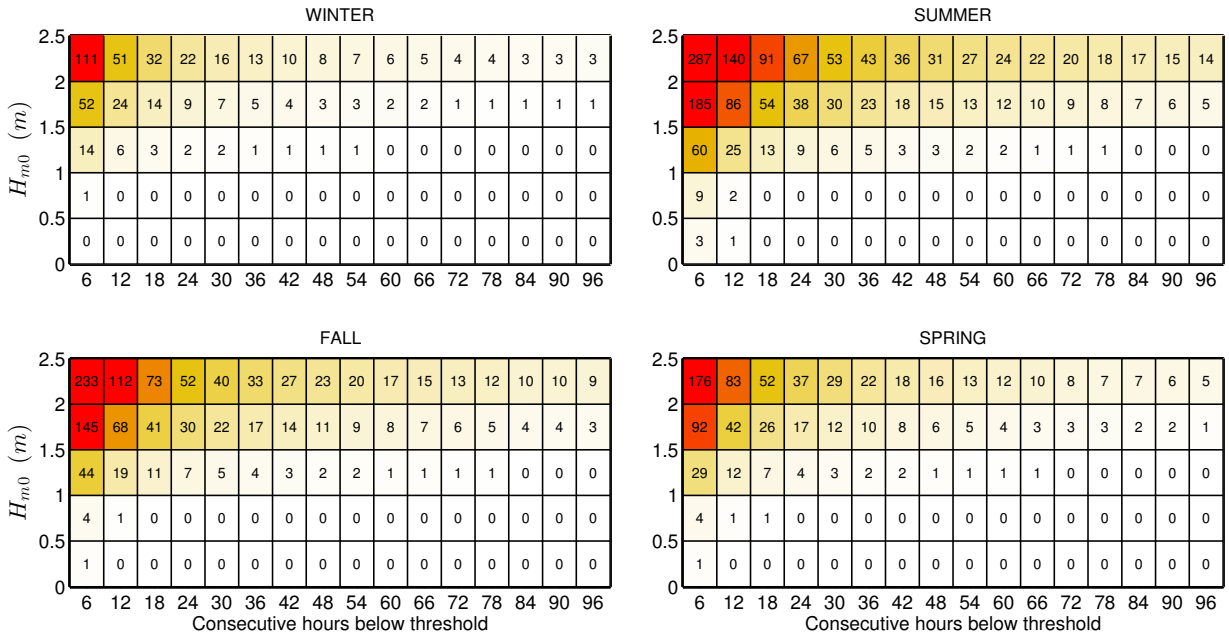

Figure 98: Average cumulative occurrences of wave height thresholds (weather windows) for each season at the South Vandenberg site. Winter is defined as December – February, spring as March – May, summer as June – August, and fall as September – November.

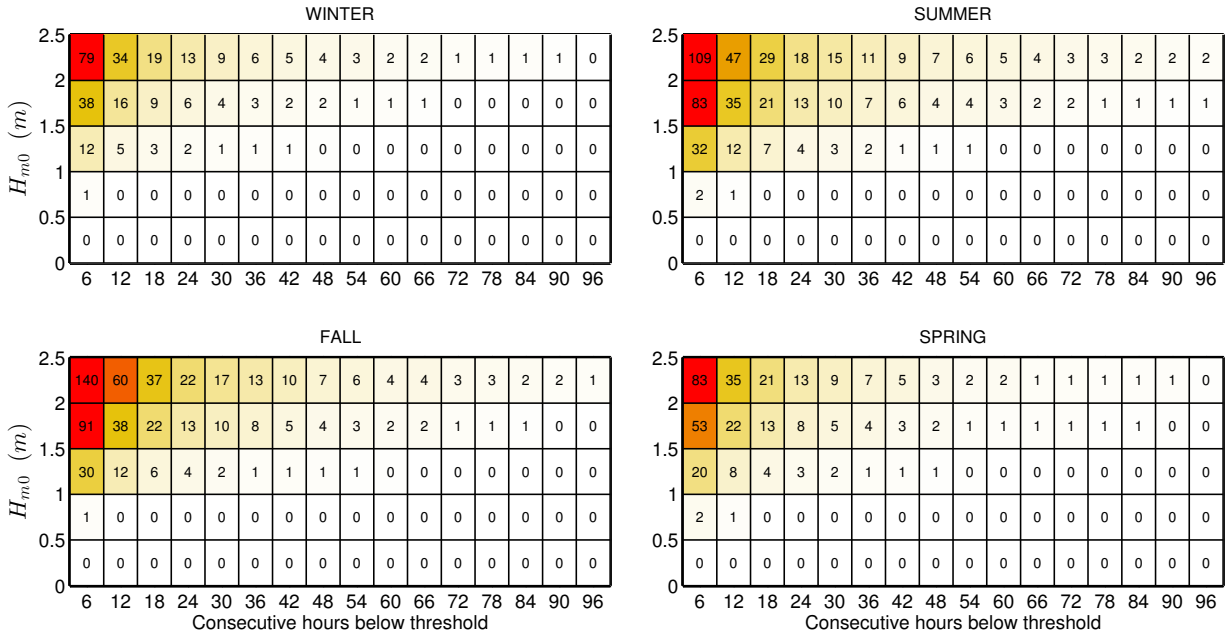

Figure 99: Average cumulative occurrences of wave height thresholds (weather windows) for each season at the South Vandenberg site with an additional restriction of U $<$ 15 mph.

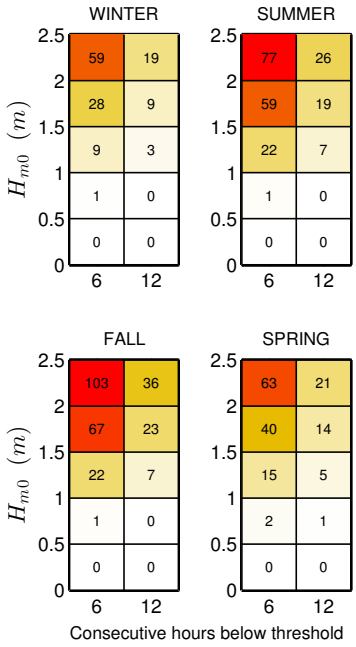

Figure 100: Average cumulative occurrences of wave height thresholds (weather windows) for 6- and 12-hour durations with $U < 15$ mph and only during daylight hours (5am – 10pm LST) at the South Vandenberg site.

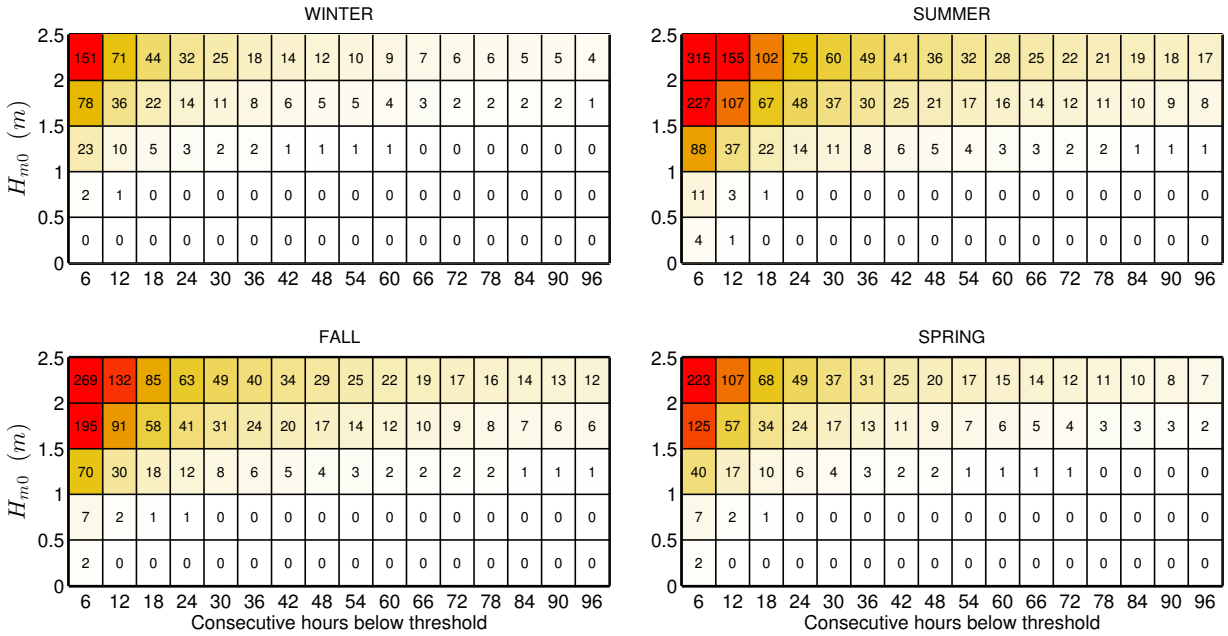

Figure 101: Average cumulative occurrences of wave height thresholds (weather windows) for each season at the SSE Vandenberg site. Winter is defined as December – February, spring as March – May, summer as June – August, and fall as September – November.

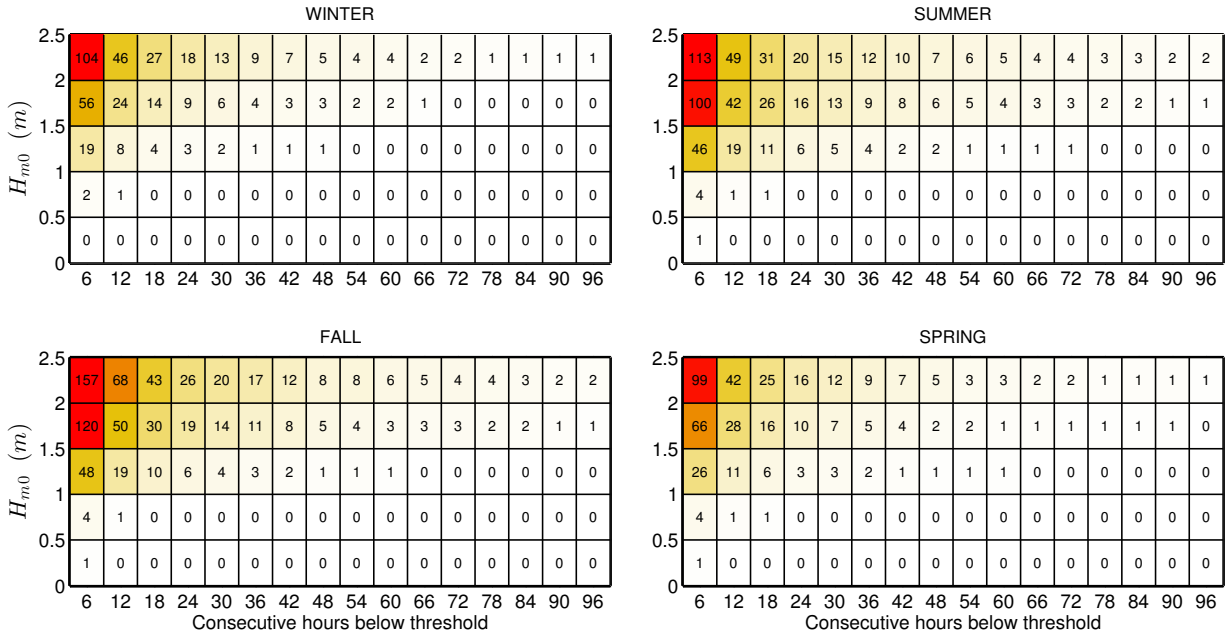

Figure 102: Average cumulative occurrences of wave height thresholds (weather windows) for each season at the SSE Vandenberg site with an additional restriction of U $<$ 15 mph.

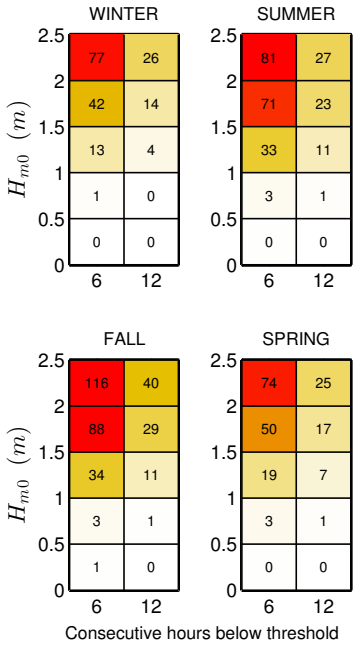

Figure 103: Average cumulative occurrences of wave height thresholds (weather windows) for 6- and 12-hour durations with $U < 15$ mph and only during daylight hours (5am – 10pm LST) at the SSE Vandenberg site.

9.4.5. Extreme Sea States

As mentioned in 2.2, the way IFORM and the modified IFORM are currently implemented, they do not work well for datasets whose variables (H_{m0} and T_e) are bimodally distributed. The CDIP071 / NDBC 46218 dataset is not well suited for IFORM, and therefore only the extreme significant wave height is estimated here using extreme value theory.

The generalized extreme value distribution (GEV) was fit to the annual significant wave height maximum in order to generate estimates of extreme values under the annual maximum method (AMM) (Rugerio et al. 2010). The peak over threshold (POT) method was also applied to the entire dataset in order to generate estimates of extreme values based on significant wave height exceedances over a certain threshold. Based on the application of this method as described by Ruggerio et al. (2010), the 99.5th percentile of significant wave height was used as a threshold value. These methods were applied using the WAFO matlab toolbox (Brodtkorb et al. 2000). The bootstrapping method (Efron and Tibshirani 1993) was applied in order to generate a 95% confidence interval around the CDFs derived using both of the extreme value distribution methods utilized in this analysis.

The 100-year H_{m0} is estimated as 9.98 m and 9.63 m using the GEV and POT methods, respectively, as shown in Figures 104 and 105. The 10-, 25-, and 50-year values are shown in the figures. It should be noted that conditions at the NDBC46218 buoy (at a depth on the order of 500 m) may differ significantly from the conditions at the test site (at depths on the order of 100 m).

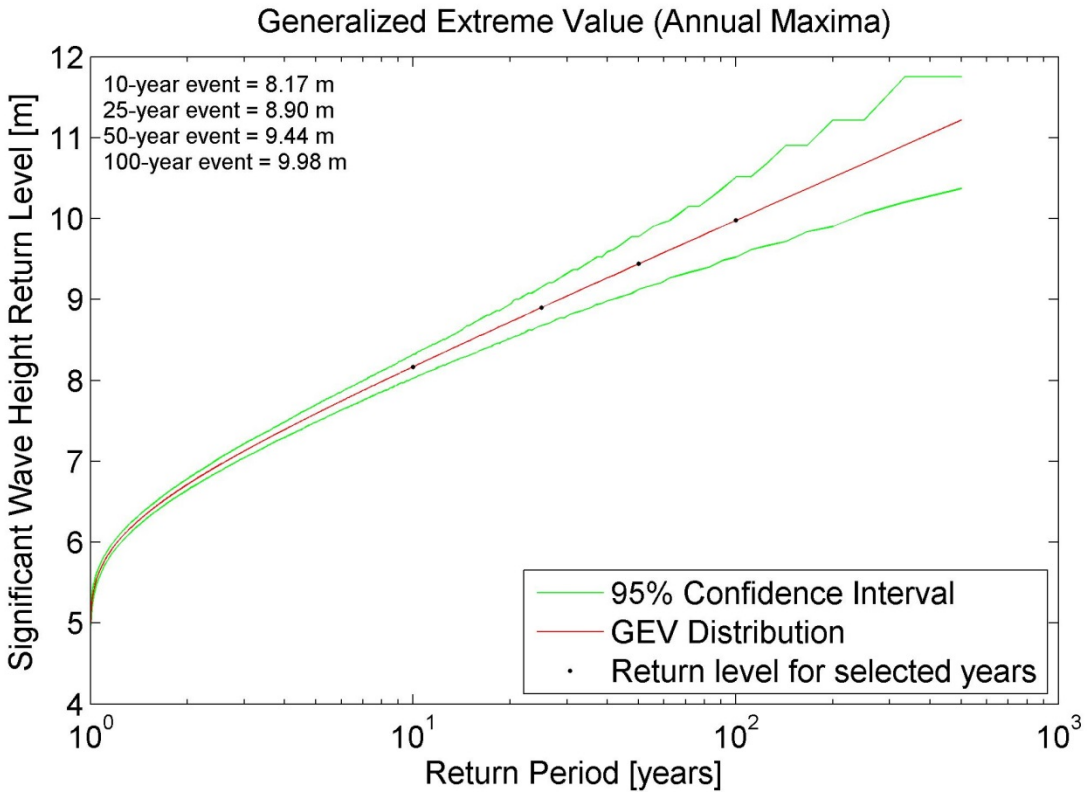

Figure 104: The generalized extreme values distribution was fit to annual maximum of significant wave height from NDBC46218 to generate estimates of extreme values. The 95% confidence interval is shown as well.

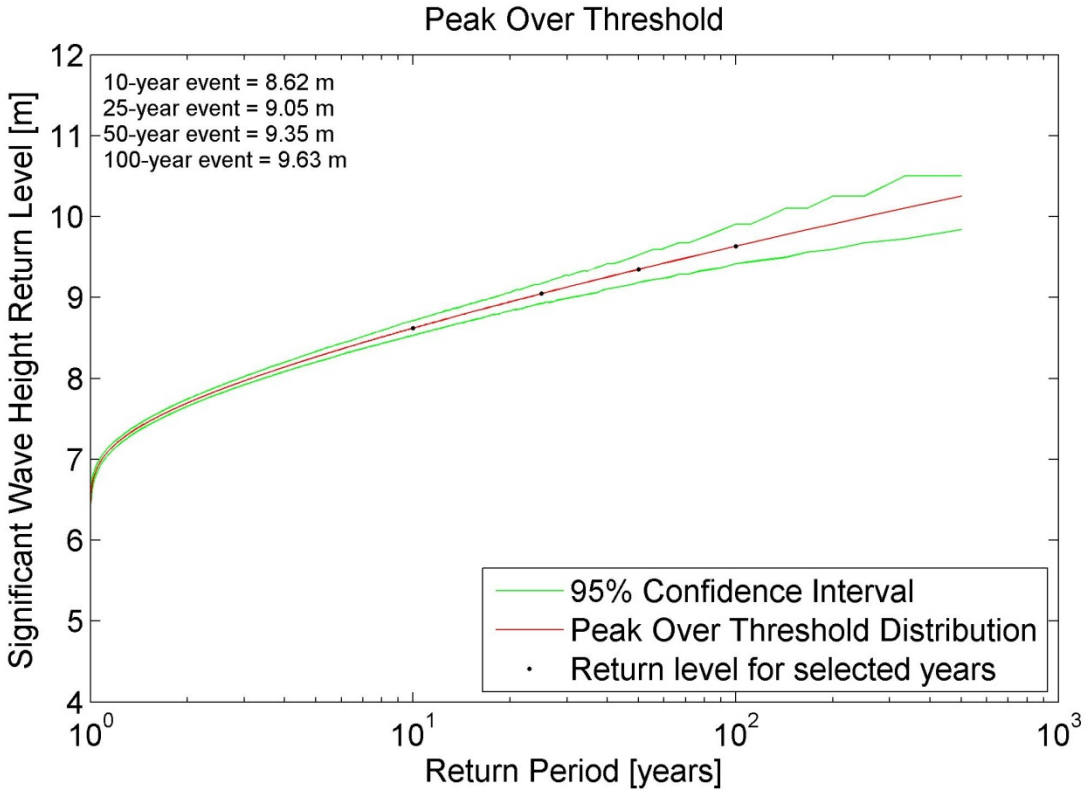

Figure 105: The peak over thresholds method was used with a threshold value of the 99.5th percentile of significant wave height from NDBC46218. The 95% confidence interval is shown as well.

9.4.6. Representative Wave Spectrum

All hourly discrete spectra measured at CDIP071 / NDBC46218 for the most frequently occurring sea states are shown in Figure 106. The most frequently occurring sea state, which is within the range 1.5 m $< H_{m0} <$ 2 m and 8 s $< T_e <$ 9 s, was selected from a JPD similar to Figures 90 & 91 in Section 9.4.1, but based on the NDBC 46218 buoy data. As a result, the JPD, and therefore the most common sea states, generated from buoy data are slightly different from that generated from hindcast data. For example, the most frequently occurring sea state for the JPD generated from hindcast data is 0.5 m higher on bounds for H_{m0} (2 m $< H_m0$ ¡ 2.5 m), and two seconds higher on bounds for T_e (10 s $< T_e <$ 11 s). Often several sea states will occur at a very similar frequency, and therefore plots of hourly discrete spectra for several other sea states are also provided for comparison. Each of these plots includes the mean spectrum and standard wave spectra, including Bretschneider and JONSWAP, with default constants as described in Section 2.2.

For the purpose of this study, the mean spectrum is the 'representative' spectrum for each sea state, and the mean spectrum at the most common sea state, shown in Figure 106 (bottom-left plot), is considered the 'representative' spectrum at the site. The hourly spectra vary considerably about this mean spectrum, but this is partly reflective of the bin size chosen for H_{m0} and T_e. Comparisons of the representative spectra in all plots with the Bretschneider

and JONSWAP spectra illustrate why modeled spectra with default constants, e.g., the shape parameter $\gamma = 3.3$ for the JONSWAP spectrum, should be used with caution. Using the constants provided in Section 2.2, the Bretschneider spectra are, at best, fair representations of the mean spectra in Figure 106, and it does not capture the bimodal nature of the spectra. The mean measured spectra is the best representation of the conditions, however, if these modeled spectra were to be used at this site, it is recommended that the constants undergo calibration against some mean spectrum, e.g., the representative spectrum constructed here. A better alternative would be to explore other methods or spectral forms to describe bimodal spectra (e.g., Mackay 2011) if it is known that the shape is not unimodal.

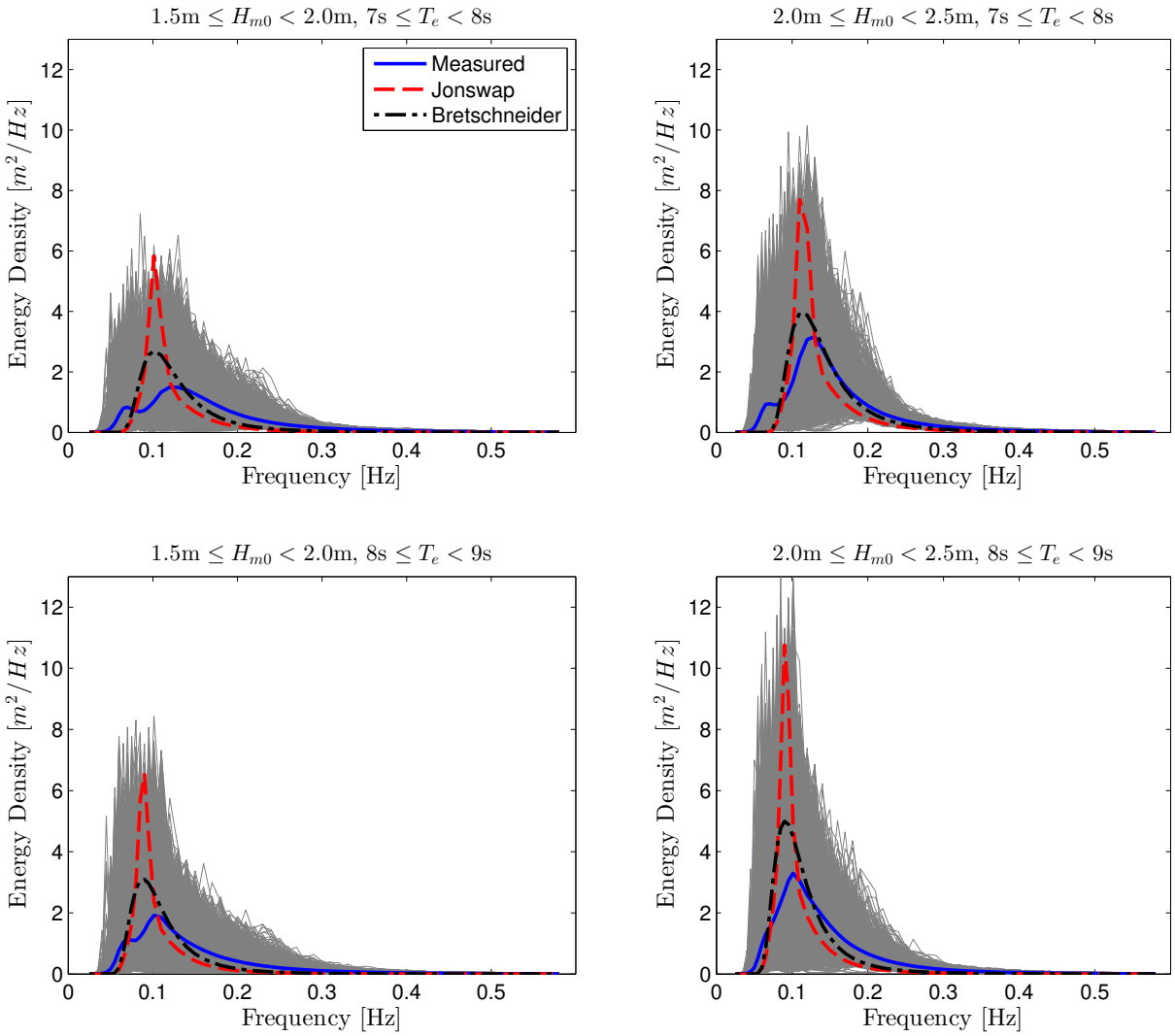

Figure 106: All hourly discrete spectra and the mean spectra measured at CDIP071 / NDBC 46218 within the sea state listed above each plot. The JONSWAP and Bretschneider spectra are represented by red and black dotted lines, respectively.

10. HUMBOLDT BAY, CALIFORNIA: POTENTIAL WEC TEST SITE

10.1. Site Description

For the purpose of this catalogue, the potential WEC site offshore of Humboldt Bay, referred to herein as the Humboldt Site, is located at 40.8418 N, 124.2477 W. As seen in Figure 107, the Humboldt Site lies in the footprint of the former Pacific Gas & Electrics (PG&E) pilot project test bed, the Humboldt WaveConnect (HWC), which was located in state waters to potentially ease permitting restrictions. PG&E considered this location for a WEC testing facility during the years 2008 – 2011 (Dooher et al. 2011). PG&E chose this test bed location based on numerous considerations, and the motivation for HWCs site placement is available in more detail in PG&Es Final Report (Dooher et al. 2011).

The Humboldt Site is approximately 9 km north/northwest of Humboldt Bay near the city of Eureka in Humboldt County, California (Figure 107). The site is at 45 m depth and lies over a sedimentary shelf consisting of sand and clay. As seen in Figure 108, the deployment site features a gently sloping seabed without many irregularities such as canyons that could disturb the local wave field (Dooher et al. 2011). The sediment and bathymetry are well suited for subsea cable burial and anchoring (Dooher et al. 2011).

The wave climate at the test site varies seasonally, with calmer seas in the summer compared to more energetic seas in the winter. The wave environment at the site is characterized by an annual average power flux of about 32.2 kW/m, including a number of events with significant wave heights exceeding 7 m each winter.

This site is not as developed as some of the other sites in this catalogue, but it has the basic infrastructure needed to support WEC testing. The surrounding area offers port facilities, an electrical substation on shore, and an abundance of high quality met-ocean data.

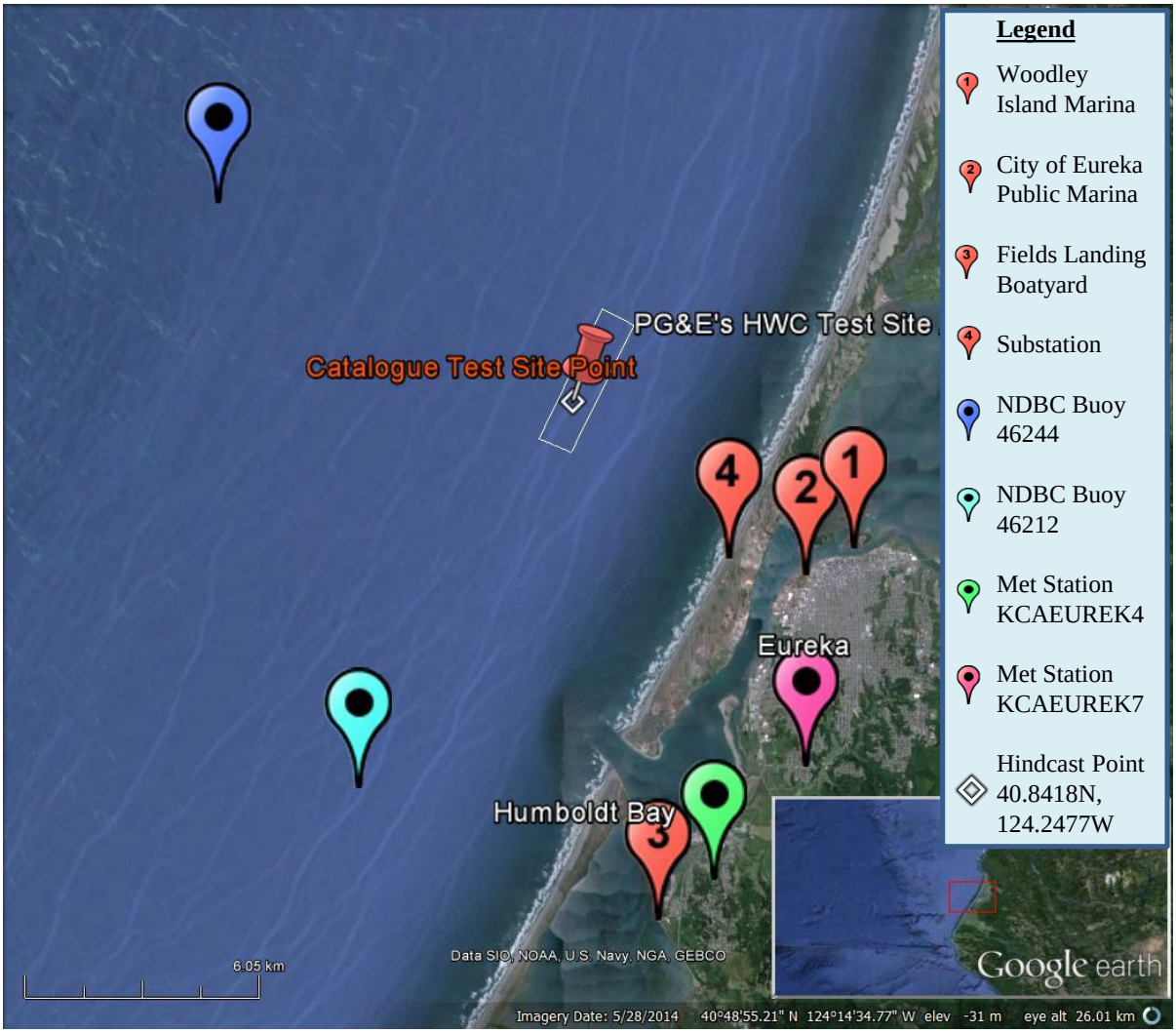

Figure 107: The proposed Humboldt Site is located on the coast of California near the city of Eureka. The test site is 5-6 km off-shore in 45 m depth water (∼25 fathoms). No berthing or ocean infrastructure exist at this time. A future grid connection could be established at the existing substation. Two National Data Buoy Center (NDBC) ocean buoys and two National Weather Service (NWS) meteorological stations are close to the test site. The Woodley Island Marina and the City of Eureka Public Marina are located in Humboldt Bay and boatyard access is available at the Fields Landing Boatyard. The point of reference for the hindcast simulation is the primary coordinate for the proposed test site. Image modified from Google Earth (2014).

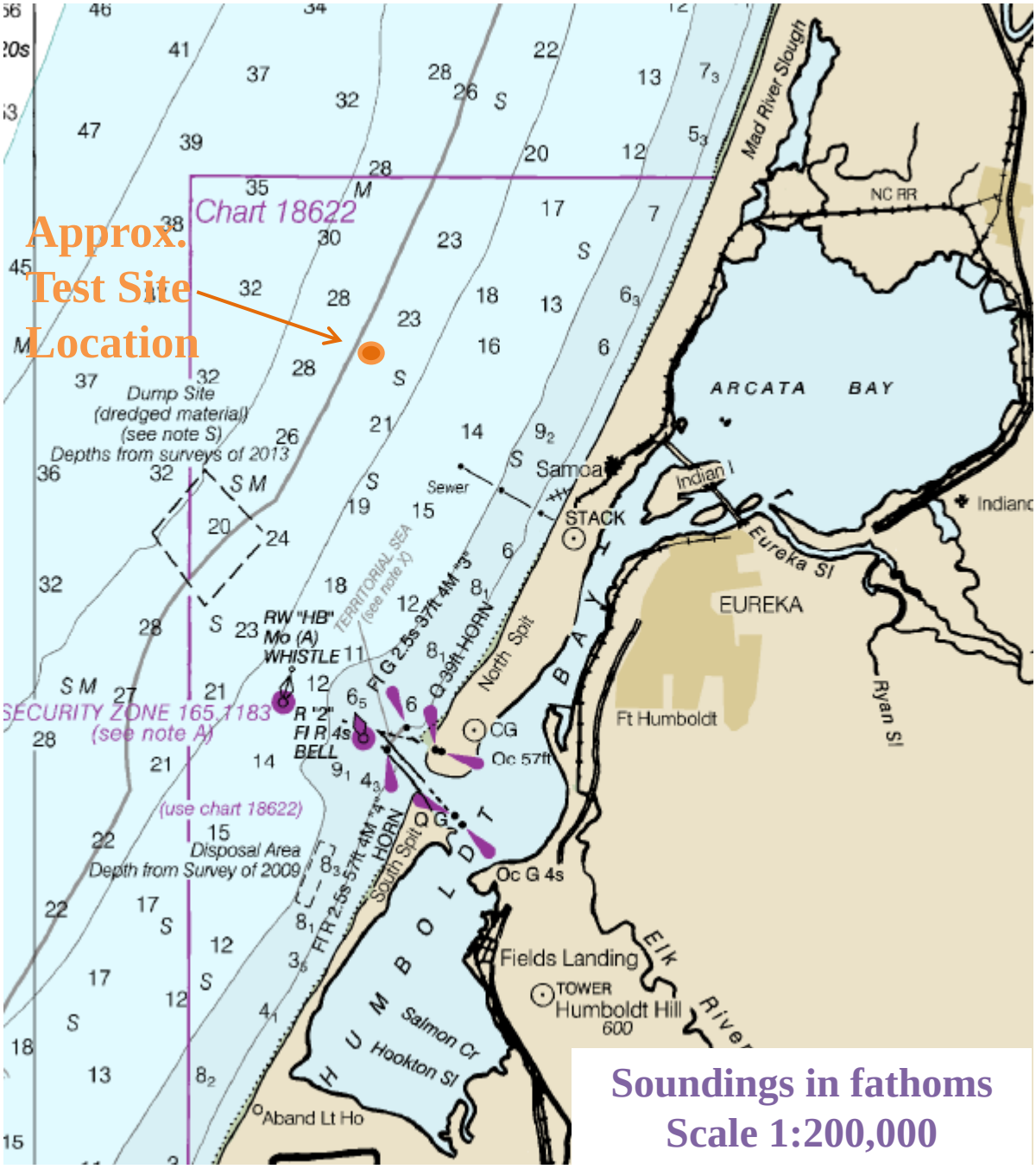

Figure 108: Nautical chart of Humboldt Bay and surrounding area shows the general bathymetry around the proposed test site. Sounds in fathoms (1 fathom = 1.8288 m). For a detailed map of Humboldt Bay, see Nautical chart #18622 (Office of Coast Survey 2013). Image modified from nautical chart #18620 (Office of Coast Survey 2012).

10.2. WEC Testing Infrastructure

10.2.1. Mooring Berths

As a potential test site, the Humboldt Site has no mooring berths installed or planned.

10.2.2. Electrical Grid Connection

There is currently no grid connection at the Humboldt Site. Future projects, however, may take advantage of the substation onshore directly landward of the test site (Waypoint #4 in Figure 107). The 60 kV PG&E Fairhaven Substation has three 60 kV lines connected to it, the highest of which accommodates 41 MW. The nearby former pulp mill facility also has a substation that interconnects to the same 60 kV transmission lines and is capable of accommodating 30 MW.

10.2.3. Facilitating Harbor

The port nearest to the test site is located within Humboldt Bay, which is the only deep-water port on California's North Coast (Department of Transportation 2012). For boat mooring, there are two options in Humboldt Bay near the city of Eureka: the Woodley Island Marina (Waypoint #1 in) and the City of Eureka Public Marina (Waypoint #2 in Figure 107).

10.2.4. On-Shore Office Space

10.2.5. Service Vessel and Engineering Boatyard Access

No dedicated service vessel is available at this time. Boats may be serviced at Fields Landing Boatyard (Waypoint #3 in Figure 107). This boatyard serves small to commercial-sized fishing boats with a travel lift. Repairs are made by the owner or hired external personnel. There may be companies such as Englund Marine & Industrial Supply Co. that can provide additional engineering services.

10.2.6. Travel and Communication Infrastructure

The Arcata/Eureka Airport services the Humboldt Bay area. The airport has several flights per day. Cellular phone service is available with moderate to full coverage.

10.2.7. Met-Ocean Monitoring Equipment

Real-time meteorological and wave data are collected by three met-ocean buoys and two meteorological stations. Instrument and data specifications for this monitoring equipment are summarized in Table 8. Buoy data is accessible online at the CDIP and NDBC databases. CDIP168 (NDBC46244) is operational and located approximately 8 km west of the test site. NDBC 46022 (Figure 109 (a)), approximately 30 km southwest of the site, has been offline

for repair and is expected to be operational in the fall of 2014. CDIP128 (NDBC 46212) (Figure 109 (b)) is approximately 12 km from the test site, but was decommissioned in 2013. In addition to the met/ocean buoys, there are two land based meteorological stations located in Eureka, California.

Figure 109: (a) Discus buoy NDBC46022 located 30 km from site, (b) Waverider buoy CDIP128/NDBC46212 located 12 km south of test site (National Data Buoy Center 2014).

Table 8: Wave monitoring equipment in close proximity to the Humboldt proposed test site.

Instrument Name (Nickname)	**CDIP128/ NDBC46212 - ("South Spit")**		**NDBC46022 (LLNR 500 / "Buoy 22")**			**CDIP168 / NDBC46244 - ("North Spit")**	
Type	Waverider Buoy		3-meter discus buoy			Waverider Buoy	
Measured parameters	-std. met. data -spectral wave density data -spectral wave direction data		-std. met. data -continuous winds data -spectral wave density data -spectral wave direction data (only from 2007-2010)			-std. met data -spectral wave density data -spectra wave directional data	
Variables reported, including derived variables (Sampling interval)	*Std. Met.:* WVHT DPD APD MWD WTMP (30 min)	-Spectral Wave Density -Spectral Wave Direction (30 min)	*Std. Met.:* WDIR WSPD GST WVHT DPD APD PRES ATMP WTMP (1 hr)	*Contin. Winds:* WDIR WSPD GDR GST GTIME (10 min)	-Spectral Wave Density -Spectral Wave Direction (1 hr)	*Std. Met.:* WDIR WSPD GST WVHT DPD APD PRES ATMP WTMP (30 min)	-Spectral Wave Density -Spectral Wave Direction (30 min)
Location	12 km South of site, 6.5 km West of Humboldt Bay entrance		30 km West/Southwest of Test site			8 km West of Test Site	
Coordinates	40.753 N 124.313 W (40°45'12" N 124°18'48" W)		40.724 N 124.578 W (40°43'25" N 124°34'41" W)			40.888 N 124.356 W (40°53'18" N 124°21'22" W)	
Depth	40 m		674.8 m			114 m	
Data Start	1/22/2004		-wave data: 1982 -spectral wave data: 01/01/1996 -directional spectra: 06/01/2007			2/9/2010	
Data End	4/3/2013		-11/13/2013 -dir. spectra ended 2/19/2010 -will be redeployed 8/2014			present	
Period of Record	∼9 yrs		-wave data: ∼32 yrs -spectral data: ∼18 yrs -directional spectra: ∼4 yrs			∼5.5 yrs	
Owner/ Contact Person	NOAA– "Information Submitted by Scripps" http://cdip.ucsd.edu/?nav=recent&sub=observed&stn=128&xitem=info&stream=p1		National Data Buoy Center http://www.ndbc.noaa.gov/station_page.php?station=46022			NOAA– "Information Submitted by Scripps" http://cdip.ucsd.edu/?ximg=search&xsearch=168&xsearch_ type=Station_ID	

Instrument Name (Nickname)	**KCAEUREK4**	**KCAEUREK7**
Type	Met station	Met Station
Measured parameters	Meteorological Data	Meteorological Data
Variables reported, including derived variables (Sampling interval)	AirTemp DewPoint Pressure WDIR WSPD Humidity (5 min)	AirTemp DewPoint Pressure WDIR WSPD Humidity Precip (5 min)
Location	Humboldt Hill, Eureka, CA	Herrick Hill, Eureka, CA
Coordinates	40.732 N 124.205 W (40° 43' 54" N, 124° 12' 17" W)	40.758 N 124.177 W
Depth	Elev.: 85 ft	Elev.: 102 ft
Data Start	3/7/2008	3/15/2011
Data End	present	present
Period of Record	∼6.5 yrs	∼3.5 yrs
Owner/ Contact Person	National Weather Service; data download wunderground.com	National Weather Service; data download wunderground.com

10.2.8. Environmental Monitoring

Environmental conditions have not been assessed at the Humboldt Site, and although some environmental studies were conducted as part of an environmental site assessment (ESA) for the HWC project site, the ESA was never completed (Dooher et al. 2011). PG&E partnered with Redwood Sciences Lab, Klamath Bird Observatory, and Humboldt State University (HSU) for their ESA related studies. Several ESA related studies reached completion including a marine life study conducted by Dr. Dawn Goley at HSU (Dooher et al. 2011: Appendix HSU E), a sediment dynamics study (Dooher et al. 2011: Appendix HSU C) and site placement in relation to local fishing economics study (Dooher et al. 2011: Appendix HSU D, Appendix HSU B). Future projects must further characterize the site and be responsible for environmental monitoring of the WEC device.

10.2.9. Permitting

The Humboldt Site has no federal, state or local permits to operate as a WEC test site. Future efforts to permit the Humboldt Site will require a substantial investment through the NEPA process, including outreach to various stakeholders, required permits for testing in California state waters, the development of an environmental impact report and monitoring, and adaptive management plans. The time required for this process is unknown and developers should be prepared for significant time uncertainty.

Although future projects must devote a significant effort to permitting at Humboldt Bay, developers can leverage the lessons learned from the HWC project site to ease the process. PG&E states in their report that they hope that their experiences may be informative for future test site developers and help future projects avoid some of the struggles they faced (Dooher et al. 2011). PG&E was issued preliminary permits for the HWC project site in 2008 through the Federal Energy Regulatory Commission (FERC), but a Pilot Project Licensing Process (PPLP) was never obtained (Dooher et al. 2011). Of all the obstacles, uncertainty regarding the expected impact of WEC devices on the environment was a major challenge in obtaining the permit. This uncertainty was partly due to the lack of specific information concerning WEC technologies to be tested at PG&Es site, and also the relative lack of understanding about the marine environment at the site. More information about PG&Es HWC project can be found in their final report, which is available from the Office of Science and Technical Information at http://www.osti.gov/scitech/biblio/1032845 (report ID 1032845).

10.3. Data used

Researchers at Sandia National Laboratories produced a 10 year hindcast dataset for the area offshore of Humboldt Bay, CA (Dallman et al. 2014). This dataset was used to calculate parameters of interest for the characterization at this site. The hindcast data at the grid point shown in Figure 110 was analyzed.

In addition to the hindcast data set, historical data from buoy CDIP128/NDBC 46212 was

used to calculate estimates of extreme events and representative spectra. As with the other sites, CFSR wind data and OSCAR current data were used. See Figures 107 and 110 for data locations.

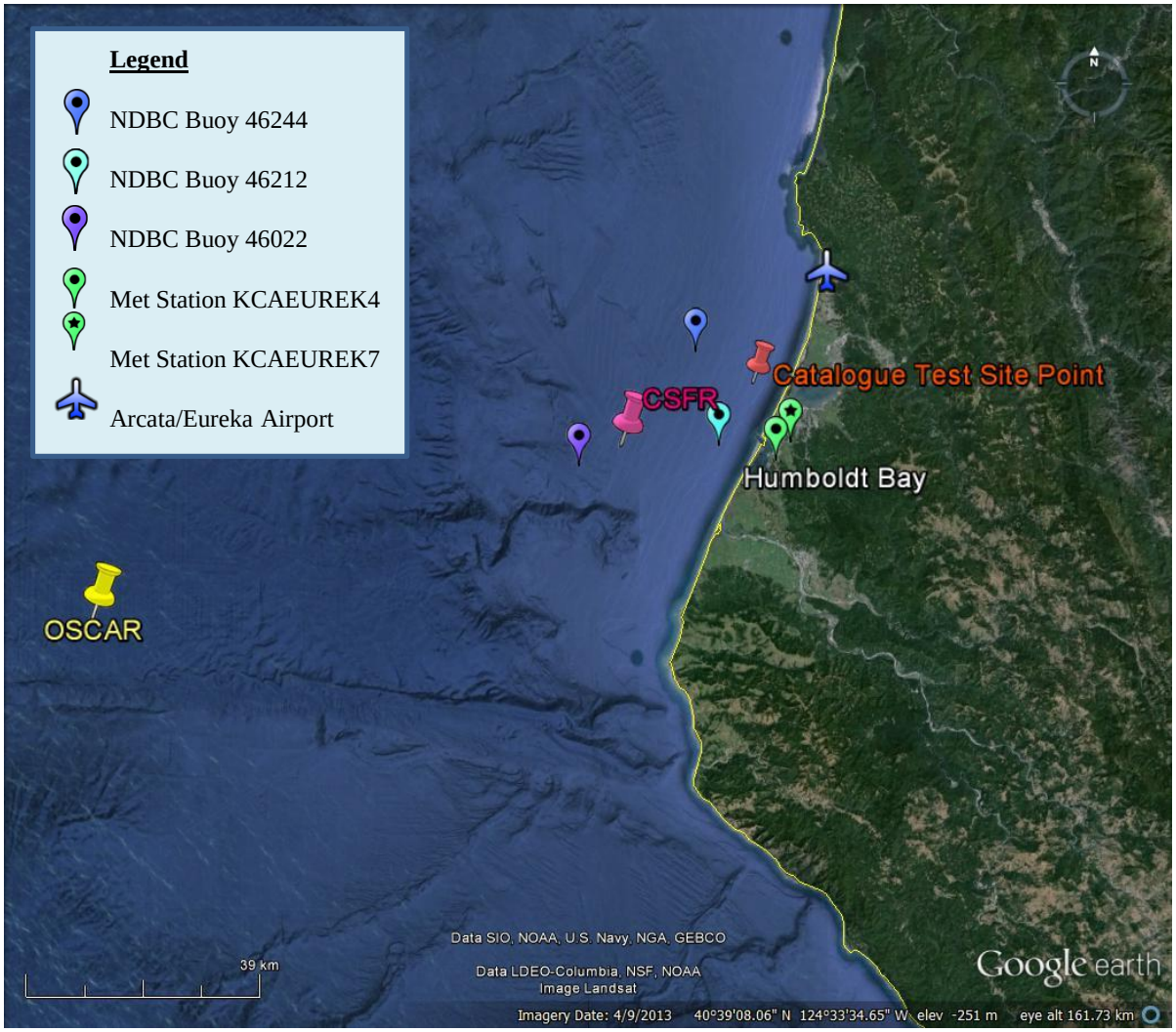

Figure 110: The catalogue test site location in relation to NDBC Buoys, OSCAR surface current data points, CSFR wind data points, and the nearest airport (Google Earth 2014).

10.4. Results

The following sections provide information on the joint probability of sea states, the variability of the IEC TS parameters, cumulative distributions, weather windows, extreme sea states, and representative spectra. This is supplemented by wave roses as well as wind and surface current data in Appendix H. The wind and surface current data provide additional information to help developers plan installation and operations & maintenance activities.

10.4.1. Sea States: Frequency of Occurrence and Contribution to Wave Energy

Joint probability distributions of the significant wave height, H_{m0}, and energy period, T_e, are shown in Figure 111. Figure 111 (top) shows the frequency of occurrence of each binned sea state and Figure 111 (bottom) shows the percentage contribution to the total wave energy. Figure 111 (top) indicates that the majority of sea states are within the range 1 m $< H_{m0} <$ 3.5 m and 6 s $< T_e <$ 11 s; but a wide range of sea states are experienced at the Humboldt Site, including extreme sea states caused by severe storms where H_{m0} exceeded 7 m. The site is well suited for testing WECs at various scales, including full-scale WECs, and testing the operation of WECs under normal sea states. This would also be a desirable site for commercial deployment. Although the occurrence of an extreme sea state for survival testing of a full scale WEC is unlikely during a normal test period, the Humboldt Site wave climate offers opportunities for survival testing of scaled model WECs.

As mentioned in the methodology (Section 2.2), previous studies show that sea states with the highest occurrence do not necessarily correspond to those with the highest contribution to total wave energy. The total wave energy in an average year is 282,600 kWh/m, which corresponds to an average annual omnidirectional wave power of 32.2 kW/m. The most frequently occurring sea state is within the range 1.5 m $< H_{m0} <$ 2 m and 6 s $< T_e <$ 7 s, while the sea state that contributes most to energy is within the range 3 m $< H_{m0} <$ 3.5 m and 10 s $< T_e <$ 11 s. Several sea states occur at a similar frequency, and sea states within 2 m $< H_{m0} <$ 4.5 m and 9 s $< T_e <$ 12 s contribute a similar amount to energy.

Frequencies of occurrence and contributions to energy of less than 0.01% are not shown in the figure for clarity. For example, the sea state within 0.5 m $< H_{m0} <$ 1 m and 4 s $< T_e <$ 5 s has an occurrence of 0.02%. The contribution to total energy, however, is only 0.001% and, therefore, does not appear in Figure 111 (bottom). Similarly, the sea state within 8 m $< H_{m0} <$ 8.5 m and 13 s $< T_e <$ 14 s has an occurrence of 0.007%, but the contribution to total energy is 0.11%.

Curves showing the mean, 5^{th} and 95^{th} percentiles of wave steepness, H_{m0}/γ, are also shown in Figure 111. The mean wave steepness at the Humboldt Site is 0.0185 ($\approx$1/54), and the 95th percentile approaches 1/33.

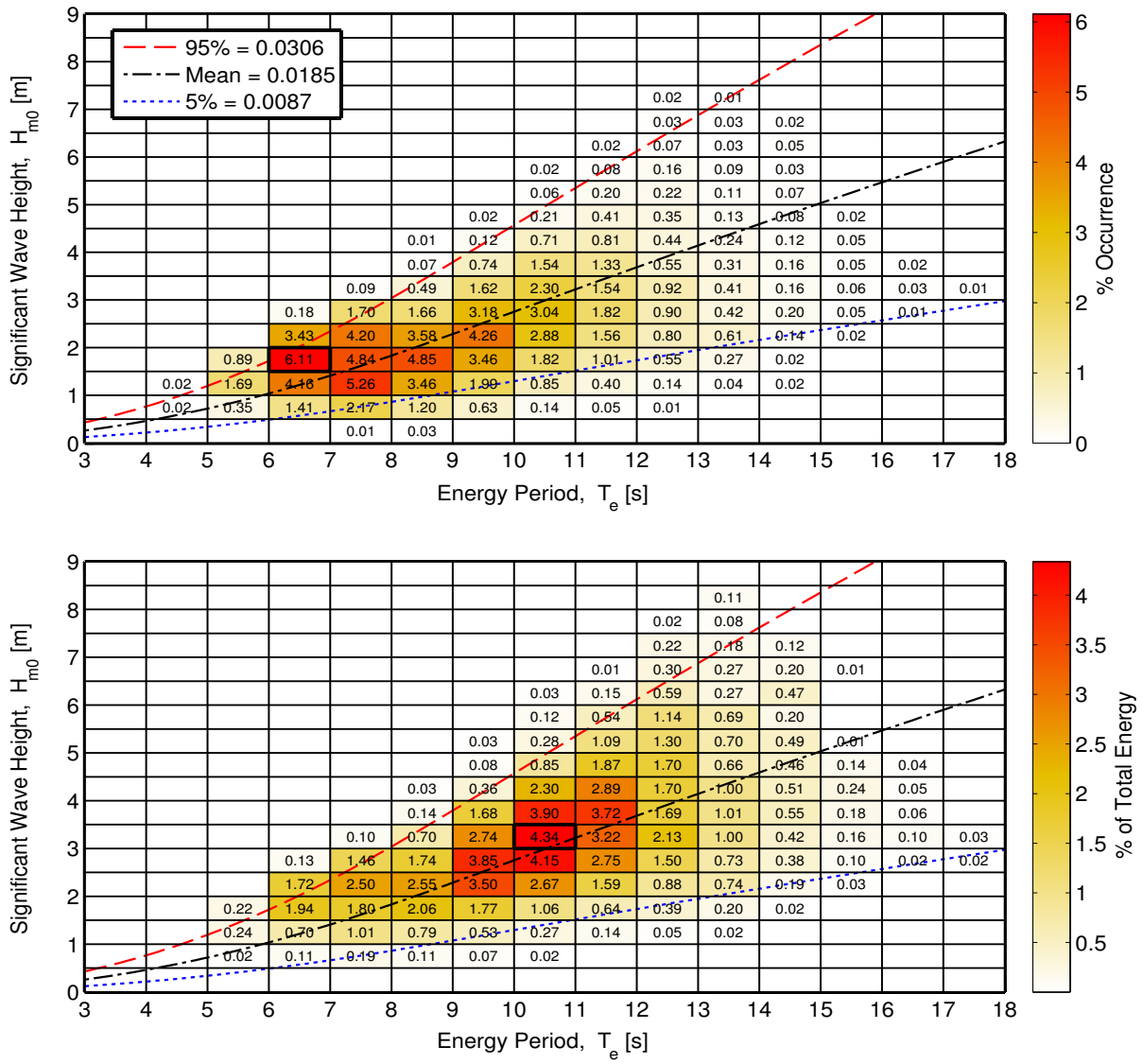

Figure 111: Joint probability distribution of sea states for the Humboldt Site. The top figure is frequency of occurrence and the bottom figure is percentage of total energy, where total energy in an average year is 282,600 kWh/m.

10.4.2. IEC TS Parameters

The monthly means of the six IEC TS parameters, along with the 5^{th} and 95^{th} percentiles, are shown in Figure 112. The values in the figure are summarized in Table 14 in Appendix C.

Monthly means of the omnidirectional wave power, J, significant wave height, H_{m0}, and energy period, T_e, show the greatest seasonal variability compared to the other parameters. Values are largest and vary the most during the winter months. These observations are consistent with the relationship between wave power density, significant wave height and energy period, where wave power density, J, is proportional to the energy period, T_e, and

the square of the significant wave height, H_{m0}.

The direction of maximum directionally resolved wave power (defined as the direction from which waves arrive in degrees clockwise from north), θ_j, is fairly consistent from west/northwest, and varies slightly between seasons. Seasonal variation of the spectral width, ϵ_0, and directionality coefficient (larger values indicate low directional spreading), is much less than the other parameters and barely discernable. Monthly means for ϵ_0 remain nearly constant between 0.3 and 0.35. Similarly, monthly means for d_θ remain nearly constant at ∼0.93.

In summary, the waves at the Humboldt Site, from the perspective of monthly means, have a fairly consistent spectral width, are predominantly from the west/northwest, and exhibit a wave power that has a narrow directional spread.

Wave roses of wave power and significant wave height, presented in Appendix C, Figure 164 and Figure 165, also show the predominant direction of the wave energy at the Humboldt Site, with small shifts to the north and west. Figure 164 shows two dominant direction sectors from west/northwest: 285° and 300°. Along the first direction sector, 285°, the omnidirectional wave power density is at or below 35 kW/m approximately 19% of the time, and greater than 35 kW/m about 15% of the time. Along the second direction sector, 300°, the omnidirectional wave power density is at or below 35 kW/m approximately 27% of the time, but greater than 35 kW/m about 9% of the time.

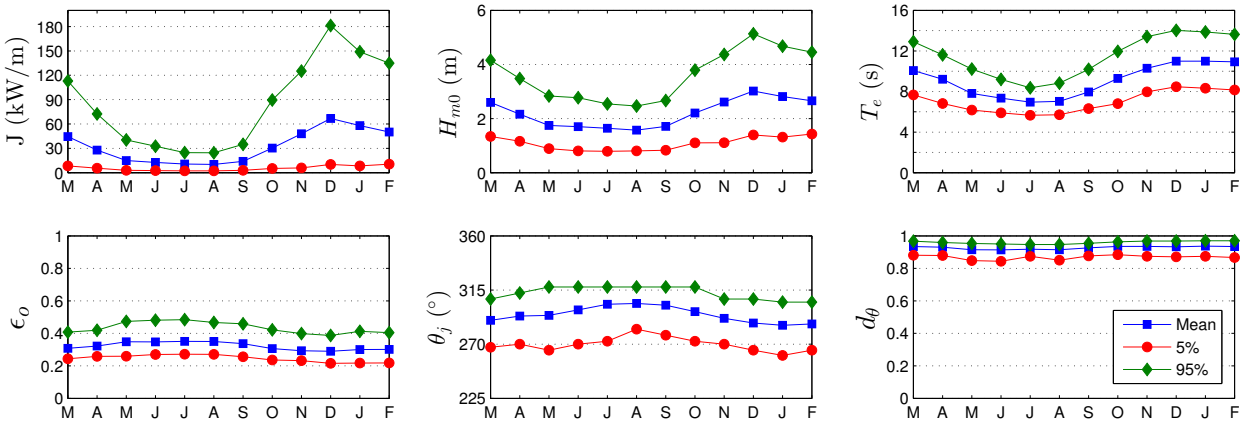

Figure 112: The average, 5th and 95th percentiles of the six parameters at the Humboldt site.

Monthly means, however, smear the significant variability of the six IEC parameters over small time intervals as shown in plots of the parameters at 1-hour intervals in Figure 113 for a representative year. While seasonal patterns described for Figure 112 are still evident, these plots show how sea states can vary abruptly at small time scales with sudden changes, e.g., jumps in the wave power as a result of a storm.

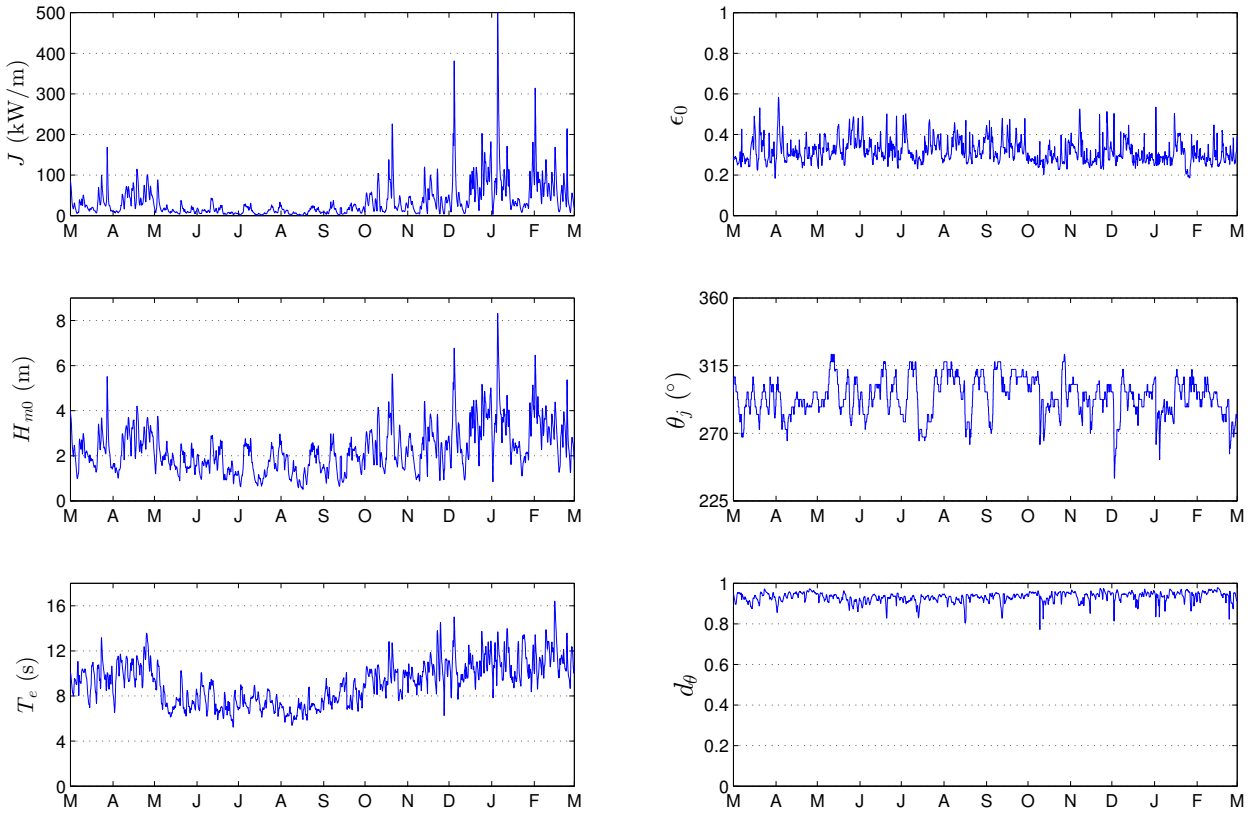

Figure 113: The six parameters of interest over a one-year period, March 2007 – February 2008 at the Humboldt site.

10.4.3. Cumulative Distributions

Annual and seasonal cumulative distributions (a.k.a., cumulative frequency distributions) are shown in Figure 114. Note that spring is defined as March - May, summer as June - August, fall as September - November, and winter as December - February. The cumulative distributions are another way to visualize and describe the frequency of occurrence of individual parameters, such as H_{m0} and T_e. A developer could use cumulative distributions to estimate how often they can access the site to install or perform operations and maintenance based on their specific device, service vessels, and diving operation constraints. For example, if significant wave heights need to be less than or equal to 1 m for installation and recovery, according to Figure 114, this condition occurs about 6% of the time on average within a given year. If significant wave heights need to be less than or equal to 2 m for emergency maintenance, according to Figure 114, this condition occurs about 48% of the time on average within a given year. Cumulative distributions, however, do not account for the duration of a desirable sea state, or weather window, which is needed to plan deployment and servicing of a WEC device at a test site. This limitation is addressed with the construction of weather window plots in the next section.

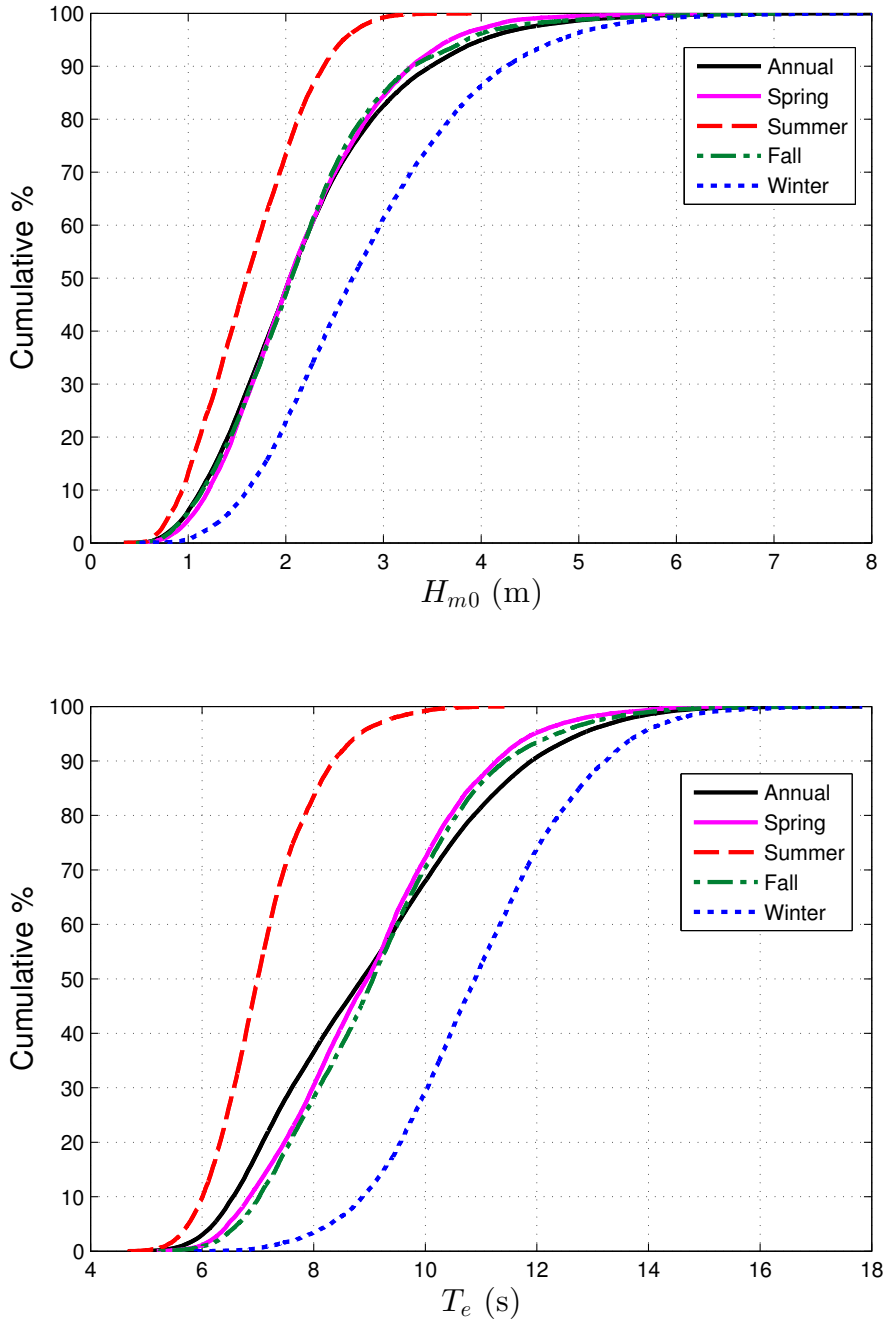

Figure 114: Annual and seasonal cumulative distributions of the significant wave height (top) and energy period (bottom) at the Humboldt site.

10.4.4. Weather Windows

Figure 115 shows the number of weather windows at the Humboldt Site, when significant wave heights are at or below some threshold value for a given duration, for an averaged winter, spring, summer, and fall. In these plots, each occurrence lasts a duration that is some multiple of 6-hours. The minimum weather window is, therefore, 6-hours in duration,

and the maximum is 96-hours (4 days). The significant wave height threshold is the upper bound in each bin and indicates the maximum significant wave height experienced during the weather window. Note that the table is cumulative, so, for example, an occurrence of $H_{m0} \leq 1m$ for at least 54 consecutive hours in the fall is included in the count for 48 consecutive hours as well. In addition, one 12-hour window counts would count as two 6-hour windows. It is clear that there are significantly more occurrences of lower wave heights during the summer than winter, which corresponds to increased opportunities for deployment or operations and maintenance.

Weather window plots provide useful information at test sites when planning schedules for deploying and servicing WEC test devices. For example, if significant wave heights need to be less than or equal to 1 m for at least 12 consecutive hours to service a WEC test device at the Humboldt Site with a given service vessel, there would be, on average, twenty weather windows in the summer, but only one in the winter. When wind speed is also considered, Figure 116 shows the average number of weather windows with the additional restriction of wind speed, $U < 15$ mph. Note that wind data was not available from the hindcast, so data from CFSR was used (see Section 2.3). For shorter durations (6- and 12-hour windows), daylight is necessary. Windows with U <15 mph and only during daylight hours are shown in Figure 117. Daylight was estimated as 5am – 10pm Local Standard Time (LST).

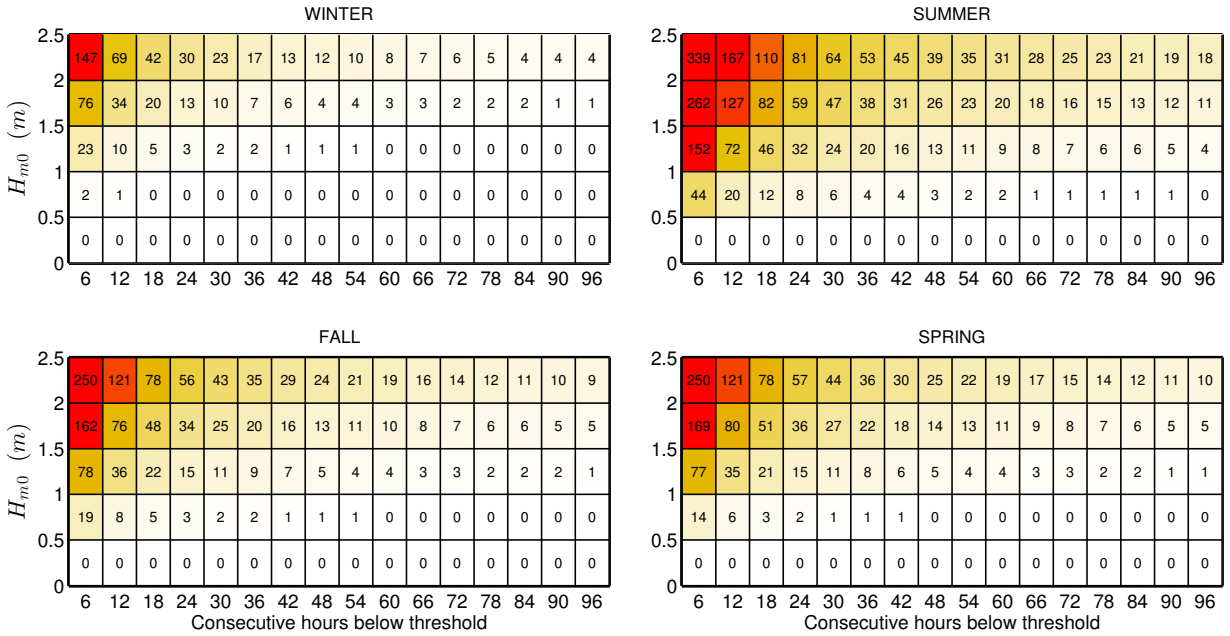

Figure 115: Average cumulative occurrences of wave height thresholds (weather windows) for each season at the Humboldt Site. Winter is defined as December - February, spring as March - May, summer as June - August, and fall as September - November.

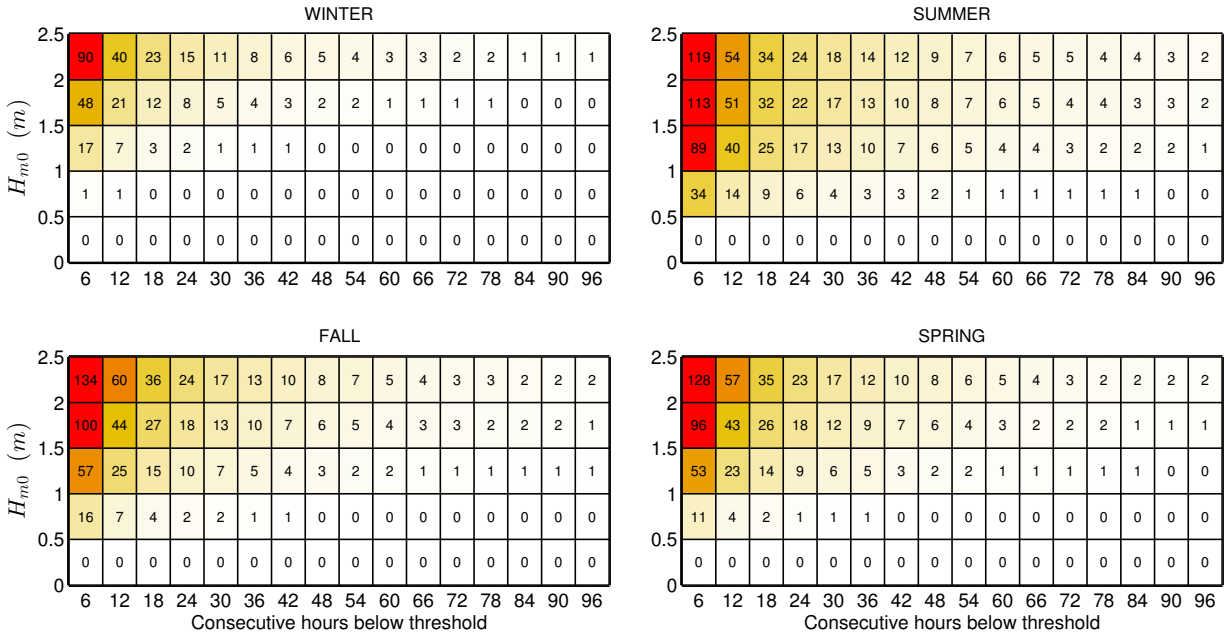

Figure 116: Average cumulative occurrences of wave height thresholds (weather windows) for each season at the Humboldt Site with an additional restriction of $U < 15$ mph.

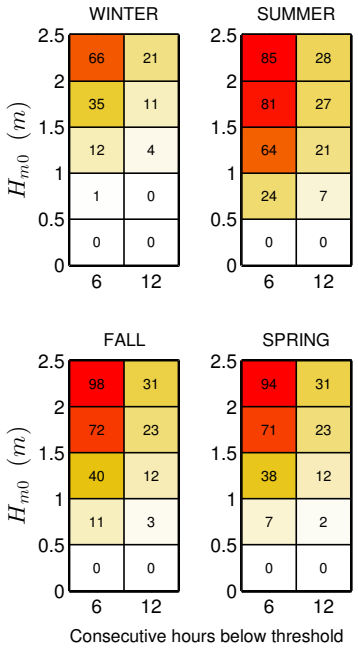

Figure 117: Average cumulative occurrences of wave height thresholds (weather windows) for 6- and 12-hour durations with $U < 15$ mph and only during daylight hours (5am – 10pm LST) at the Humboldt Site.

10.4.5. Extreme Sea States

The modified IFORM was applied using CDIP128 / NDBC46212 to generate the 100-year environmental contour for the Humboldt Site shown in Figure 118. Selected sea states along this contour are listed in Appendix H, Table 44. As stated in Section 1.2, environmental contours are used to determine extreme wave loads on marine structures and design these structures to survive extreme sea states of a given recurrence interval, typically 100-years. For the Humboldt Site, the largest significant wave height estimated to occur every 100-years, is approximately 10.9 m, and has an energy period of about 17.8 s. However, significant wave heights lower than 10.9 m, with energy period less than or greater than 17.8 s, listed in Appendix H, Table 44, could also compromise the survival of the WEC test device under a failure mode scenario in which resonance occurred between the incident wave and WEC device, or its subsystem. For comparison, 50- and 25-year return period contours are also shown in Figure 118. The largest significant wave height on the 50-year contour is 10.4 m with an energy period of about 17.5 s, and on the 25-year contour is 9.9 m and 17.1 s.

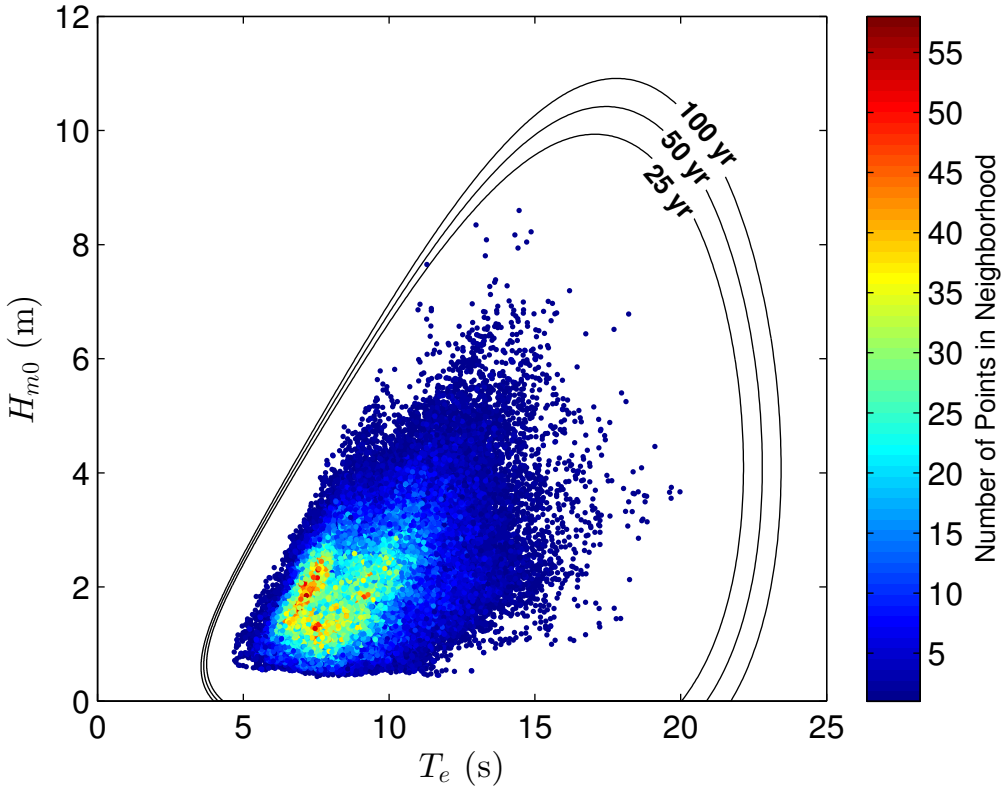

Figure 118: 100-year contour for CDIP128 / NDBC 46212 (2004-2012).

10.4.6. Representative Wave Spectrum

All hourly discrete spectra measured at CDIP128 / NDBC 46212 for the most frequently occurring sea states are shown in Figure 119. The most frequently occurring sea state, which is within the range 1 m $< H_{m0} <$ 1.5 m and 7 s $< T_e <$ 8 s, was selected from a JPD similar to Figure 36 in Section 5.4.1, but based on the CDIP128 / NDBC46212 buoy data. As a result, the JPD, and therefore the most common sea states, generated from buoy data are slightly different from that generated from hindcast data. For example, the most frequently occurring sea state for the JPD generated from hindcast data is a half-meter higher on bounds for H_{m0} (1.5 m $< H_{m0} <$ 2 m) and one second lower for T_e (6 s $< T_e <$ 7 s). Often several sea states will occur at a very similar frequency, and therefore plots of hourly discrete spectra for several other sea states are also provided for comparison. Each of these plots includes the mean spectrum and standard wave spectra, including Bretschneider and JONSWAP, with default constants as described in 2.2.

For the purpose of this study, the mean spectrum is the 'representative' spectrum for each sea state, and the mean spectrum at the most common sea state, shown in Figure 44 (bottom-left plot), is considered the 'representative' spectrum at the site. The hourly spectra vary considerably about this mean spectrum, but this is partly reflective of the bin size chosen for H_{m0} and T_e. Comparisons of the representative spectra in all plots with the Bretschneider and JONSWAP spectra illustrate why modeled spectra with default constants, e.g., the shape

parameter $\gamma = 3.3$ for the JONSWAP spectrum, should be used with caution. Using the constants provided in Section 2.2, the Bretschneider spectra are, at best, fair representations of the mean spectra in Figure 119. If these modeled spectra were to be used at this site, it is recommended that the constants undergo calibration against some mean spectrum, e.g., the representative spectrum constructed here. Using the constants provided in Section 2.2, the Bretschneider spectra are fair representations of the mean spectra in Figure 119, however it does not capture the bimodal nature of the spectra. The mean measured spectra is the best representation of the conditions, however, if these modeled spectra were to be used at this site, it is recommended that the constants undergo calibration against some mean spectrum, e.g., the representative spectrum constructed here. A better alternative may be to explore other methods or spectral forms to describe bimodal spectra (e.g., Mackay 2011) if it is known that the shape is not unimodal.

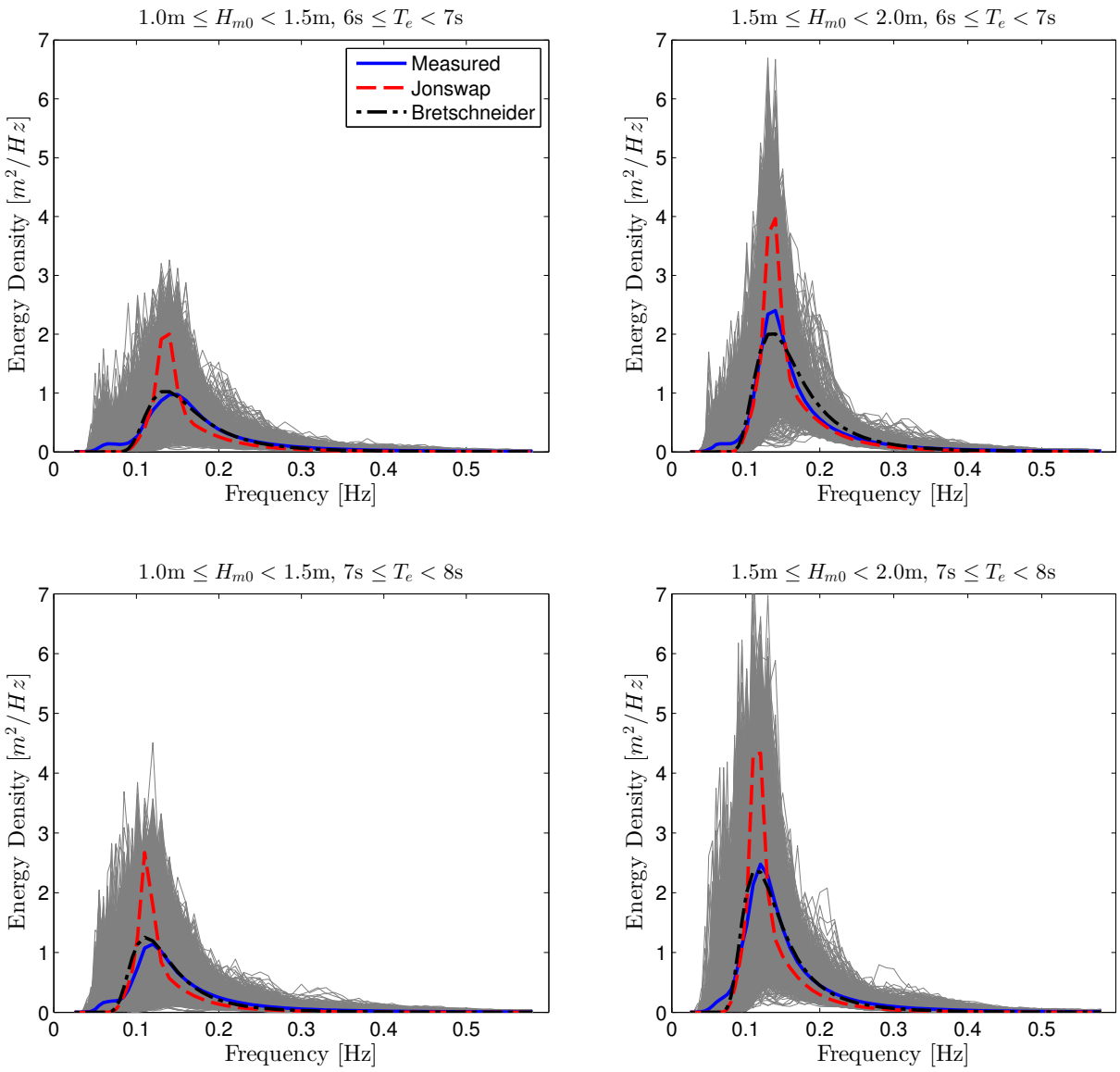

Figure 119: All hourly discrete spectra and the mean spectra measured at CDIP128 / NDBC 46212 within the sea state listed above each plot. The JONSWAP and Bretschneider spectra are represented by red and black dotted lines, respectively.

11. SUMMARY AND CONCLUSIONS

This study provides a comprehensive characterization of eight U.S. WEC test sites. It includes important information on test site infrastructure and services, and catalogues detailed met-ocean data and information derived from numerous data sources. Although there are some differences in the quality of the data sources, e.g., the location of the buoy observations with respect to the test site, and the period of record of the hindcast or buoy observations, the data are processed using uniform and consistent methods. The characterization results, therefore, allow reasonable comparisons between the wave resource characteristics among the different test sites, and selection of test sites that are most suitable for a given device or current testing needs and objectives.

Plots useful for designing WEC test devices include the JPDs, seasonal variation of the six IEC bulk parameters, representative wave spectra, and environmental contours (extreme sea states). They also provide a useful and comprehensive summary of the wave climate and wave energy resource. Cumulative distributions and weather windows can aid in planning WEC deployments and servicing schedules based on the requirements of the service vessel.

The characterization results also allow assessment of the opportunities and risks of testing at each site, how they vary seasonally, and how they can change abruptly within a matter of hours or days. Large waves, associated with both normal and extreme sea states, provide opportunities for testing full scale WEC devices, but they can increase the challenges and risks of testing at the site. These include reduced access to the test device, for deployment or operation and maintenance, and increased risk of damaging or destroying the test device.

NETS is a test site offshore of Newport, OR, where the average annual omnidirectional wave power is 36.8 kW/m. The wave climate at the site varies significantly by season. Calmer seas (lower significant wave heights and energy periods) occur in the summer, while energetic seas occur in the winter, dominated by swells further away in the North Pacific. Larger wave heights occur in the winter months, with a number of events each year exceeding 7 m, and some severe storms producing significant wave heights over 10 m. There are significantly more weather windows that would allow for deployment, and operations and maintenance, in the summer than any other season. Winter would provide opportunities for survival testing for devices at high TRL levels.

WETS is a test site offshore of Oahu, HI, where the average annual omnidirectional wave power is 14.3 kW/m at the 80 m berth. The wave climate varies seasonally, but with less variability than the Pacific Northwest. Calmer seas occur during the summer, produced by year-round trade winds from the northeast, while more energetic seas occur in the winter made up of both wind waves and swell from the North Pacific. Year-round testing has been done at the site because significant wave heights rarely exceed 3 m in the winter. Weather windows are higher in summer, but with less of a difference from winter as other sites, and there are relatively few longer weather windows that might be appropriate for deployment. However, shorter weather windows (opportunities for operations and maintenance),

especially for H_{m0} limits of 1.5 m or more remain high throughout the year.

The Jennette's Pier Wave Energy Test Site is offshore of Nags Head, NC, where the average annual omnidirectional wave power is 6.08 kW/m at 12.6 m depth. The wave climate varies seasonally, but with less variability than the Pacific Northwest. Calmer seas occur during the summer, while more energetic seas occur in the winter. Significant wave heights rarely exceed 3 m, however there are some instances greater than 5 m. Weather windows are high throughout the year due to the lower wave heights, including longer windows that might be appropriate for deployment. There are significantly more weather windows in the summer than winter.

The USACE FRF is offshore of Duck, NC, where the average annual omnidirectional wave power is 3.29 kW/m at 4.8 m depth, although areas in state waters up to depths of approximately 25 m are available for testing. The test site has similar characteristics to the Jennette's Pier Wave Energy Test Site, with calmer seas during the summer, and more energetic seas in the winter. Significant wave heights rarely exceed 3 m at the 4.8 m depth location, and would not typically exceed 5 m at depths available for testing. Similarly to the Jennette's Pier site, weather windows are high throughout the year, including longer windows that might be appropriate for deployment. There are significantly more weather windows in the summer than winter.

The PMEC Lake Washington test site can be considered a proof of concept or 'nursery' site, where the average annual omnidirectional wave power is 0.04 kW/m. The wave climate varies by season, with calm conditions in the summer due to weak northerly winds and more energetic conditions in the winter due to strong southerly winds. The climate is event driven by local wind, and there are periods of very low waves throughout the year. There are no occurrences of significant wave height greater than 1 m, so it is assumed there are ample opportunities for deployment and mainteance in any season, depending on wind restrictions and competing uses of the area in the lake.

SETS is a potential test site located west of NETS, in slightly deeper water depths (58-75 m), where the average annual omnidirectional wave power is 40.7 kW/m. The characteristics are very similar to NETS, however the wave power is greater and there is slightly more directional spreading. Larger wave heights occur in the winter months, with a number of events each year exceeding 8 m. Similarly to NETS, there are significantly more weather windows that would allow for deployment, and operations and maintenance, in the summer than any other season. Winter would provide opportunities for survival testing for devices at high TRL levels.

The CalWave proposed Central Coast WEC Test Site at Vandenberg Air Force Base includes several options for berth locations, although this catalogue focuses on two potential offshore siting alternatives, the 'South', and 'South by Southeast' sites, which are located outside state waters. The average annual omnidirectional wave power is 39.9 kW/m at the South site and 31.4 kW/m at the South by Southeast site. The wave climate at the site varies significantly by season. Calmer seas occur in the summer, while energetic seas occur in the winter, dominated by swells further away in the North Pacific. Typically the site experiences low

directional spread in the waves (nearly unidirectional), however there are occasional swells from the south/southwest that increase the directional spreading. There are significantly more weather windows that would allow for deployment, and operations and maintenance, in the summer than any other season. Depending on restrictions for deployment, finding a suitable weather window may be difficult given that there are, on average, no windows longer than 18 hours for significant wave heights less than 1 m. Winter could provide opportunities for survival testing for devices at high TRL levels.

The Humboldt site is a potential test or commercial deployment site, where the average annual omnidirectional wave power is 32.2 kW/m. Similarly to NETS, the wave climate varies significantly by season with calmer wind waves in the summer and much more energetic seas dominated by swell in the winter. A small percentage of sea states exceed 7 m each winter. The Humboldt Site exhibits the very low directional spreading (nearly unidirectional waves). Similarly to SETS, NETS, and the CalWave Central Coast site, winter storms can be severe at Humboldt, with significant wave heights exceeding 5 m approximately 5% of the time in December.

With the exception of the Lake Washington site, wave direction at the sites generally does not align with the local wind direction because the waves are associated with swells and far-field winds, and they tend to align with the bathymetric contours as they approach shore. However, at most of the sites there is a slight shift towards the wind direction in the summer when swells are less dominant. The local wind data is important for servicing, and is incorporated into the weather windows. It may also be important for determining loads on a low-draft device with a significant above-water profile.

In general, the standard spectra did not match the mean ('representative') measured spectra at the sites very well, and the typical forms of JONSWAP and Bretschneider do not capture bimodal spectra. Therefore these standard spectra should be used with caution, and the mean measured spectra should be considered the best representation of conditions. This should be kept in mind especially for sites that do not exhibit unimodal spectra, and if the measured spectra cannot be used for an analysis, alternative parametric forms should be explored (e.g., Mackay 2011). The wide spread of spectral shapes that occur within a bin of H_{m0} and T_e) should also be considered, and perhaps smaller bin sizes should be used when characterizing the typical spectra.

The monthly mean surface currents at all sites are below 0.4 m/s, well below the IEC TS value of 1.5 m/s for depth-averaged current speed, which is recommended as the threshold beyond which it is important to account for ocean current effects in wave modeling. As surface currents are generally higher than depth-averaged currents, ocean currents at all the sites are not expected to significantly influence the wave dynamics.

REFERENCES

Batten, Belinda. E-mail correspondence to Director of Northwest National Marine Renewable Energy Center, July 24 – September 9, 2014.

Batten, Belinda. Monitoring at North Ocean Test Site, Newport OR. [Powerpoint slides], 2013. Retreived from Tethys: http://tethys.pnnl.gov/sites/default/files/attachments/2013-04-09%201%20Belinda%20Batten.pdf.

Berg, J.C., *Extreme Ocean Wave Conditions for Northern California Wave Energy Conversion Device*, SAND 2011-9304. Sandia National Laboratories, Albuquerque, NM, 2011.

Bitner-Gregersen, E.M, 2001, *Extreme Wave Steepness Estimated from Environmental Contour Plots Contra Traditional Design Practice*, Proceedings of the 20th International Conference on Offshore Mechanics and Arctic Engineering, Rio de Janeiro, Brazil.

Brodtkorb, P.A., Johannesson, P., Lindgren, G., Rychlik, I., Rydén, J. and Sjö, E., 2000, *WAFO - a Matlab toolbox for analysis of random waves and loads.* Proceedings of the 10th International Offshore and Polar Engineering conference, Seattle, Vol III, 343-350 p.

Cahill, B.G., and Lewis, A.W., 2011, *Wave Energy Resource Characterization of the Atlantic Marine Energy Test Site*. Proceedings of the 9th European Wave and Tidal Energy Conference, Southampton, United Kingdom.

Cahill, B.G., and Lewis, A.W., 2013, *Wave energy resource characterization of the Atlantic Marine Energy Test Site*, International Journal of Marine Energy 1, 3-15 p.

Chakrabarti, S.K., 1987, *Hydrodynamics of offshore structures.* WIT Press / Computational Mechanics, UK / Germany.

Coast and Harbor Engineering, 2015, Lake Washington Wave Energy Resource Assessment – Wave Energy Converter (WEC) Test Site, Technical Report.

Coastal Data Information Program, "Station 098-Mokapu Point, HI." Photo taken November 18, 2013. http://cdip.ucsd.edu/?ximg=search&xsearch=098&xsearch_type=Station_ID.

Coastal Data Information Program, "Station 198-Kaneohe Bay, HI." Photo taken November 18, 2013. http://cdip.ucsd.edu/?nav=historic&sub=data&units=metric&tz=UTC&pub=public&stn=198&stream=p1&xitem=stn_gallery3.

Coastal Data Information Program, "Station 192 - Oregon Inlet, NC." Photo taken July 18, 2013. http://cdip.ucsd.edu/?ximg=search&xsearch=192&xsearch_type=Station_ID.

D'Asaro, E. , J. Thomson, A. Shcherbina, R. Harcourt, M. Cronin, M. Hemer, B. Fox-Kemper, Quantifying upper ocean turbulence driven by surface waves, Geophys. Res. Letters, 41 (2014).

Dallman, A.R., Neary, V.S., Stephenson, M., *Investigation of Spatial Variation of Sea States Offshore of Humboldt Bay, CA Using a Hindcast Model,* SAND2014-18207. Sandia National Laboratories, Albuquerque, NM, 2014.

Davey, T., Venugopal, V., Smith, H., Smith, G., Lawrence, J., Luigi, C., Bertotti, L., Prevosto, M., Girard, F., Holmes, B., *EquiMar D2.7 Protocols for wave and tidal resource assessment,* December 2010.

Department of the Navy, *Wave Energy Test Site: Final Environmental Assessment,* Prepared by Alan Suwa, Caroleen Toyama, Jeffrey Fong, Jackie Sanehira, Sean Hanser, Kate Winters, Justin Fujimoto, T.A.F.,Thomas A. Fee, Gail Renard, Corlyn Olson Orr and John Clark, Marine Corps Base Hawaii: January 2014.

De Visser, A., and Vega, L.A., *"Wave Energy Test Site,"* Proceedings of the 7th Annual Global Marine Renewable Energy Conference, April 15-18, 2014.

Det Norske Veritas, 2005, *Guidelines on design and operation of wave energy converters.* Det Norske Veritas, The Carbon Trust, 2005.

Det Norske Veritas, 2014, *Environmental Conditions and Environmental Loads.* Recommended Practice DNV-RP-C205.

Department of Transportation, 2012, *Port of Humboldt Bay* Freight Planning Fact Sheet for Caltrans. http://dot.ca.gov/hq/tpp/offices/ogm/CFMP/Fact_Sheets/Seaports/Humboldt.pdf.

Dooher, B.P., Cheslak, E., Booth, R., Davy, D., Faraglia, A., Caliendo, I. Morimoto, G. and Herman, D. 2011, *PG&E WaveConnect Program Final Report.* DOE/GO/18170-1. Pacific Gas and Electric Company, San Francisco, CA, December 2011. doi: 10.2172/1032845.

Eckert-Gallup, A.C., Sallaberry, C.J., Dallman, A.R., Neary, V.S., *Modified Inverse First Order Reliability Method (I-FORM) for Predicting Extreme Sea States,* SAND2014-17550. Sandia National Laboratories, Albuquerque, NM, September 2014.

Eckert-Gallup, A.C., Sallaberry, C.J., Dallman, A.R., Neary, V.S., 2016, *Application of principal component analysis (PCA) and improved joint probability distributions to the inverse first-order reliability method (I-FORM) for predicting extreme sea states,* Ocean Engineering, 112, 307-319 pp.

Efron, B., Tibshirani, R.J., 1993, *An Introduction to the Bootstrap - Monographs on Statistics and Applied Probability,* Chapman & Hall, New York.

Feld, G., Mork, G., 2004, *A Comparison of Hindcast and Measured Wave Spectra Based on a Directional Spectral Fitting Algorithm,* Proceedings of the 8th International Workshop on Wave Hindcasting & Forecasting, North Shore, Oahu, HI, November 14-19.

Folley, M., Cornett, A., Holmes, B., Lenee-Bluhm, P., Liria, P., 2012, *Standardising resource assessment for wave energy converters,* Proceedings of the 4th Annual International

Conference on Ocean Energy, Dublin.

GarcíaMedina, G., Özkan-Haller, H.T., Ruggiero, P., 2014, *Wave resource assessment in Oregon and southwest Washington, USA*, Renew Energy 64, 203-214 p.

Google Earth, *Duck, NC,* 36°10' N 75°44' W. Data from SIO, NOAA, U.S. Navy, NGA, GEBCO. Image from Landsat. Accessed July 22, 2015.

Google Earth, *Humboldt Bay,* 41°00'07.85" N 124°16'03.18" W. Data from SIO, NOAA, U.S. Navy, NGA, GEBCO, LDEO-Columbia, NSF. Image from Landsat. Accessed July 16, 2014.

Google Earth, *Jennette's Pier, NC,* 35°55' N 75°36' W. Data from SIO, NOAA, U.S. Navy, NGA, GEBCO. Image from Landsat. Accessed July 22, 2015.

Google Earth, *Kaneohe Bay,* 21°27'50.53" N 157°44'19.06"W. Data from USGS. Image from USGS. Accessed July 16, 2014.

Google Earth, *Lake Washington,* 47°37' N 122°16' W. Data from SIO, NOAA, U.S. Navy, NGA, GEBCO, MBARI. Image from Landsat. Accessed July 22, 2015.

Google Earth, *Lompoc, CA,* 34°38' N 120°28' W. Image from Landsat. Accessed July 22, 2015.

Google Earth, *Newport, OR,* 44°38' N 124°3' W. Data from SIO, NOAA, U.S. Navy, NGA, GEBCO, MBARI, LDEO-Columbia, NSF. Image from Landsat. Accessed July 22, 2015.

Hasselmann, K., Barnett, T.P., Bouws, E., Carlson H., Cartwright D.E., Enke, K., Ewing J.A., Gienapp, H., Hasselmann, D.E., Kruseman, P., Meerburg, A., Mller, P., Olbers, D.J., Richter, K., Sell, W., Walden, H., 1973, *Measurements of Win-Wave Growth and Swell Decay During the Joint North sea Wave Project (JONSWAP),* Deutschen Hydro-graphischen Institut, No. 12, Hamburg, Germany.

Hawaii National Marine Renewable Energy Center, "Kaneohe Site." April 25, 2013. Accessed July 14, 2014. http://hinmrec.hnei.hawaii.edu/.

IEC TS 62600-101 Ed. 1.0 Marine energy – Wave, tidal and other water current converters – Part 101: Wave energy resource assessment and characterization.

Johnson, E.S., F. Bonjean, G.S.E. Lagerloef, J.T. Gunn, and G.T. Mitchum, 2007, *Validation and Error Analysis of OSCAR Sea Surface Currents.* Journal of Atmospheric and Oceanic Technology 24, 688701 p. doi: 10.1175/JTECH1971.1.

Jouanne, Annette von, Lettenmaier, Terry, and Sean Moran, *Wave Energy Testing Using the Ocean Sentinel Instrumentation Buoy.* Presented at the 1st Marine Energy Technology Symposium, Washington, DC, April 10-11, 2013. http://www.globalmarinerenewable.com/images/wave%20energy%20testing%20using%20the%20ocean%20sentinel%20instrumentation%20buoy.pdf.

Lenee-Bluhm, P., Paasch, R., Özkan-Haller, H.T., 2011, *Characterizing the wave energy*

resource of the US Pacific Northwest. Renew Energy 36, 2106-2119 p.

Lenee-Bluhm, P., 2010, *The Wave Energy Resource of the US Pacific Northwest,* MS Thesis, Oregon State University, http://ir.library.oregonstate.edu/xmlui/handle/1957/16384.

Li, N. and Cheung, K.F., 2014, *Wave Energy Resource Characterization at the US Navy Wave Energy Test Site and Other Locations in Hawai'i.* Technical Report November 2014. http://hinmrec.hnei.hawaii.edu/.

Li, N., Cheung, K.F., Stopa, J.E., Hisao, F., Chen, Y.-L., Vega, L., Cross, P., 2015, *Thirty-four Years of Hawaii Wave Hindcast from Downscaling of Climate Forecast System Reanalysis.* Ocean Modeling, In review.

Mackay, E., 2011. Modeling and description of omnidirectional wave spectra, In: Proceedings of the 9th Europeam Wave and Tidal Conference, Japan.

Nair, B., Shendure, R., Nachlas, J., Gill, A., Murphree, Z., Campbell, J., Challa, V., Thomson, J., Talbert, J., deKlerk, A., Rusch, C. 2013. Low-Cost Utility-Scale Wave Energy Enabled by Magnetostriction. 1st Marine Energy Technology Symposium, April 2013, Washington, D.C.

National Data Buoy Center, "Station 44014 (LLNR 550) - Virginia Beach 64 NM East of Virginia Beach, VA" http://www.ndbc.noaa.gov/station_page.php?station=44014.

National Data Buoy Center, "Station 44095 - Oregon Inlet, NC - 192" http://www.ndbc.noaa.gov/station_page.php?station=44095.

National Data Buoy Center, "Station 46022 (LLNR 500) - Eel River 17 NM WSW of Eureka, CA" http://www.ndbc.noaa.gov/station_page.php?station=46022.

National Data Buoy Center, "Station 46094 - Buoy NH-10 - West of Newport, OR" http://www.ndbc.noaa.gov/station_page.php?station=46094.

National Data Buoy Center, "Station 46212 - Humboldt Bay South Spit, CA (128)" http://www.ndbc.noaa.gov/station_page.php?station=46212.

National Data Buoy Center, "Station 46218 - Harvest, CA (071)" http://www.ndbc.noaa.gov/station_page.php?station=46218.

National Data Buoy Center, "Station 51202 Mokapu Point, HI (098)" http://www.ndbc.noaa.gov/station_page.php?station=51202.

National Data Buoy Center, "Station 51207 Kaneohe Bay, HI (198)" http://www.ndbc.noaa.gov/station_page.php?station=51207.

National Data Buoy Center, "Station MOKH1 1612480 Mokuoloe, HI" http://www.ndbc.noaa.gov/station_page.php?station=mokh1.

National Data Buoy Center, "Station NWPO3 - Newport, OR" http://www.ndbc.noaa.gov/

station_page.php?station=NWPO3.

National Data Buoy Center, "Station PTGC1 - Point Arguello, CA" http://www.ndbc.noaa.gov/station_page.php?station=PTGC1.

National Oceanic Atmospheric Administration, "OSCAR: Ocean Surface Current Analysis-Real Time." Accessed June 26, 2014. http://www.oscar.noaa.gov/index.html.

NNMREC (Northwest National Marine Renewable Energy Center), Oregon State University. "Northwest National Marine Renewable Energy Center." Accessed July 14th, 2014. http://nnmrec.oregonstate.edu/.

NNMREC (Northwest National Marine Renewable Energy Center), Oregon State University. "Northwest National Marine Renewable Energy Center." Accessed March 3rd, 2015. http://nnmrec.oregonstate.edu/.

NNMREC (Northwest National Marine Renewable Energy Center), Oregon State University. "Northwest National Marine Renewable Energy Center – South Energy Test Site." Accessed March 3rd, 2015. http://nnmrec.oregonstate.edu/facilities/pmec-sets.

O'Connor, M, Holmes, B., *EquiMar D4.3 Test Sites Catalogue,* April 2011.

Oregon State University, "Northwest National Marine Renewable Energy Center." Accessed July 14, 2014. http://nnmrec.oregonstate.edu/pmec-facilities.

Office of Coast Survey, *Chart 19357.* National Ocean and Atmospheric Association, printed March 1, 2013, accessed August 1, 2014. http://www.nauticalcharts.noaa.gov/staff/chartpubs.html

Office of Coast Survey, *Chart 18620.* National Ocean and Atmospheric Association, printed February 1, 2012, accessed August 1, 2014. http://www.nauticalcharts.noaa.gov/staff/chartspubs.html.

Office of Coast Survey, *Chart 18622.* National Ocean and Atmospheric Association, printed June 1, 2010, accessed August 1, 2014. http://www.nauticalcharts.noaa.gov/staff/chartspubs.html.

Office of Coast Survey, *Chart 18561.*, National Ocean and Atmospheric Association, printed December 1, 2011, accessed August 1, 2014. http://www.nauticalcharts.noaa.gov/staff/chartspubs.html.

Port of Newport. "South Beach Marina." Accessed July 28, 2014. http://www.portofnewport.com/recreational-marina/.

Port of Toledo, "Yaquina Boatyard." Accessed July 24, 2014. http://portoftoledo.org/yaquina-boatyard/.

Ruggiero, P., Komar, P.D., Allan, J.C., 2010, *Increasing wave heights and extreme value projections: The wave climate of the U.S. Pacific Northwest.* Coastal Engineering, 57:5,

539-552 p.

State of Hawaii Division of Boating and Ocean Recreation, "Heeia Kea Small Boat Harbor." Accessed July 21, 2014. http://state.hi.us/dlnr/dbor/oahuharbors/heeiahrbr.htm.

Saha, Suranjana, and Coauthors, 2010: *The NCEP Climate Forecast System Reanalysis.* Bull. Amer. Meteor. Soc., 91, 1015-1057 p. doi: 10.1175/2010BAMS3001.1

Saha, Suranjana and Coauthors, 2014: *The NCEP Climate Forecast System Version 2.* J. Climate, 27, 2185-2208 p. doi: http://dx.doi.org/10.1175/JCLI-D-12-00823.1.

Stopa, J.E., Filipot, J.-F., Li, N., Cheung, K.F., Chen, Y.-L., Vega, L., 2013, *Wave energy resources along the Hawaiian Island chain,* Renew Energy 55, 305-321 p.

Thomson, J., Observations of wave breaking dissipation from a SWIFT drifter, J. Atmos. & Ocean. Tech., 29, (2012).

Thomson, J. J.R. Gemmrich, and A.T. Jessup, Energy dissipation and the spectral distribution of whitecaps, Geophys. Res. Let., 36 (2009).

UNC Coastal Studies Institute. E-mail correspondence with Billy Edge, Brian Blanton, and Lindsay Dubbs, 2015.

United States Army Corps of Engineers, "Field Research Facility" (FRF). Accessed March 2015. http://www.frf.usace.army.mil/frf.shtml.

United States Army Corps of Engineers Field Research Facility, "Report for station wvrdr430". Accessed March 2015. http://www.frf.usace.army.mil/realtime.shtml?staid=wvrdr430&dirg=1.

U.S. Census Bureau, *Newport (city) Oregon,* State & County QuickFacts, 2012. Retrieved from http://quickfacts.census.gov/qfd/states/41/4152450.html.

Williams, R.B, Davy, D.M., Sheppard, C., Thomson, J., West, A., Toman, W.I, 2015, *Final Report of the Feasibility Study for the California Wave Energy Test Center (CalWavesm) Final Report.* DOE Contract DE-EE0006517. Cal Poly Corporation, Institute of Advanced Technology and Public Policy, California Polytechnic University, San Luis Obispo, California. July 2015.

Winterstein, S.R., Ude, T.C., Cornell, C.A., Bjerager, P., Haver, S., *Environmental Parameters for Extreme Response: Inverse FORM with Omission Factors,* Proceedings of ICOSSAR-93, Innsbruck, Austria, 1993.

Vega, Luis: University of Hawaii, e-mail correspondence, July 23 – August 29, 2014.

DISTRIBUTION:

1	MS 1124	Ann R. Dallman, 6122
1	MS 1124	Vincent S. Neary, 6122
1	MS 0899	Technical Library, 9536 (electronic copy)

Appendix A: PACIFIC MARINE ENERGY CENTER (PMEC): NORTH ENERGY TEST SITE (NETS)

A.1. IEC TS Parameter Values

Table 9: The average, 5^{th} and 95^{th} percentiles of the six parameters at NETS (see Figure 7).

	$J[kW/m]$			$H_{m0}[m]$			$T_e[s]$		
	5%	**Mean**	**95%**	**5%**	**Mean**	**95%**	**5%**	**Mean**	**95%**
March	9.4	52.2	141.6	1.46	2.86	4.75	7.65	9.92	12.80
April	6.5	36.8	96.3	1.16	2.39	4.03	7.65	9.75	12.04
May	3.6	16.1	42.1	0.87	1.71	2.84	7.01	8.76	10.84
June	3.7	12.2	33.6	0.88	1.52	2.68	6.89	8.84	11.39
July	2.3	9.3	19.0	0.73	1.39	2.05	6.72	8.41	10.46
August	2.8	8.7	20.5	0.83	1.33	2.09	6.60	8.45	10.70
September	4.3	18.1	52.7	0.98	1.74	3.04	7.37	9.31	11.78
October	7.8	38.5	106.5	1.26	2.43	4.19	7.86	9.79	12.28
November	9.1	62.4	162.8	1.35	3.09	5.10	7.75	10.05	12.90
December	8.6	69.3	203.0	1.25	3.13	5.45	8.12	10.66	13.95
January	11.3	66.6	173.5	1.43	3.08	5.06	8.19	10.88	14.13
February	11.1	52.4	141.4	1.43	2.77	4.70	8.24	10.70	13.44

	ϵ_0			$\theta_j[^\circ]$			d_θ		
	5%	**Mean**	**95%**	**5%**	**Mean**	**95%**	**5%**	**Mean**	**95%**
March	0.33	0.43	0.54	242.5	276.0	297.5	0.82	0.91	0.96
April	0.33	0.45	0.55	252.5	280.3	297.5	0.79	0.91	0.96
May	0.32	0.43	0.55	247.5	274.6	302.5	0.80	0.89	0.95
June	0.33	0.45	0.59	242.5	272.1	302.5	0.79	0.88	0.94
July	0.34	0.45	0.56	242.5	278.6	302.5	0.75	0.86	0.93
August	0.33	0.44	0.58	252.5	279.0	302.5	0.78	0.86	0.94
September	0.31	0.43	0.57	247.5	280.6	302.5	0.81	0.89	0.95
October	0.30	0.41	0.52	247.5	281.2	302.5	0.84	0.92	0.96
November	0.29	0.41	0.51	247.5	280.2	302.5	0.83	0.92	0.97
December	0.27	0.41	0.53	237.5	276.5	297.5	0.82	0.92	0.97
January	0.28	0.42	0.53	242.5	275.4	297.5	0.85	0.93	0.97
February	0.27	0.41	0.54	237.5	276.8	302.5	0.82	0.92	0.97

A.2. Wave Roses

The annual wave rose of omnidirectional wave power, J, and direction of maximum directionally resolved wave power, θ_j, is shown in Figure 120, and essentially mirrors that for significant wave height, H_{m0}, and θ_j shown in Figure 121.

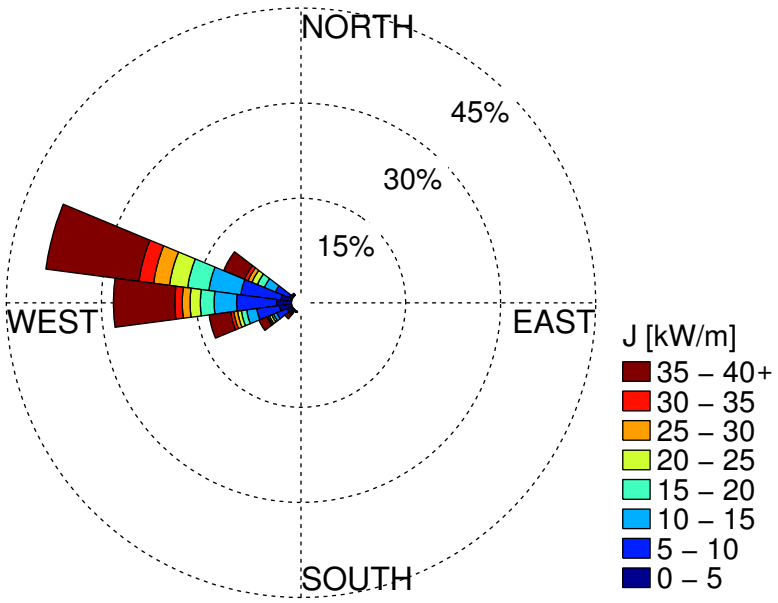

Figure 120: Annual wave rose of omnidirectional wave power and direction of maximally resolved wave power. Values of J greater than 40 kW/m are included in the top bin as shown in the legend.

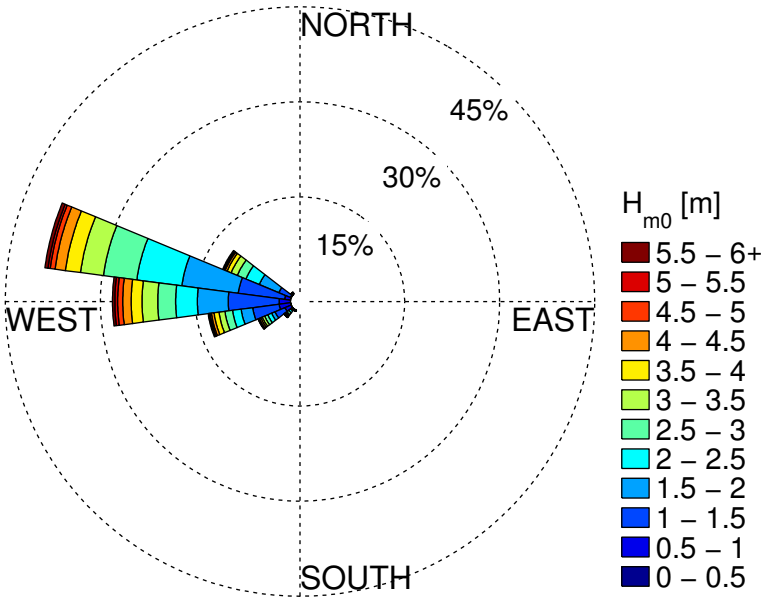

Figure 121: Annual wave rose of significant wave height and direction of maximally resolved wave power. Values of H_{m0} greater than 6 m are included in the top bin as shown in the legend.

A.3. Extreme Sea States

Table 10: Selected values along the 100-year contour for NDBC46050 (see Figure 13).

Significant wave height [m]	Energy period [s]
1	3.80
2	4.58
3	5.32
4	6.00
5	6.64
6	7.25
7	7.83
8	8.39
9	8.95
10	9.50
11	10.07
12	10.65
13	11.27
14	11.94
15	12.71
16	13.66
17	15.14
17.31	16.57
17	18.04
16	19.63
15	20.65
14	21.48
13	22.18
12	22.79
11	23.34
10	23.84
9	24.29
8	24.69
7	25.05
6	25.36
5	25.63
4	25.85
3	26.02
2	26.12
1	26.15

A.4. Wind Data

The wind data for this site (obtained from CFSR), is the mean of magnitude and direction taken at 44.5 N, 124.5 W and 45 N, 124.5 W, which are the nearest data points to NETS. Note that the central location between these two points is approximately 30 km west/northwest of the test site (Figure 1). The average monthly values, along with the 5^{th} and 95^{th} percentiles, of wind are shown in Figure 122. The values are also tabulated in Table 11. The annual and seasonal wind roses are shown in Figure 123.

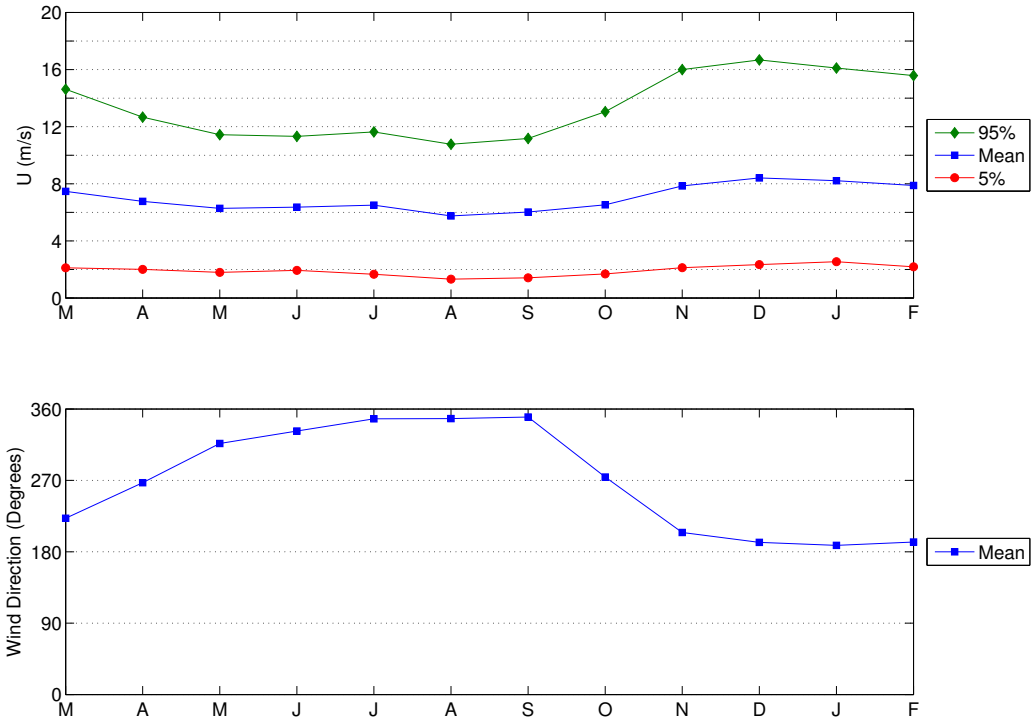

Figure 122: Monthly wind velocity and direction obtained from CSFR data during the period 1/1/1979 to 12/31/2014 at 44.75 N, 124.5 W, located 30 km west/northwest of NETS (Figure 1).

(a)

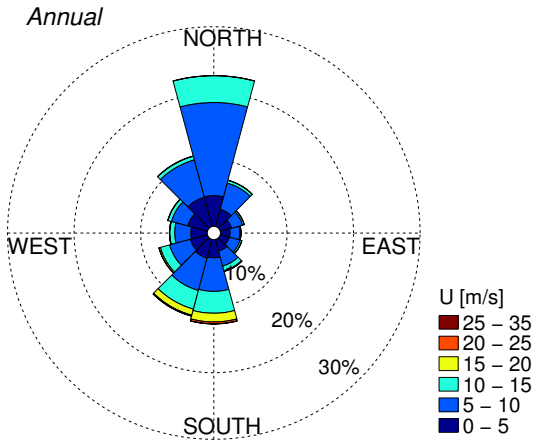

(b)

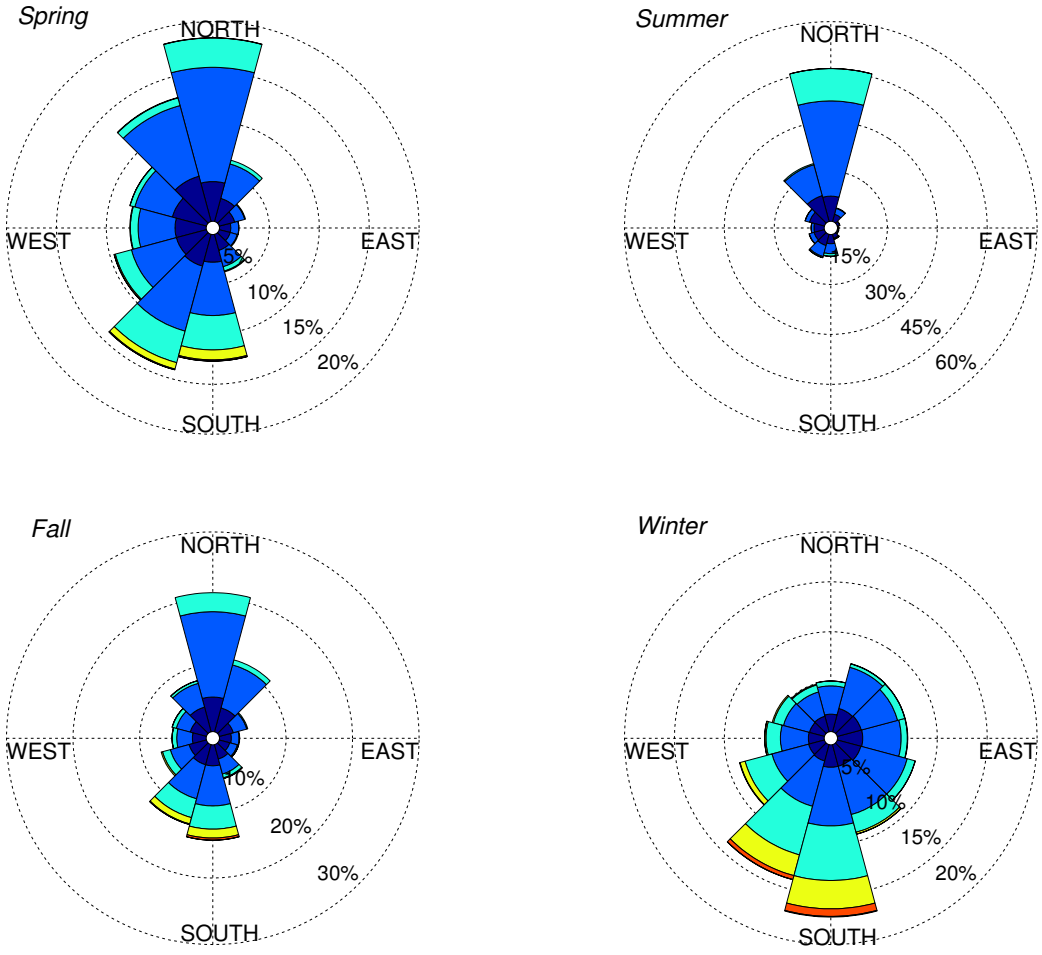

Figure 123: (a) Annual and (b) seasonal wind roses of velocity and direction obtained from CSFR data during the period 1/1/1979 to 12/31/2014. Data taken at 44.75 N, 124.5 W, located approximately 30 km west/northwest of NETS (Figure 1).

Table 11: Monthly wind velocity and direction obtained from CSFR data during the period 1/1/1979 to 12/31/2014 at 44.75 N, 124.5 W, located approximately 30 km west/northwest of NETS.

	$U[m/s]$			$Direction[^\circ]$
	5%	**Mean**	**95%**	**Mean**
March	2.1	7.5	14.6	222
April	2.0	6.8	12.7	267
May	1.8	6.3	11.4	316
June	1.9	6.4	11.3	332
July	1.7	6.5	11.6	348
August	1.3	5.7	10.8	348
September	1.4	6.0	11.2	350
October	1.7	6.5	13.0	274
November	2.1	7.8	16.0	204
December	2.3	8.4	16.7	192
January	2.5	8.2	16.1	188
February	2.2	7.9	15.6	192

A.5. Ocean Surface Current Data

The surface current data (obtained from OSCAR) used for this site is located at 44.5 N, 125.5 W. There is data located closer to the site at 44.5 N, 124.5 W, however the period of record is short (about 2 years). Data from the two years available was compared at both locations. Surface current speeds at 124.5 W are slightly higher in the summer than at 125.5 W, however overall the patterns are similar. Therefore, the data point further out (125.5 W) with the longer period of record (about 20 years) was used for consistency with the other sites. The average monthly values, along with the 5^{th} and 95^{th} percentiles, of current are shown in Figure 124. These data points are listed in Table 12. The annual and seasonal current roses are shown in Figure 125.

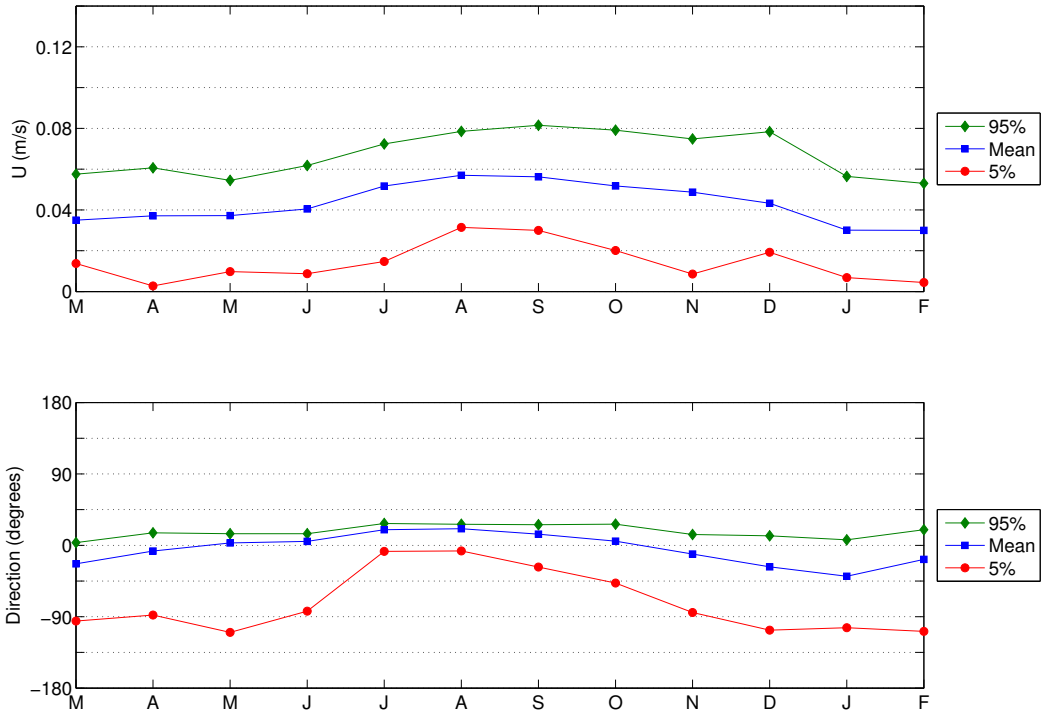

Figure 124: Monthly ocean surface current velocity and direction obtained from OSCAR at 44.5 N, 125.5 W, located approximately 110 km southwest of NETS. Data period 1/1/1993 to 12/30/2014.

(a)

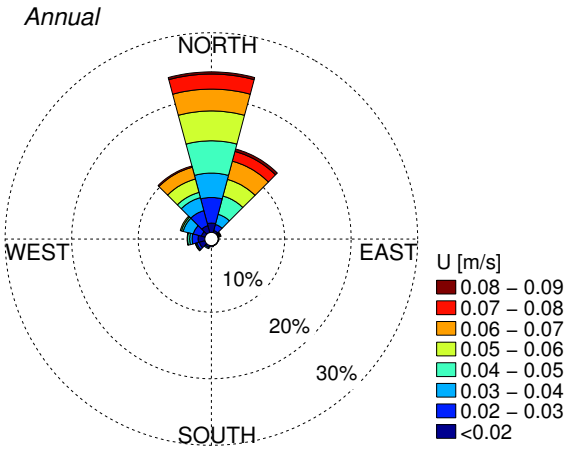

(b)

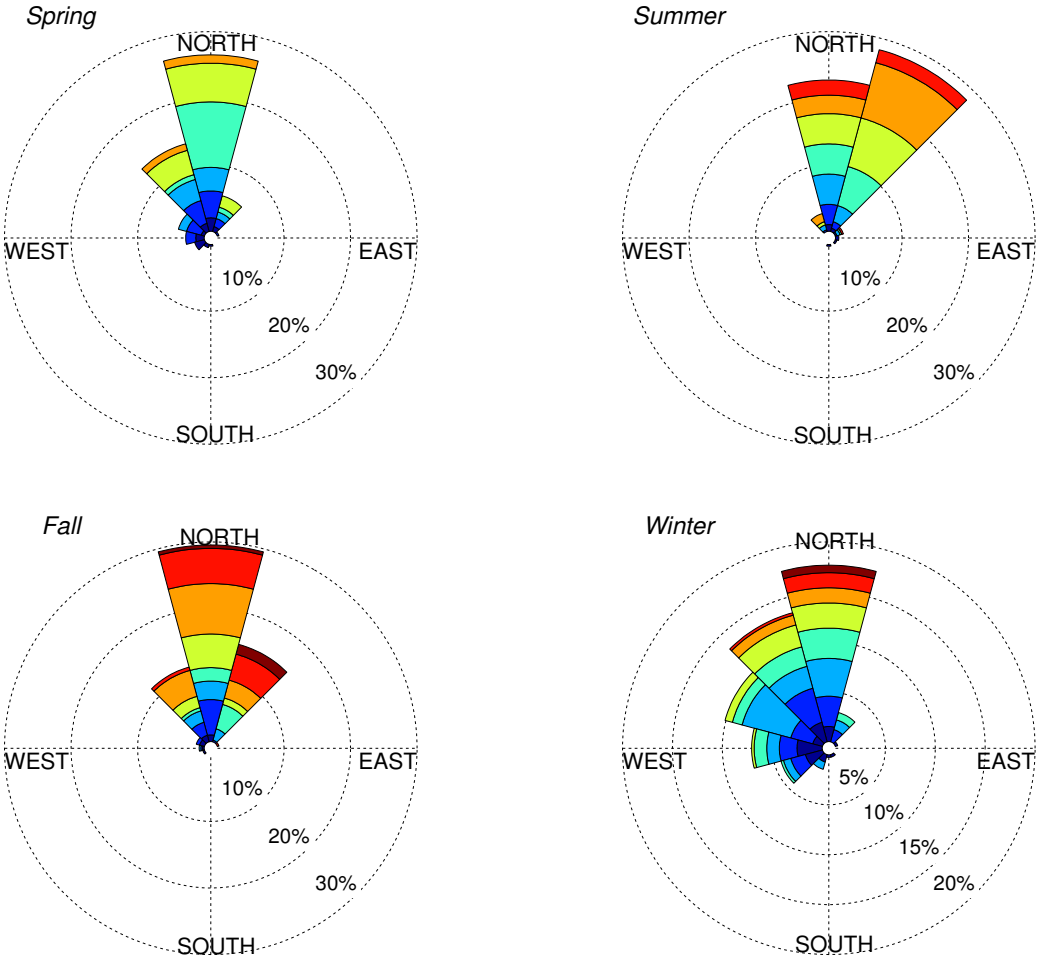

Figure 125: (a) Annual and (b) seasonal current roses of ocean surface current velocity and direction obtained from OSCAR at 44.5 N, 125.5 W. Data period 1/1/1993 to 12/30/2014.

Table 12: Monthly surface current velocity and direction obtained from OSCAR data during the period 1/1/1993 to 12/30/2014 at 44.5 N, 125.5 W.

	$U[m/s]$			$Direction[^\circ]$		
	5%	**Mean**	**95%**	**5%**	**Mean**	**95%**
March	0.014	0.035	0.058	-95	-23	3
April	0.003	0.037	0.061	-88	-7	16
May	0.010	0.037	0.055	-110	3	15
June	0.009	0.040	0.062	-83	5	15
July	0.015	0.052	0.072	-8	20	28
August	0.031	0.057	0.079	-7	21	27
September	0.030	0.056	0.082	-27	14	26
October	0.020	0.052	0.079	-48	5	27
November	0.009	0.049	0.075	-85	-11	14
December	0.019	0.043	0.078	-107	-27	12
January	0.007	0.030	0.056	-104	-39	7
February	0.004	0.030	0.053	-108	-18	20

Appendix B: U.S. NAVY WAVE ENERGY TEST SITE (WETS)

B.1. IEC TS Parameter Values

Table 13: The average, 5^{th} and 95^{th} percentiles of the six parameters at Kaneohe II (see Figure 23).

	$J[kW/m]$			$H_{m0}[m]$			$T_e[s]$		
	5%	**Mean**	**95%**	**5%**	**Mean**	**95%**	**5%**	**Mean**	**95%**
March	4.0	18.1	47.5	0.93	1.85	3.07	6.8	8.7	11.8
April	3.9	14.1	33.1	1.01	1.76	2.68	6.4	7.9	10.5
May	2.5	8.6	18.9	0.82	1.45	2.17	6.1	7.3	9.3
June	2.6	6.9	13.1	0.90	1.41	1.94	5.7	6.6	8.1
July	3.0	7.4	14.2	0.97	1.46	2.00	5.7	6.6	7.6
August	2.4	6.6	13.3	0.87	1.36	1.91	5.6	6.6	8.0
September	2.7	7.3	15.4	0.88	1.33	1.88	6.0	7.4	9.8
October	4.1	11.3	25.9	1.00	1.55	2.27	6.4	8.2	11.1
November	5.1	19.0	50.6	1.09	1.87	2.99	6.9	8.9	12.0
December	5.0	19.7	50.6	1.02	1.87	3.05	7.1	9.5	12.7
January	4.6	18.1	46.3	0.95	1.76	2.90	7.2	9.7	13.0
February	4.6	18.2	46.5	0.98	1.80	2.92	7.0	9.3	12.4

	ϵ_0			$\theta_j[^\circ]$			d_θ		
	5%	**Mean**	**95%**	**5%**	**Mean**	**95%**	**5%**	**Mean**	**95%**
March	0.29	0.38	0.51	-22.5	23.4	67.5	0.66	0.82	0.94
April	0.28	0.37	0.49	-7.5	34.4	67.5	0.67	0.81	0.91
May	0.28	0.37	0.48	-7.5	40.2	67.5	0.68	0.82	0.92
June	0.31	0.37	0.46	22.5	50.9	67.5	0.71	0.84	0.91
July	0.31	0.35	0.43	37.5	53.3	67.5	0.78	0.87	0.91
August	0.30	0.36	0.45	37.5	54.3	67.5	0.74	0.86	0.91
September	0.28	0.38	0.49	-7.5	36.7	67.5	0.71	0.82	0.91
October	0.27	0.38	0.51	-7.5	25.2	52.5	0.69	0.81	0.93
November	0.27	0.38	0.50	-7.5	22.6	67.5	0.68	0.82	0.93
December	0.28	0.38	0.50	-22.5	16.6	67.5	0.67	0.82	0.94
January	0.29	0.38	0.50	-22.5	10.4	67.5	0.67	0.84	0.95
February	0.28	0.38	0.52	-22.5	15.0	67.5	0.66	0.83	0.95

Table 14: The average, 5^{th} and 95^{th} percentiles of the six parameters at WETS (see Figure 24).

	$J[kW/m]$			$H_{m0}[m]$			$T_e[s]$		
	5%	**Mean**	**95%**	**5%**	**Mean**	**95%**	**5%**	**Mean**	**95%**
March	4.4	20.1	52.5	1.00	1.98	3.29	6.81	8.70	11.72
April	4.5	15.9	36.5	1.08	1.89	2.88	6.46	7.93	10.38
May	2.8	9.8	21.1	0.88	1.57	2.35	6.09	7.30	9.33
June	3.1	8.1	15.4	0.97	1.52	2.10	5.75	6.68	8.11
July	3.5	8.6	16.7	1.04	1.57	2.17	5.79	6.63	7.71
August	2.8	7.7	15.6	0.94	1.47	2.08	5.67	6.65	8.10
September	3.1	8.2	17.4	0.94	1.43	2.02	6.01	7.43	9.73
October	4.5	12.4	27.7	1.06	1.65	2.41	6.46	8.22	11.09
November	5.8	20.8	53.9	1.17	2.00	3.17	6.95	8.89	11.92
December	5.6	21.7	54.7	1.09	2.00	3.24	7.19	9.44	12.63
January	5.0	19.7	49.9	1.01	1.86	3.06	7.26	9.73	12.89
February	5.1	19.8	49.7	1.04	1.91	3.08	7.08	9.33	12.39

	ϵ_0			$\theta_j[^\circ]$			d_θ		
	5%	**Mean**	**95%**	**5%**	**Mean**	**95%**	**5%**	**Mean**	**95%**
March	0.28	0.38	0.50	-22.5	28.4	67.5	0.64	0.81	0.94
April	0.27	0.36	0.48	-7.5	39.8	67.5	0.66	0.80	0.91
May	0.28	0.36	0.47	-7.5	45.5	82.5	0.67	0.81	0.92
June	0.30	0.36	0.45	22.5	55.9	67.5	0.70	0.84	0.92
July	0.30	0.35	0.42	37.5	58.2	67.5	0.78	0.87	0.91
August	0.30	0.35	0.44	37.5	59.9	67.5	0.74	0.86	0.92
September	0.28	0.37	0.48	-7.5	41.5	67.5	0.69	0.82	0.91
October	0.27	0.37	0.50	-7.5	29.6	67.5	0.67	0.80	0.93
November	0.26	0.37	0.49	-7.5	27.5	67.5	0.66	0.81	0.93
December	0.27	0.37	0.49	-22.5	21.6	67.5	0.65	0.81	0.94
January	0.28	0.37	0.49	-22.5	14.5	67.5	0.65	0.83	0.95
February	0.27	0.37	0.51	-22.5	19.2	67.5	0.64	0.82	0.95

B.2. Wave Roses

The annual wave rose of omnidirectional wave power, J, and direction of maximum directionally resolved wave power, θ_j, is shown in Figure 126, and essentially mirrors that for significant wave height, H_{m0}, and θ_j shown in Figure 127.

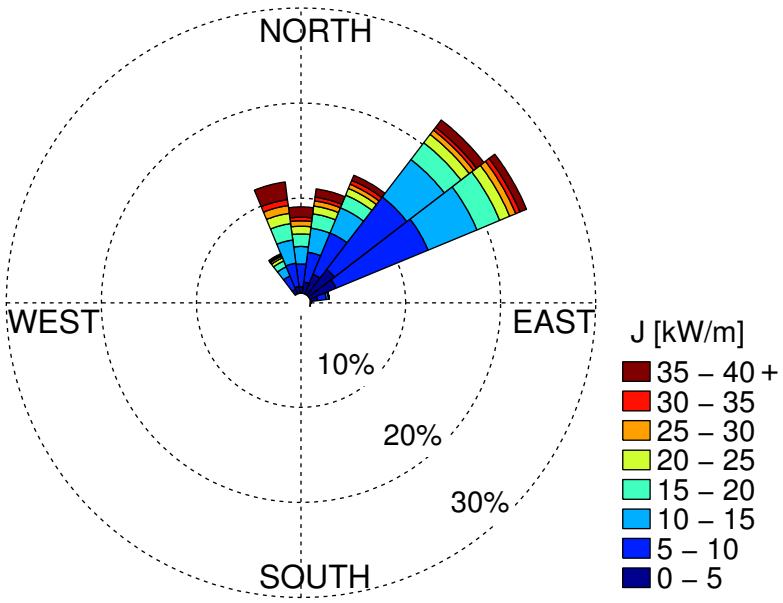

Figure 126: Annual wave rose of omnidirectional wave power and direction of maximum directionally resolved wave power. Values of J greater than 40 kW/m are included in the top bin as shown in the legend. Figure produced by Ning Li (Li and Cheung 2014).

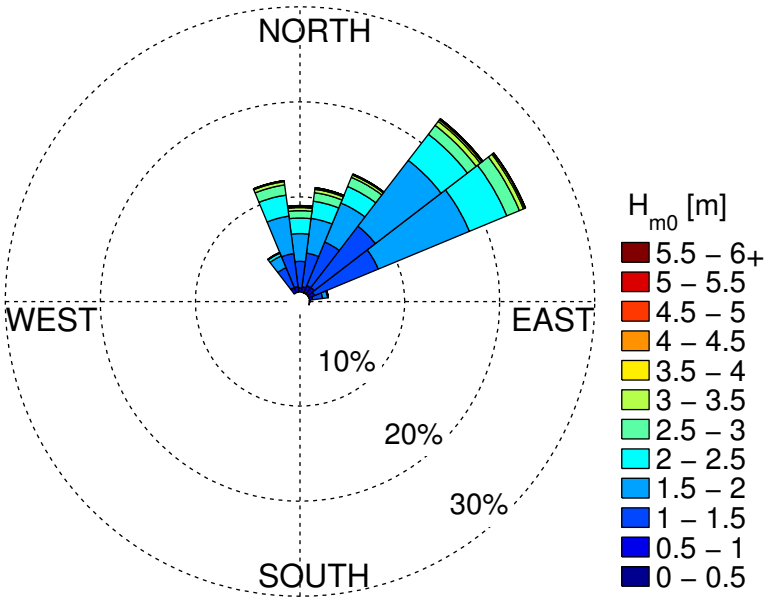

Figure 127: Annual wave rose of significant wave height and direction of maximum directionally resolved wave power. Values of H_{m0} greater than 6 m are included in the top bin as shown in the legend. Figure produced by Ning Li (Li and Cheung 2014).

B.3. Extreme Sea States

Table 15: Selected values along the 100-year contour for CDIP098 (NDBC 51202) (see Figure 30).

Significant wave height [m]	Energy period [s]
1	4.24
2	4.17
3	5.72
4	7.11
5	8.44
6	9.85
7	11.74
7.24	12.98
7	14.05
6	15.18
5	15.72
4	16.05
3	16.24
2	16.31
1	16.25

B.4. Wind Data

The wind data for this site (obtained from CFSR), is taken at 21.5 N, 157.5 W located approximately 25 km east of WETS (Figure 20), which is the nearest data point to the site. The average monthly values, along with the 5^{th} and 95^{th} percentiles, of wind are shown in Figure 128. The values are also tabulated in Table 16. The annual and seasonal wind roses are shown in Figure 129.

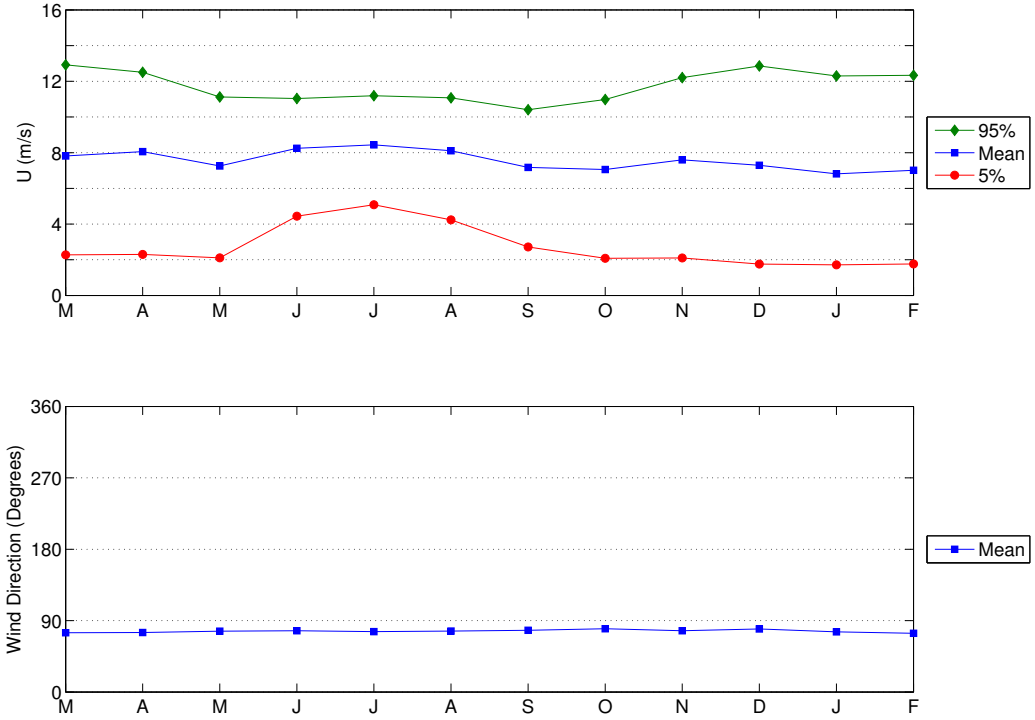

Figure 128: Monthly wind velocity and direction obtained from CSFR data during the period 1/1/1979 to 12/31/2014 at 21.5 N, 157.5 W, located approximately 25 km east of WETS (Figure 20).

(a)

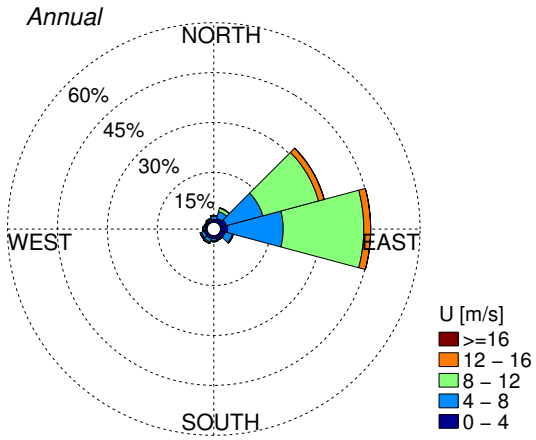

(b)

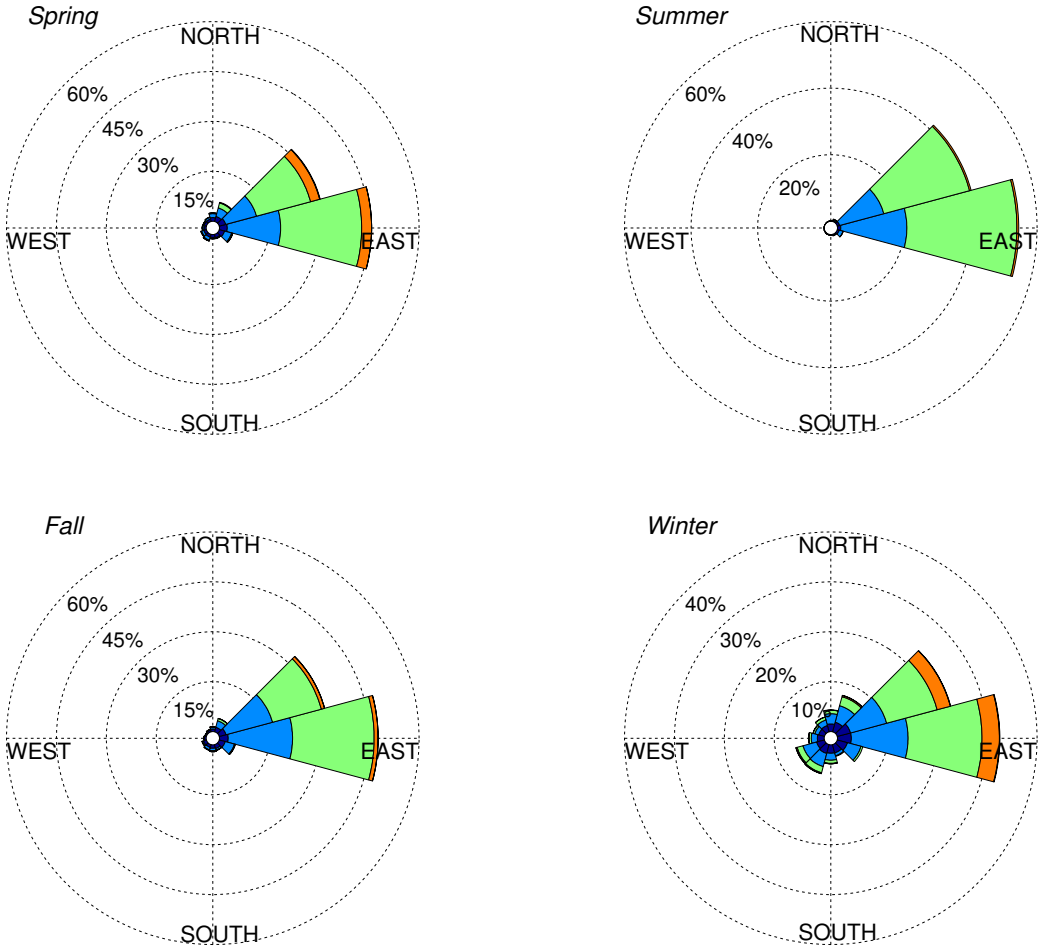

Figure 129: (a) Annual and (b) seasonal wind roses of velocity and direction obtained from CSFR data during the period 1/1/1979 to 12/31/2014. Data taken at 21.5 N, 157.5 W, located approximately 25 km east of WETS (Figure 20).

Table 16: Monthly wind velocity and direction obtained from CSFR data during the period 1/1/1979 to 12/31/2014 at 21.5 N, 157.5 W, located approximately 25 km east of WETS.

	$U[m/s]$			$Direction[^\circ]$
	5%	**Mean**	**95%**	**Mean**
March	2.3	7.8	12.9	75
April	2.3	8.1	12.5	75
May	2.1	7.3	11.1	77
June	4.4	8.2	11.0	77
July	5.1	8.4	11.2	76
August	4.2	8.1	11.1	77
September	2.7	7.2	10.4	78
October	2.1	7.1	11.0	80
November	2.1	7.6	12.2	77
December	1.8	7.3	12.9	79
January	1.7	6.8	12.3	76
February	1.8	7.0	12.3	74

B.5. Ocean Surface Current Data

The surface current data (obtained from OSCAR), is located at 21.5 N, 157.5 W, the closest data point to shore. The average monthly values, along with the 5^{th} and 95^{th} percentiles, of current are shown in Figure 130. These data points are listed in Table 17. The annual and seasonal current roses are shown in Figure 131.

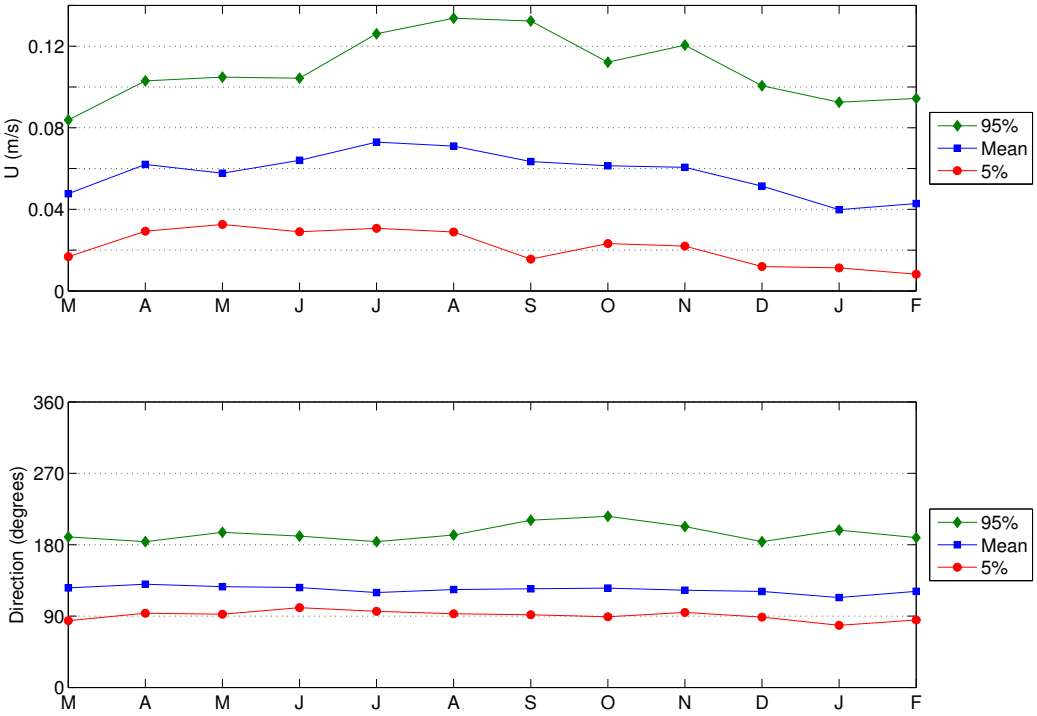

Figure 130: Monthly ocean surface current velocity and direction obtained from OSCAR at 21.5 N, 157.5 W, located approximately 25 km east of WETS. Data period 1/1/1993 to 12/30/2014.

(a)

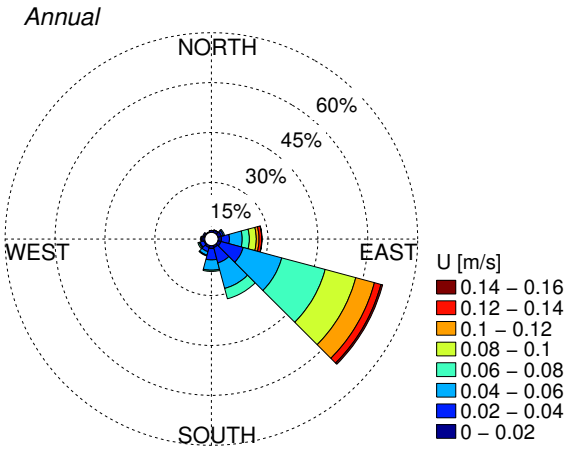

(b)

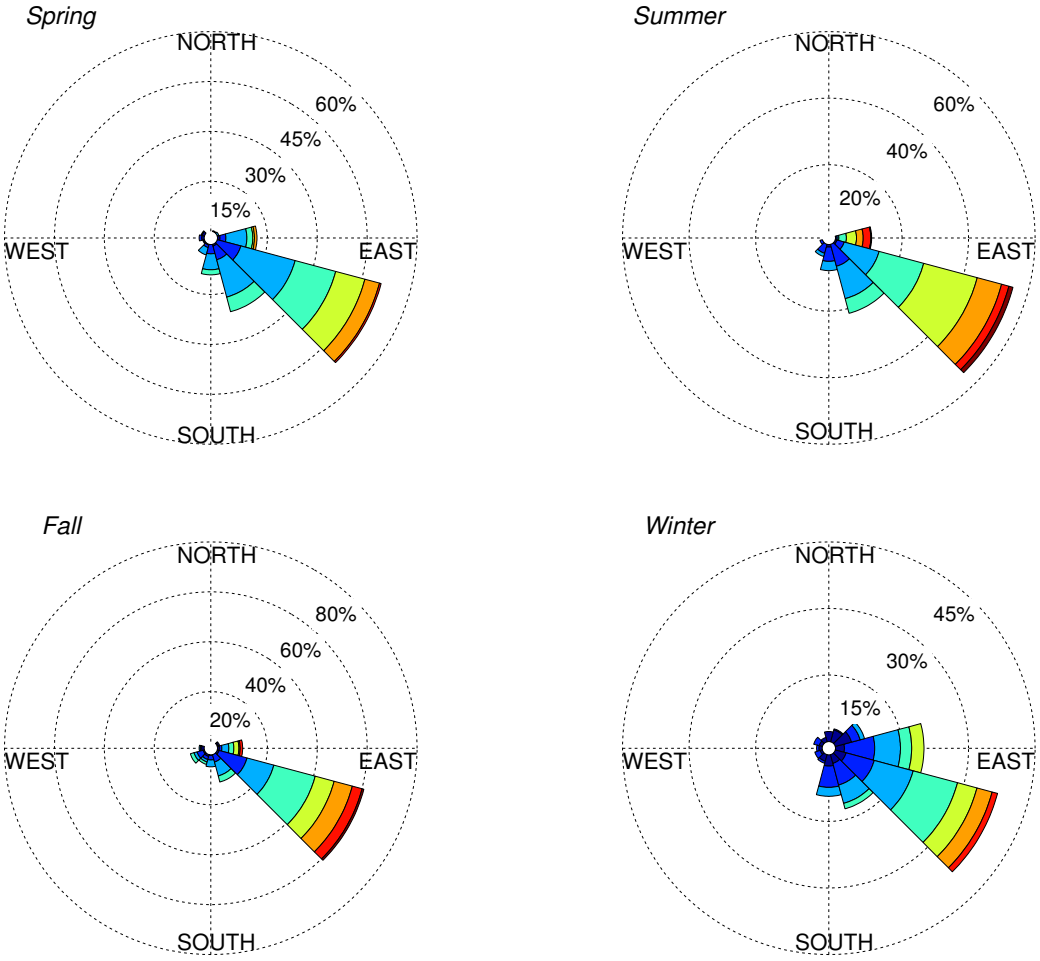

Figure 131: (a) Annual and (b) seasonal current roses of ocean surface current velocity and direction obtained from OSCAR at 21.5 N, 157.5 W, located approximately 25 km east of WETS. Data period 1/1/1993 to 12/30/2014.

Table 17: Monthly surface current velocity and direction obtained from OSCAR data during the period 1/1/1993 to 12/30/2014 at 21.5 N, 157.5 W, located approximately 25 km east of WETS.

	$U[m/s]$			$Direction[^\circ]$		
	5%	**Mean**	**95%**	**5%**	**Mean**	**95%**
March	0.017	0.048	0.084	84	126	190
April	0.029	0.062	0.103	94	130	184
May	0.033	0.058	0.105	92	127	196
June	0.029	0.064	0.104	101	126	191
July	0.031	0.073	0.126	96	120	184
August	0.029	0.071	0.134	93	123	192
September	0.016	0.063	0.132	92	124	211
October	0.023	0.062	0.112	89	125	216
November	0.022	0.061	0.121	95	122	202
December	0.012	0.052	0.099	88	122	183
January	0.011	0.040	0.093	78	113	198
February	0.008	0.043	0.094	85	121	189

Appendix C: JENNETTE'S PIER WAVE ENERGY TEST CENTER

C.1. IEC TS Parameter Values

Table 18: The average, 5^{th} and 95^{th} percentiles of the six parameters at Jennette's Pier (see Figure 37).

	$J[kW/m]$			$H_{m0}[m]$			$T_e[s]$		
	5%	**Mean**	**95%**	**5%**	**Mean**	**95%**	**5%**	**Mean**	**95%**
March	0.80	9.07	31.42	0.50	1.28	2.56	4.74	7.08	10.35
April	0.57	5.83	20.03	0.43	1.04	2.15	4.67	6.74	9.54
May	0.46	4.19	14.25	0.39	0.88	1.88	4.61	6.42	8.68
June	0.39	1.90	5.83	0.36	0.68	1.28	4.51	6.06	7.60
July	0.35	1.41	3.03	0.33	0.59	0.97	4.63	6.06	7.49
August	0.36	3.00	8.54	0.35	0.74	1.48	4.48	6.06	8.35
September	0.56	7.35	28.90	0.43	1.11	2.52	4.58	6.67	10.30
October	0.57	8.06	31.62	0.44	1.19	2.62	4.59	6.61	9.83
November	0.60	8.04	24.05	0.43	1.21	2.34	4.72	6.80	9.84
December	0.69	8.12	28.45	0.47	1.24	2.49	4.73	6.82	9.88
January	0.72	7.74	26.58	0.46	1.24	2.46	4.87	6.85	9.50
February	0.88	8.41	32.16	0.51	1.27	2.63	4.89	6.97	9.84

	ϵ_0			$\theta_j[^\circ]$			d_θ		
	5%	**Mean**	**95%**	**5%**	**Mean**	**95%**	**5%**	**Mean**	**95%**
March	0.24	0.35	0.46	25	73.1	115	0.72	0.87	0.96
April	0.24	0.34	0.46	35	79.1	115	0.70	0.87	0.96
May	0.24	0.33	0.44	45	86.8	115	0.72	0.88	0.96
June	0.24	0.33	0.44	55	96.9	125	0.73	0.89	0.96
July	0.24	0.33	0.44	65	102.7	125	0.74	0.90	0.96
August	0.24	0.33	0.44	55	93.7	115	0.75	0.89	0.96
September	0.24	0.34	0.46	45	81.6	115	0.73	0.88	0.96
October	0.24	0.34	0.45	35	73.2	115	0.72	0.88	0.96
November	0.25	0.35	0.46	25	70.3	115	0.70	0.87	0.96
December	0.25	0.36	0.47	15	65.6	115	0.68	0.86	0.95
January	0.25	0.36	0.47	15	66.6	115	0.68	0.85	0.95
February	0.24	0.35	0.47	25	68.8	115	0.69	0.86	0.96

C.2. Wave Roses

The annual wave rose of omnidirectional wave power, J, and direction of maximum directionally resolved wave power, θ_j, is shown in Figure 132, and essentially mirrors that for significant wave height, H_{m0}, and θ_j shown in Figure 133.

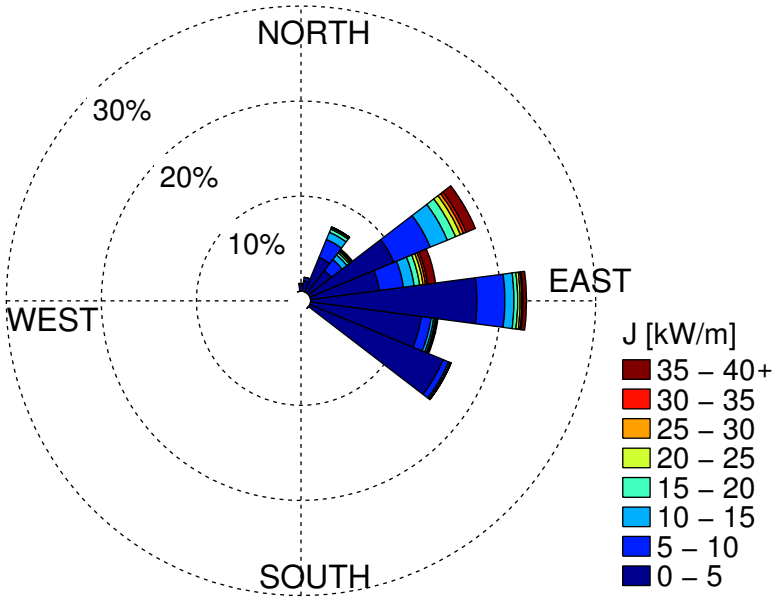

Figure 132: Annual wave rose of omnidirectional wave power and direction of maximally resolved wave power. Values of J greater than 40 kW/m are included in the top bin as shown in the legend.

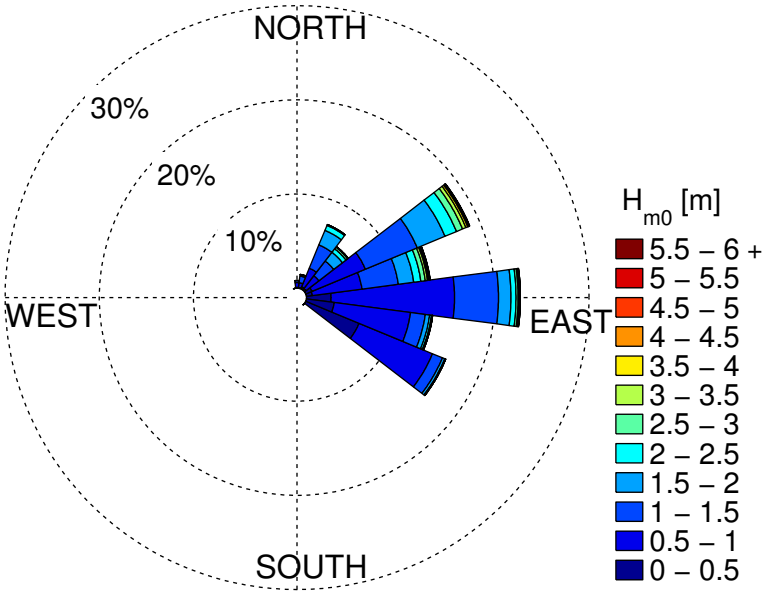

Figure 133: Annual wave rose of significant wave height and direction of maximally resolved wave power. Values of H_{m0} greater than 6 m are included in the top bin as shown in the legend.

C.3. Extreme Sea States

Table 19: Estimates of extreme significant wave height values using the generalized extreme value distribution (see Figure 43).

Return period [years]	Significant wave height [m]
10	6.23
25	6.79
50	7.19
100	7.55

Table 20: Estimates of extreme significant wave height values using the peak over thresholds method (see Figure 44).

Return period [years]	Significant wave height [m]
10	7.34
25	7.81
50	8.14
100	8.46

C.4. Wind Data

The wind data for this site (obtained from CFSR), is taken at 36 N, 75.5 W located approximately 12 km northeast of the site (Figure 35, which is the nearest data point to the site). The average monthly values, along with the 5^{th} and 95^{th} percentiles, of wind are shown in Figure 134. The values are also tabulated in Table 21. The annual and seasonal wind roses are shown in Figure 135.

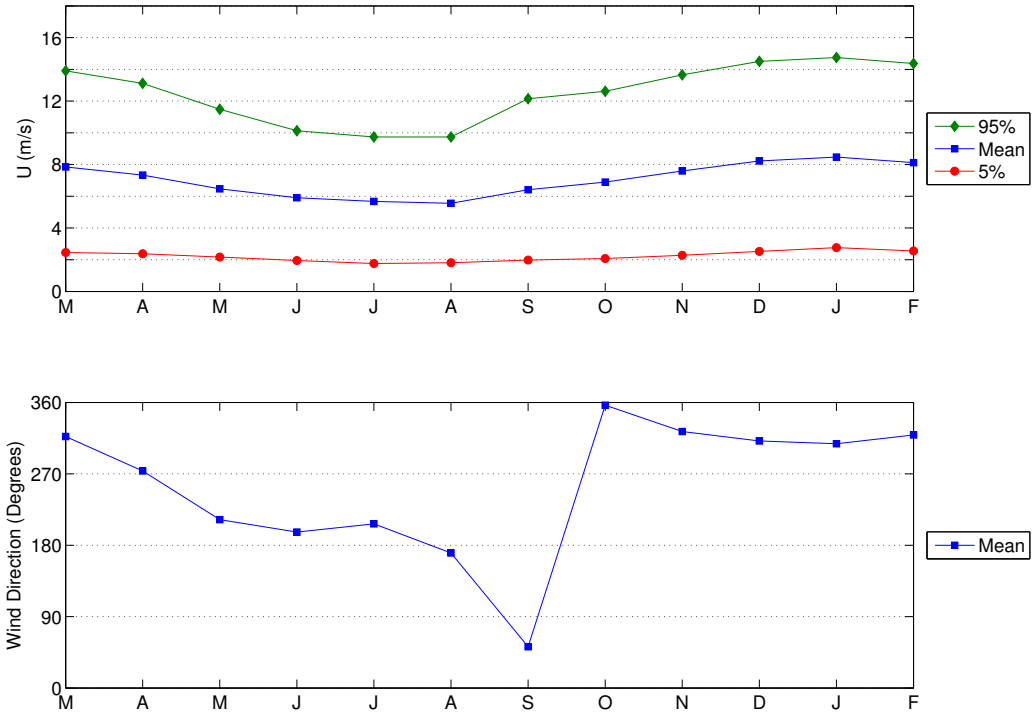

Figure 134: Monthly wind velocity and direction obtained from CSFR data during the period 1/1/1979 to 12/31/2014 at 36 N, 75.5 W, located approximately 12 km northeast of the the Jennette's Pier site (Figure 35).

(a)

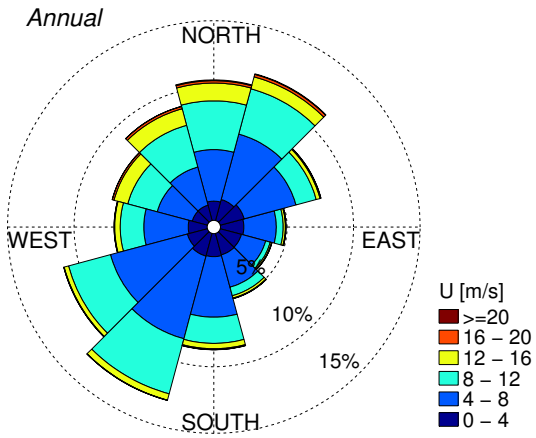

(b)

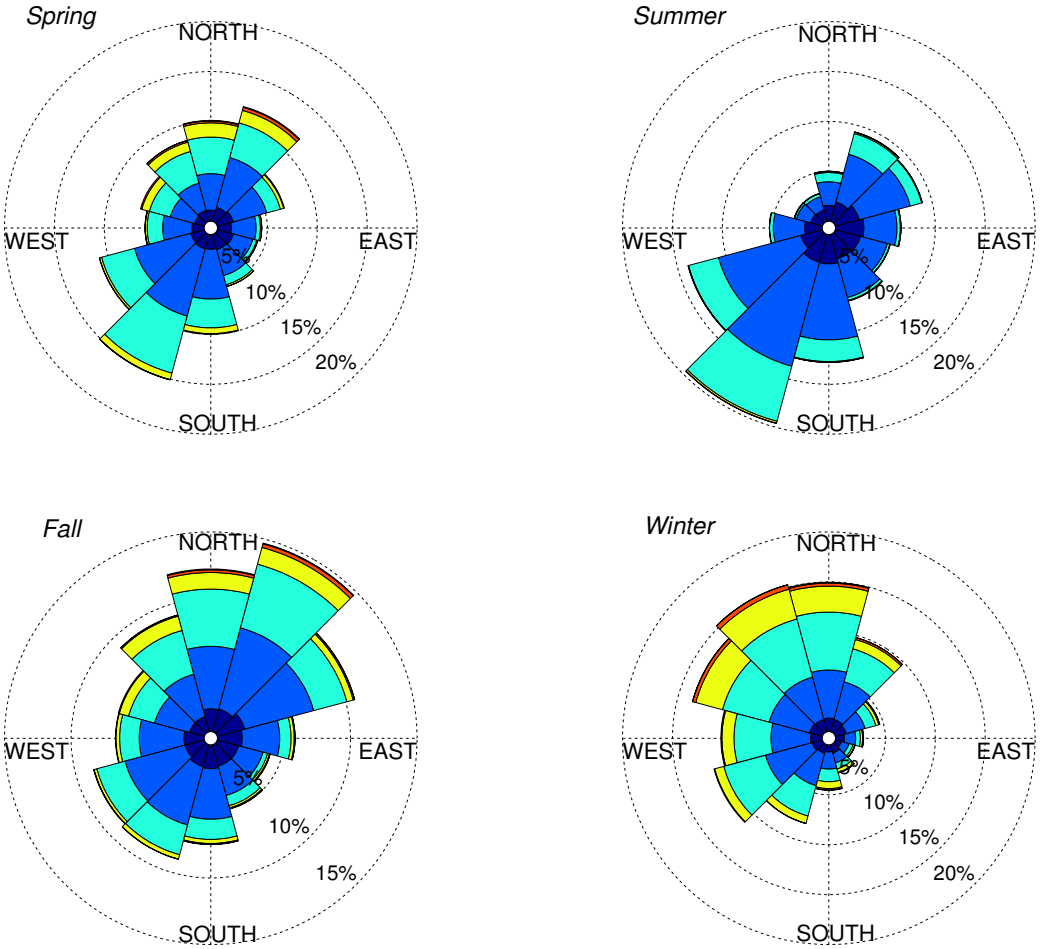

Figure 135: (a)Annual and (b) seasonal wind roses of velocity and direction obtained from CSFR data during the period 1/1/1979 to 12/31/14. Data taken at 36 N, 75.5 W, located approximately 12 km northeast of the the Jennette's Pier site (Figure 35).

Table 21: Monthly wind velocity and direction obtained from CSFR data during the period 1/1/1979 to 12/31/2014 at 36 N, 75.5 W, located approximately 12 km northeast of Jennette's Pier.

	$U[m/s]$			$Direction[^\circ]$
	5%	**Mean**	**95%**	**Mean**
March	2.5	7.8	13.9	317
April	2.4	7.3	13.1	274
May	2.2	6.5	11.5	212
June	1.9	5.9	10.1	197
July	1.8	5.7	9.7	207
August	1.8	5.6	9.7	170
September	2.0	6.4	12.1	52
October	2.1	6.9	12.6	357
November	2.3	7.6	13.7	323
December	2.5	8.2	14.5	311
January	2.8	8.5	14.7	308
February	2.6	8.1	14.4	319

C.5. Ocean Surface Current Data

The surface current data (obtained from OSCAR), is located at 36.5 N, 75.5.5 W, the closest data point to shore. The data point at 35.5 N, 75.5 W, which would be closer to the site, is located west of the Outer Banks. The average monthly values, along with the 5^{th} and 95^{th} percentiles, of current are shown in Figure 136. These data points are listed in Table 22. The annual and seasonal current roses are shown in Figure 137.

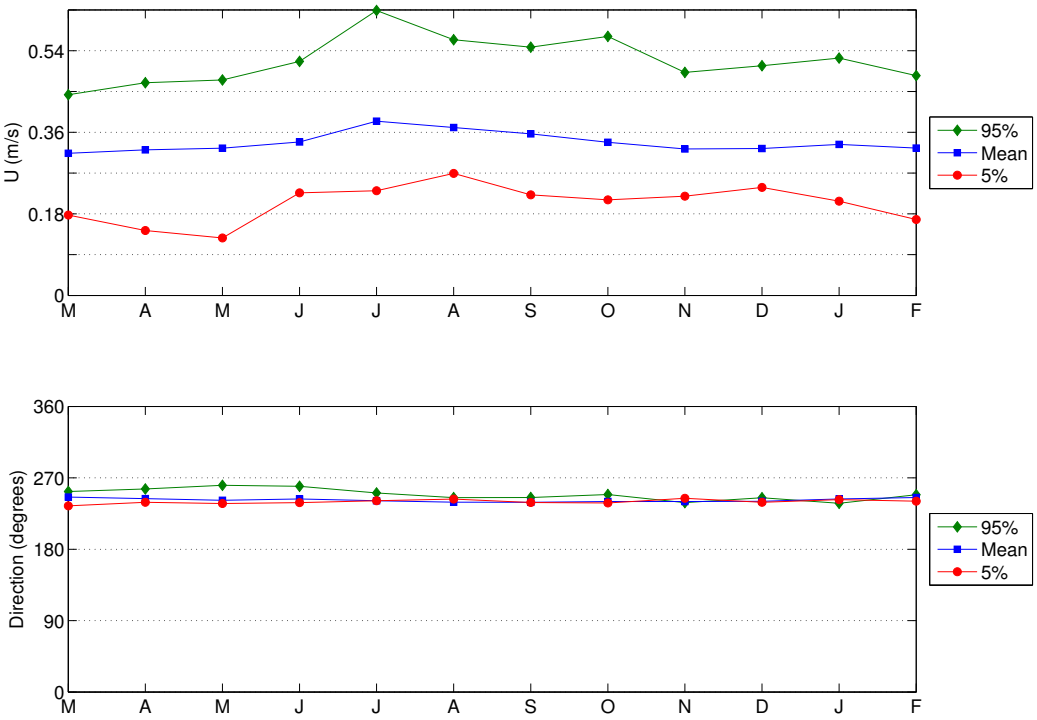

Figure 136: Monthly ocean surface current velocity and direction obtained from OSCAR at 36.5 N, 75.5 W, located approximately 60 km north/northeast of Jennette's Pier. Data period 1/1/1993 to 12/31/2014.

(a)

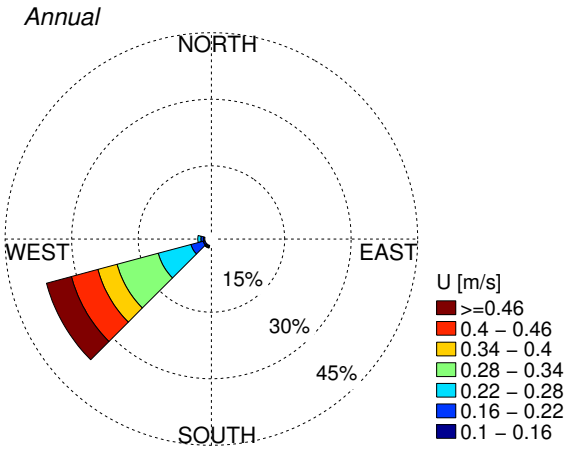

(b)

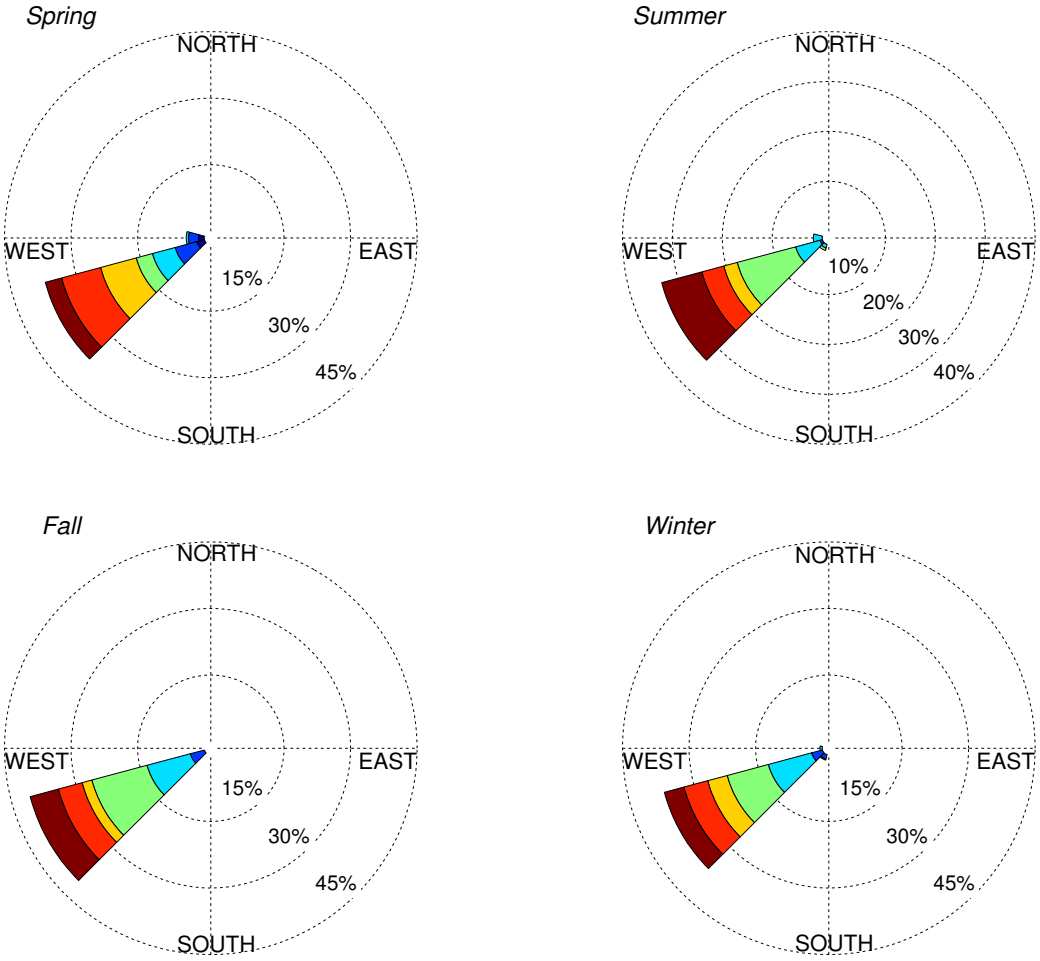

Figure 137: (a) Annual and (b) seasonal current roses of velocity and direction obtained from OSCAR at 36.5 N, 75.5 W, located approximately 60 km north/northeast of Jennette's Pier. Data period 1/1/1993 to 12/31/2014.

Table 22: Monthly surface current velocity and direction obtained from OSCAR data during the period 1/1/1993 to 12/31/2014 at 36.5 N, 75.5 W, located approximately 60 km north/northeast of Jennette's Pier.

	$U[m/s]$			$Direction[^\circ]$		
	5%	**Mean**	**95%**	**5%**	**Mean**	**95%**
March	0.177	0.314	0.443	235	246	253
April	0.143	0.321	0.469	239	244	256
May	0.127	0.325	0.476	238	242	261
June	0.226	0.339	0.516	239	243	259
July	0.231	0.385	0.629	241	241	251
August	0.269	0.370	0.564	243	239	245
September	0.222	0.357	0.548	239	239	245
October	0.211	0.338	0.572	238	240	249
November	0.219	0.323	0.492	244	240	239
December	0.238	0.324	0.507	239	241	245
January	0.208	0.333	0.524	242	243	238
February	0.168	0.325	0.485	241	245	249

Appendix D: U.S. ARMY CORPS OF ENGINEERS (USACE) FIELD RESEARCH FACILITY (FRF)

D.1. IEC TS Parameter Values

Table 23: The average, 5^{th} and 95^{th} percentiles of the six parameters at USACE FRF (see Figure 37).

	$J[kW/m]$			$H_{m0}[m]$			$T_e[s]$		
	5%	**Mean**	**95%**	**5%**	**Mean**	**95%**	**5%**	**Mean**	**95%**
March	0.54	4.54	13.05	0.45	1.07	1.93	4.42	6.86	10.03
April	0.40	3.15	10.53	0.38	0.89	1.76	4.35	6.53	9.10
May	0.32	2.35	8.46	0.34	0.76	1.61	4.40	6.28	8.39
June	0.28	1.30	3.82	0.32	0.61	1.12	4.30	5.95	7.62
July	0.25	1.02	2.23	0.29	0.55	0.87	4.36	5.94	7.62
August	0.26	1.75	5.81	0.31	0.66	1.34	4.26	5.96	8.45
September	0.41	3.89	14.10	0.38	0.95	2.01	4.41	6.64	10.44
October	0.41	4.09	14.01	0.40	1.00	1.99	4.34	6.48	9.66
November	0.42	4.23	12.13	0.41	1.03	1.87	4.43	6.65	9.74
December	0.47	4.29	13.15	0.42	1.05	1.94	4.42	6.65	9.68
January	0.47	4.39	13.21	0.43	1.07	1.95	4.48	6.70	9.36
February	0.62	4.51	14.04	0.47	1.08	1.99	4.54	6.80	9.66

	ϵ_0			$\theta_j[^\circ]$			d_θ		
	5%	**Mean**	**95%**	**5%**	**Mean**	**95%**	**5%**	**Mean**	**95%**
March	0.25	0.37	0.51	35	73.4	105	0.79	0.90	0.97
April	0.25	0.37	0.52	45	78.4	105	0.78	0.90	0.97
May	0.24	0.35	0.49	55	83.5	105	0.79	0.91	0.97
June	0.24	0.36	0.49	65	90.4	115	0.80	0.91	0.96
July	0.24	0.36	0.50	65	94.2	115	0.80	0.91	0.96
August	0.24	0.35	0.48	55	88.0	115	0.80	0.91	0.96
September	0.24	0.35	0.48	55	79.5	105	0.81	0.91	0.97
October	0.25	0.36	0.48	45	73.6	105	0.79	0.91	0.97
November	0.25	0.37	0.51	35	71.7	105	0.77	0.89	0.97
December	0.25	0.38	0.53	35	68.0	105	0.75	0.89	0.96
January	0.25	0.38	0.55	35	68.6	105	0.73	0.88	0.96
February	0.25	0.38	0.53	35	70.0	105	0.76	0.89	0.97

D.2. Wave Roses

The annual wave rose of omnidirectional wave power, J, and direction of maximum directionally resolved wave power, θ_j, is shown in Figure 138, and essentially mirrors that for significant wave height, H_{m0}, and θ_j shown in Figure 139.

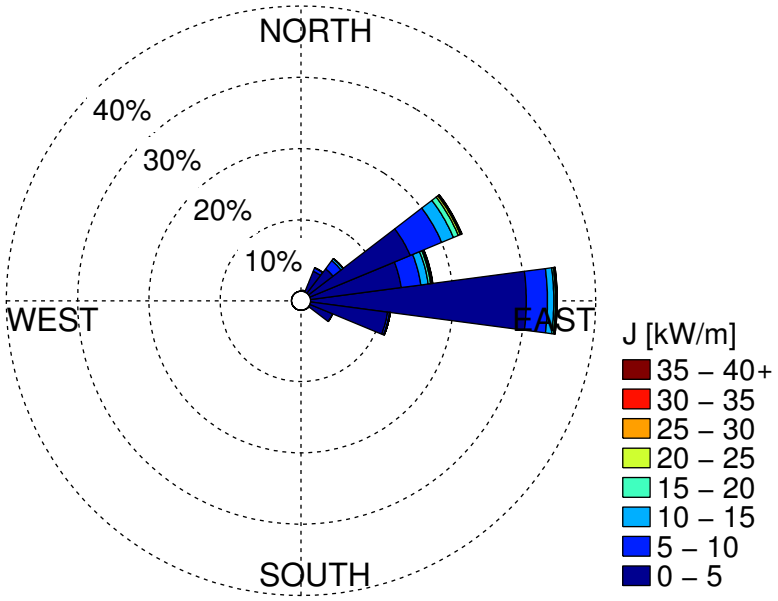

Figure 138: Annual wave rose of omnidirectional wave power and direction of maximally resolved wave power. Values of J greater than 40 kW/m are included in the top bin as shown in the legend.

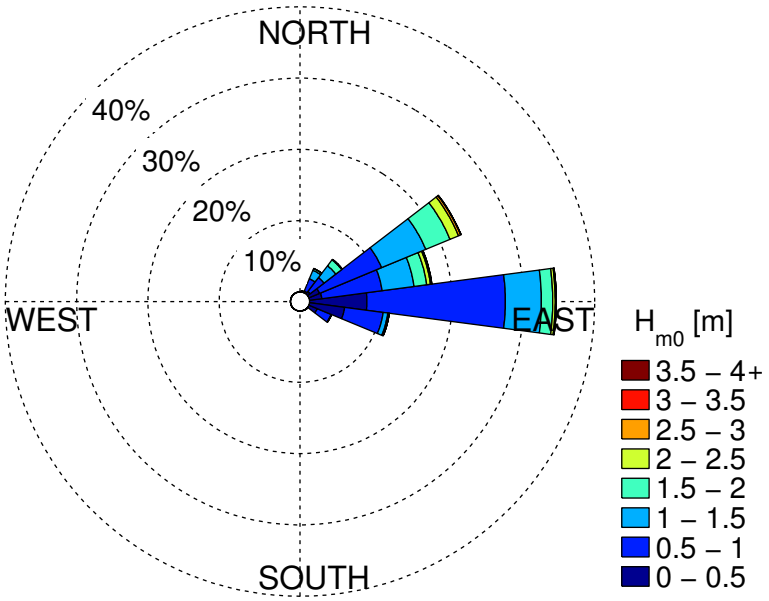

Figure 139: Annual wave rose of significant wave height and direction of maximally resolved wave power. Values of H_{m0} greater than 4 m are included in the top bin as shown in the legend.

D.3. Extreme Sea States

Table 24: Estimates of extreme significant wave height values using the generalized extreme value distribution (see Figure 57).

Return period [years]	Significant wave height [m]
10	6.23
25	6.79
50	7.19
100	7.55

Table 25: Estimates of extreme significant wave height values using the peak over thresholds method (see Figure 58).

Return period [years]	Significant wave height [m]
10	7.34
25	7.81
50	8.14
100	8.46

D.4. Wind Data

The wind data for this site (obtained from CFSR), is taken at 36.25 N, 75.5 W located approximately 23 km northeast of the USACE FRF site (Figure 35), which is the nearest data point to the site. The average monthly values, along with the 5^{th} and 95^{th} percentiles, of wind are shown in Figure 140. The values are also tabulated in Table 26. The annual and seasonal wind roses are shown in Figure 141.

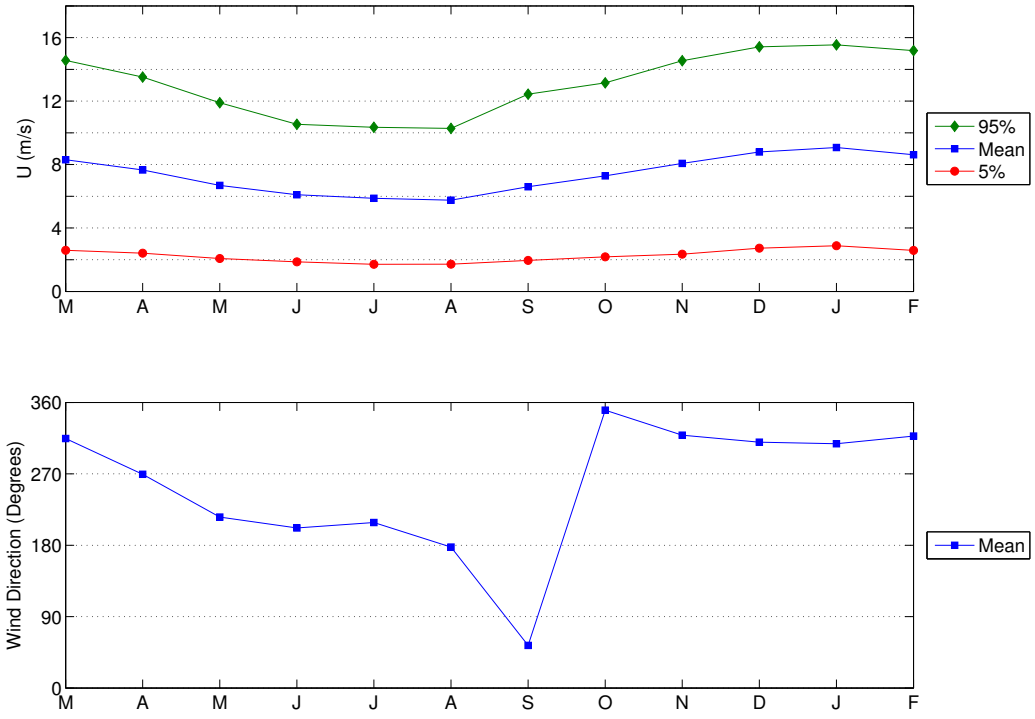

Figure 140: Monthly wind velocity and direction obtained from CSFR data during the period 1/1/1979 to 12/31/2014 at 36.25 N, 75.5 W.

(a)

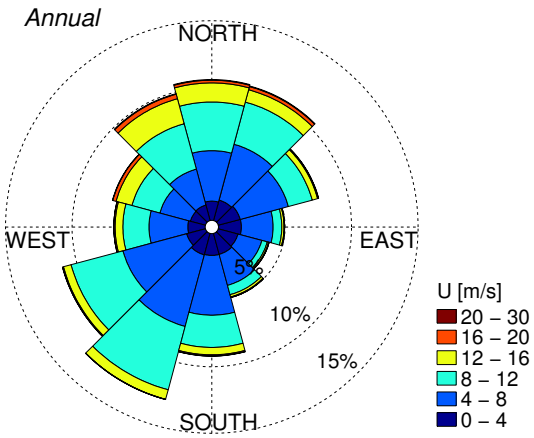

(b)

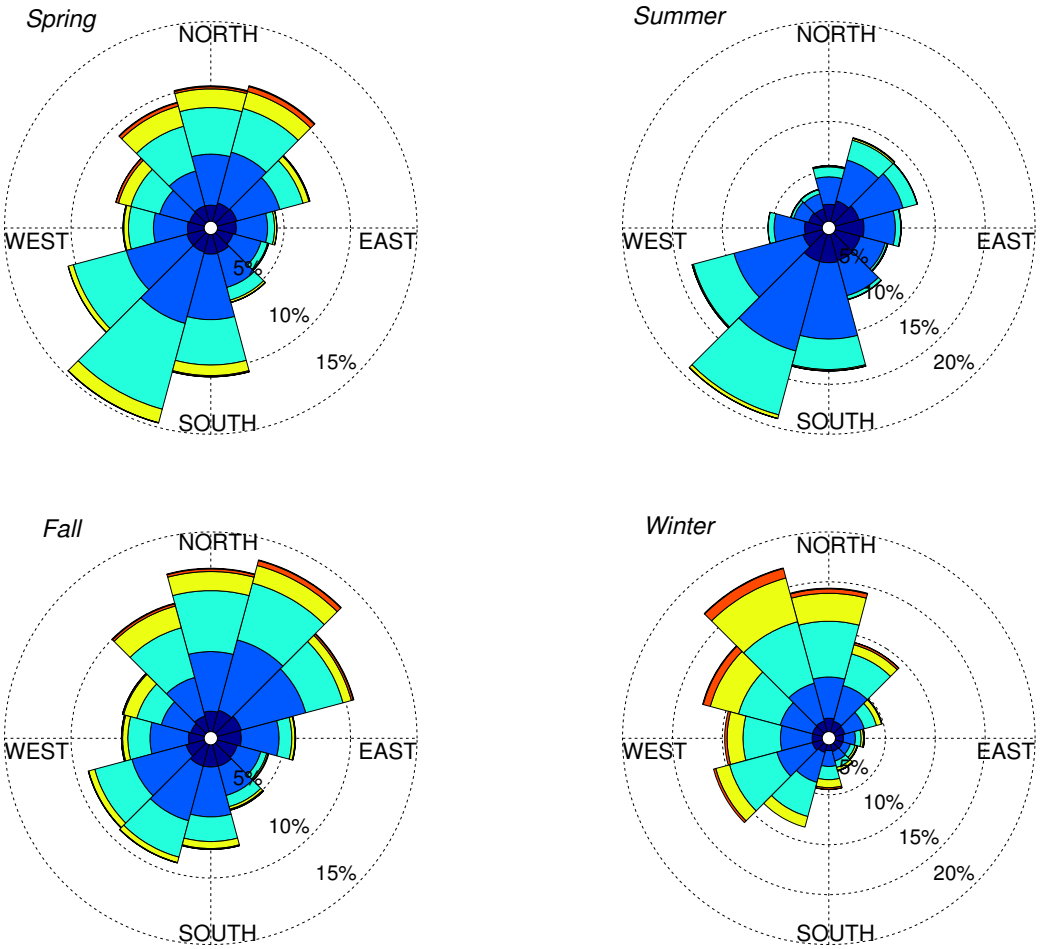

Figure 141: (a) Annual and (b) seasonal wind roses of velocity and direction obtained from CSFR data during the period 1/1/1979 to 12/31/14 at 36.25 N, 75.5 W.

Table 26: Monthly wind velocity and direction obtained from CSFR data during the period 1/1/1979 to 12/31/2014 at 36.25 N, 75.5 W, located approximately 23 km northeast of USACE FRF.

	$U[m/s]$			$Direction[^\circ]$
	5%	**Mean**	**95%**	**Mean**
March	2.6	8.3	14.6	315
April	2.4	7.7	13.5	269
May	2.1	6.7	11.9	215
June	1.9	6.1	10.5	202
July	1.7	5.9	10.4	209
August	1.7	5.8	10.3	178
September	2.0	6.6	12.4	54
October	2.2	7.3	13.1	350
November	2.3	8.1	14.5	319
December	2.7	8.8	15.4	310
January	2.9	9.1	15.5	308
February	2.6	8.6	15.2	318

D.5. Ocean Surface Current Data

The surface current data (obtained from OSCAR), is located at 36.5 N, 75.5 W, the closest data point to shore. The average monthly values, along with the 5^{th} and 95^{th} percentiles, of current are shown in Figure 142. These data points are listed in Table 27. The annual and seasonal current roses are shown in Figure 143.

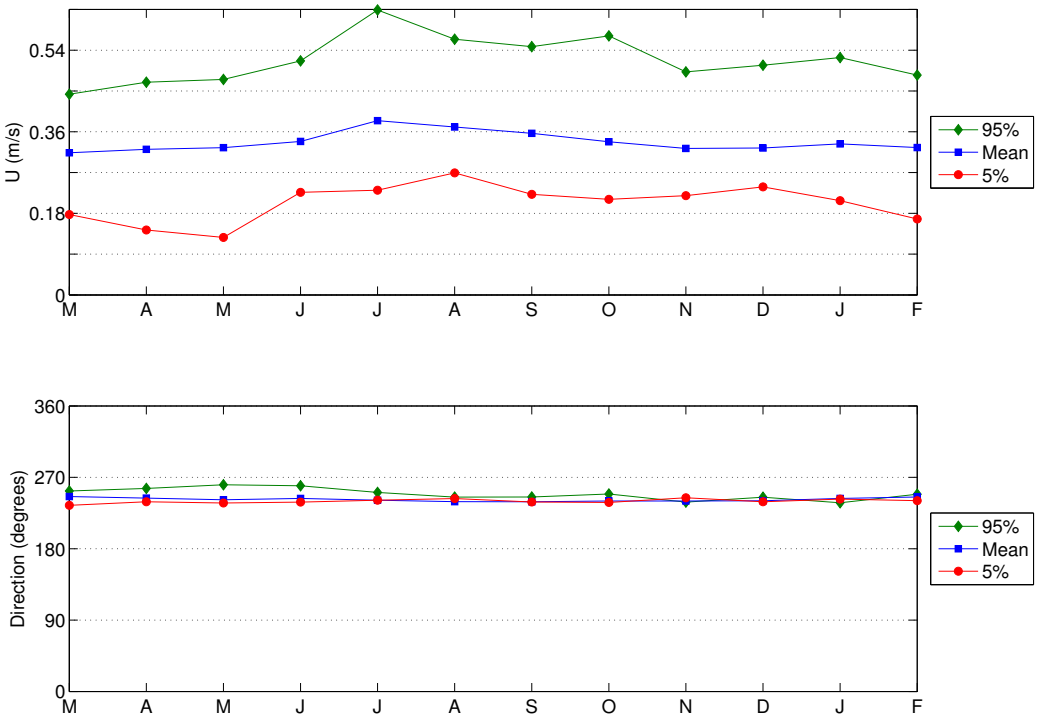

Figure 142: Monthly current velocity and direction obtained from CSFR data during the period 1/1/1993 to 12/31/2014 at 36.5 N, 75.5 W.

(a)

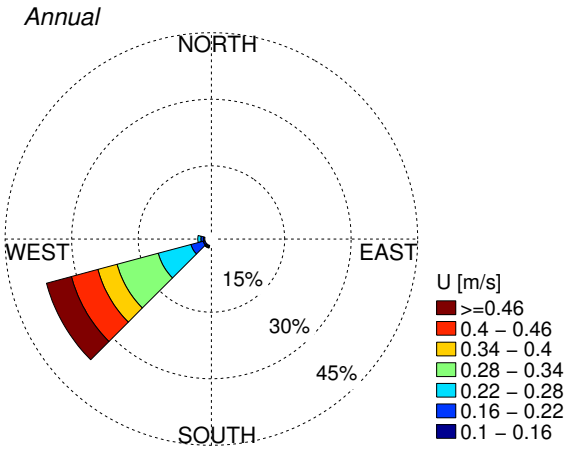

(b)

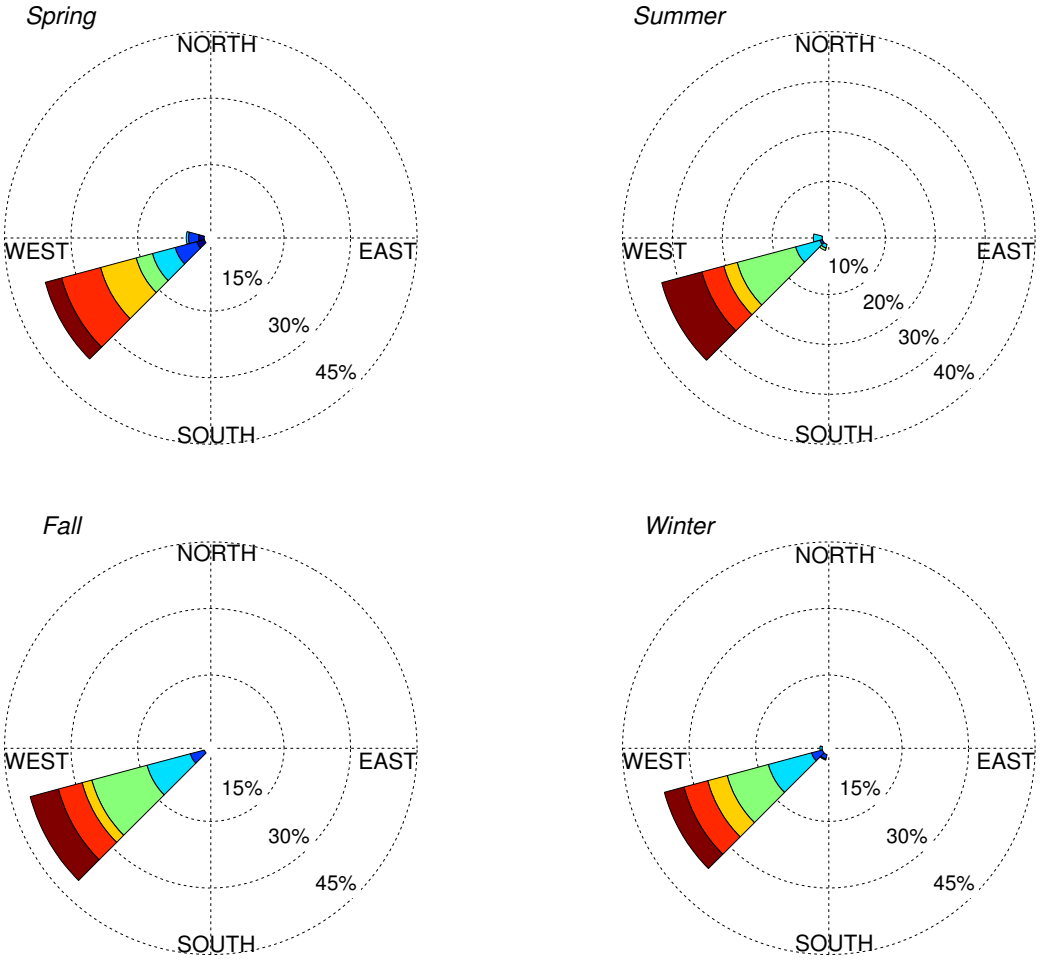

Figure 143: (a)Annual and (b) seasonal current roses of velocity and direction obtained from CSFR data during the period 1/1/1993 to 12/31/14 at 36.5 N, 75.5 W.

Table 27: Monthly surface current velocity and direction obtained from OSCAR data during the period 1/1/1993 to 12/30/2014 at 36.5 N, 75.5 W, located approximately 40 km northeast of the USACE FRF site.

	$U[m/s]$			$Direction[^\circ]$		
	5%	**Mean**	**95%**	**5%**	**Mean**	**95%**
March	0.177	0.314	0.443	235	246	253
April	0.143	0.321	0.469	239	244	256
May	0.127	0.325	0.476	238	242	261
June	0.226	0.339	0.516	239	243	259
July	0.231	0.385	0.629	241	241	251
August	0.269	0.370	0.564	243	239	245
September	0.222	0.357	0.548	239	239	245
October	0.211	0.338	0.572	238	240	249
November	0.219	0.323	0.492	244	240	239
December	0.238	0.324	0.507	239	241	245
January	0.208	0.333	0.524	242	243	238
February	0.168	0.325	0.485	241	245	249

Appendix E: PACIFIC MARINE ENERGY TEST CENTER (PMEC): LAKE WASHINGTON TEST SITE

E.1. IEC TS Parameter Values

Table 28: The average, 5^{th} and 95^{th} percentiles of the six parameters at Lake Washington (see Figure 64).

	$J[kW/m]$			$H_{m0}[m]$			$T_e[s]$		
	5%	**Mean**	**95%**	**5%**	**Mean**	**95%**	**5%**	**Mean**	**95%**
March	0.0026	0.052	0.219	0.071	0.200	0.444	1.06	1.56	2.26
April	0.0025	0.040	0.169	0.070	0.180	0.401	1.05	1.50	2.16
May	0.0024	0.029	0.107	0.069	0.161	0.331	1.05	1.45	2.01
June	0.0024	0.025	0.100	0.069	0.152	0.320	1.04	1.41	1.98
July	0.0023	0.019	0.063	0.068	0.138	0.264	1.03	1.37	1.84
August	0.0023	0.017	0.064	0.068	0.133	0.266	1.03	1.35	1.84
September	0.0023	0.027	0.124	0.067	0.150	0.353	1.02	1.40	2.05
October	0.0023	0.047	0.205	0.067	0.184	0.432	1.02	1.50	2.24
November	0.0026	0.054	0.218	0.070	0.201	0.444	1.05	1.56	2.26
December	0.0024	0.051	0.209	0.069	0.190	0.437	1.03	1.52	2.23
January	0.0024	0.063	0.279	0.069	0.207	0.491	1.04	1.57	2.37
February	0.0023	0.056	0.256	0.068	0.197	0.474	1.02	1.54	2.32

	ϵ_0			$\theta_j[^\circ]$			d_θ		
	5%	**Mean**	**95%**	**5%**	**Mean**	**95%**	**5%**	**Mean**	**95%**
March	0.226	0.241	0.252	75	188.4	325	0.79	0.88	0.95
April	0.226	0.241	0.254	35	191.7	335	0.78	0.88	0.95
May	0.227	0.242	0.255	15	206.5	335	0.77	0.89	0.95
June	0.225	0.242	0.255	25	206.2	345	0.77	0.89	0.95
July	0.223	0.243	0.256	15	260.6	345	0.72	0.88	0.96
August	0.226	0.242	0.255	15	243.6	345	0.73	0.89	0.96
September	0.222	0.241	0.255	15	218.4	345	0.76	0.89	0.96
October	0.223	0.241	0.254	25	190.5	335	0.79	0.89	0.95
November	0.227	0.241	0.254	115	188.0	335	0.83	0.89	0.95
December	0.224	0.240	0.255	75	178.8	335	0.80	0.88	0.95
January	0.226	0.241	0.253	25	187.8	335	0.82	0.89	0.95
February	0.220	0.240	0.254	25	186.3	335	0.77	0.88	0.95

E.2. Wave Roses

The annual wave rose of omnidirectional wave power, J, and direction of maximum directionally resolved wave power, θ_j, is shown in Figure 144, and essentially mirrors that for significant wave height, H_{m0}, and θ_j shown in Figure 145.

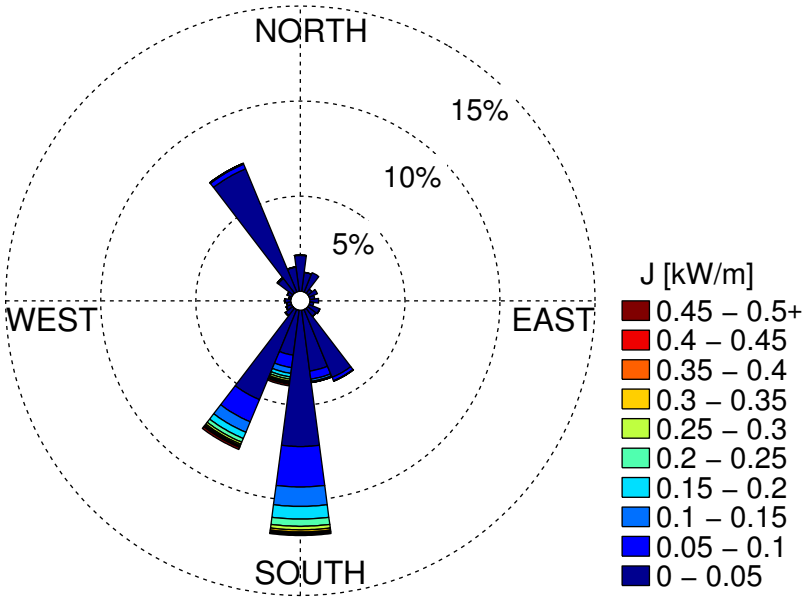

Figure 144: Annual wave rose of omnidirectional wave power and direction of maximally resolved wave power. Values of J greater than 0.5 kW/m are included in the top bin as shown in the legend.

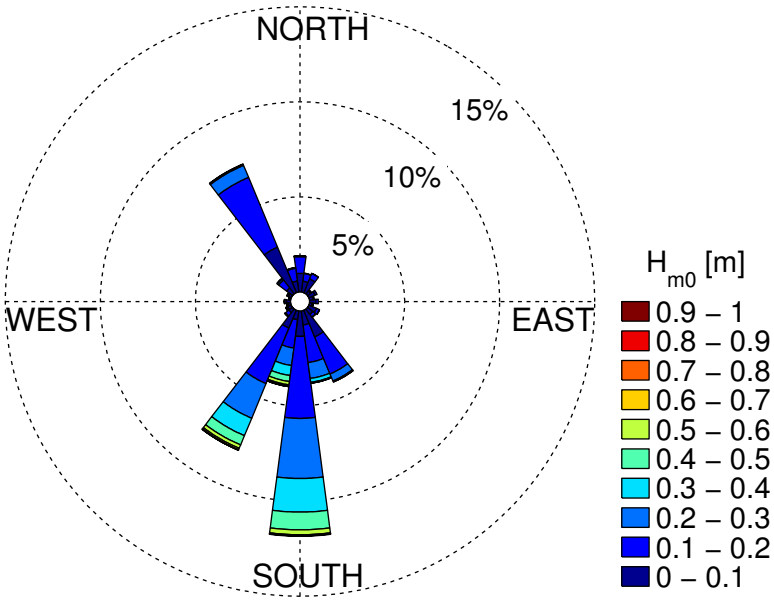

Figure 145: Annual wave rose of significant wave height and direction of maximally resolved wave power. Values of H_{m0} greater than 1 m are included in the top bin as shown in the legend.

E.3. Extreme Sea States

Table 29: Estimates of extreme significant wave height values using the generalized extreme value distribution (see Figure 70).

Return period [years]	Significant wave height [m]
10	0.94
25	1.01
50	1.07
100	1.13

Table 30: Estimates of extreme significant wave height values using the peak over thresholds method (see Figure 71).

Return period [years]	Significant wave height [m]
10	0.93
25	0.98
50	1.01
100	1.04

E.4. Wind Data

The wind data for this site (obtained from the SR 520 bridge weather station), is located approximately 5 km south of the site (Figure 60). The average monthly values, along with the 5^{th} and 95^{th} percentiles, of wind are shown in Figure 146. The values are also tabulated in Table 31. The annual and seasonal wind roses are shown in Figure 147.

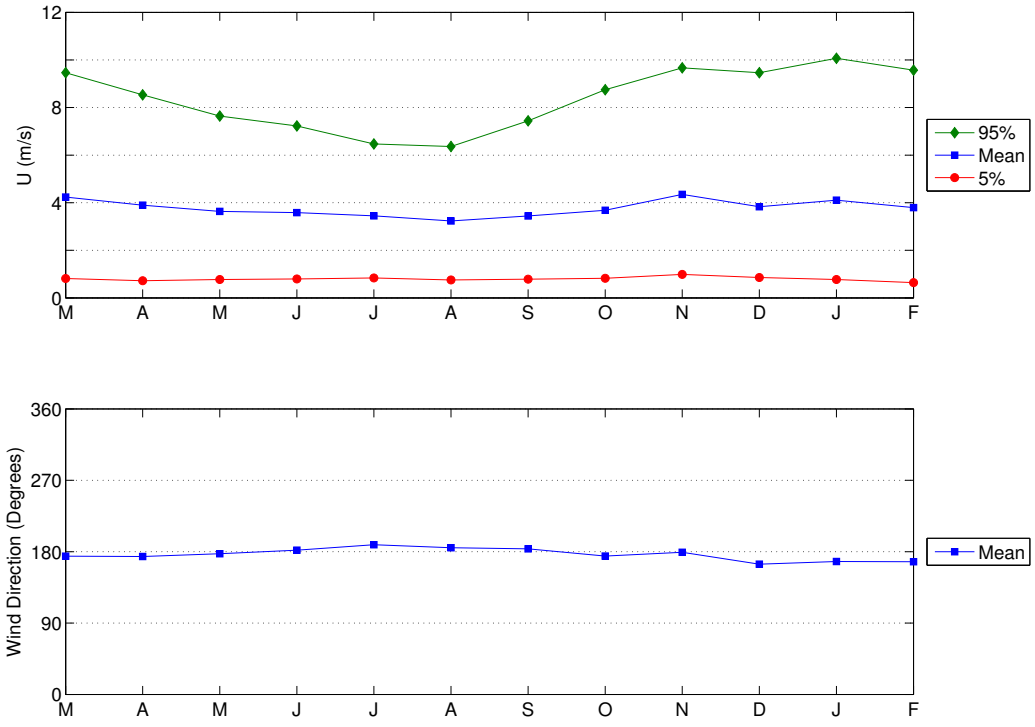

Figure 146: Monthly wind velocity and direction obtained from the SR 520 bridge weather station on Lake Washington during the period 1/1/2005 to 12/31/2014.

(a)

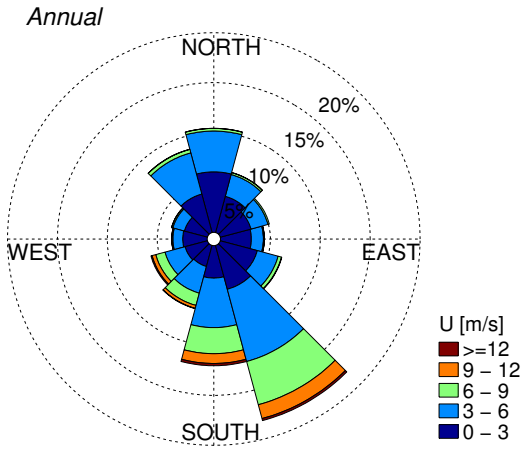

(b)

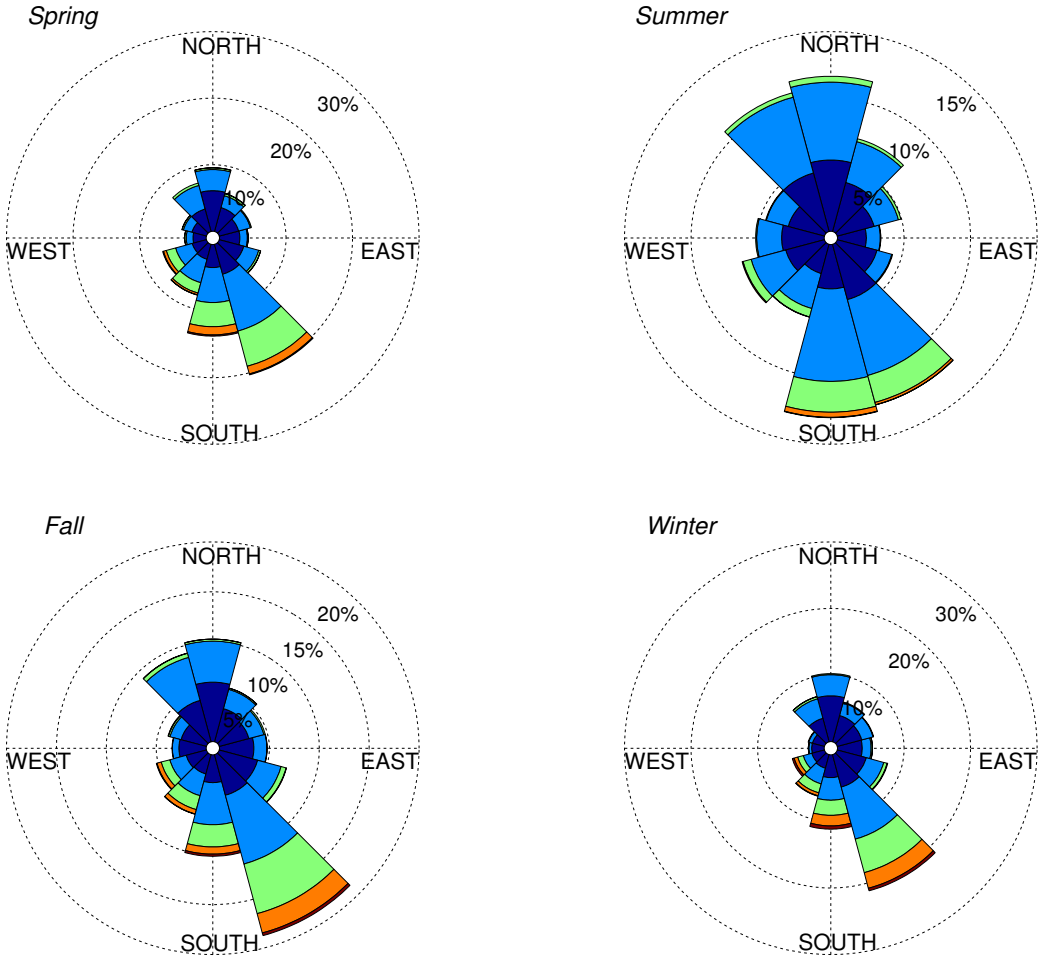

Figure 147: (a) Annual and (b) seasonal wind roses of velocity and direction obtained from the SR 520 bridge weather station during the period 1/1/2005 to 12/31/14.

Table 31: Monthly wind velocity and direction obtained from the SR 520 bridge weather station on Lake Washington during the period 1/1/2005 to 12/31/2014.

	$U[m/s]$			$Direction[^\circ]$
	5%	**Mean**	**95%**	**Mean**
March	0.81	4.2	9.5	174
April	0.72	3.9	8.5	174
May	0.77	3.6	7.6	177
June	0.80	3.6	7.2	182
July	0.84	3.4	6.5	189
August	0.75	3.2	6.4	185
September	0.79	3.4	7.4	184
October	0.83	3.7	8.7	175
November	0.99	4.4	9.7	179
December	0.86	3.8	9.5	164
January	0.77	4.1	10.1	168
February	0.64	3.8	9.6	167

E.5. Ocean Surface Current Data

Neither OSCAR data nor measured surface current data was available at this site. Therefore the surface current data was estimated using the empirical relationship in Madsen (1977), where surface current speeds are approximately 3% of the wind speed measured at 10 m elevation. Note this is a rough estimation of current speeds and should be used with caution. The average monthly values, along with the 5^{th} and 95^{th} percentiles, of current are shown in Figure 148. These data points are listed in Table 32. The annual and seasonal current roses are shown in Figure 149, which exactly mirror the wind roses because the direction is assumed to be the same.

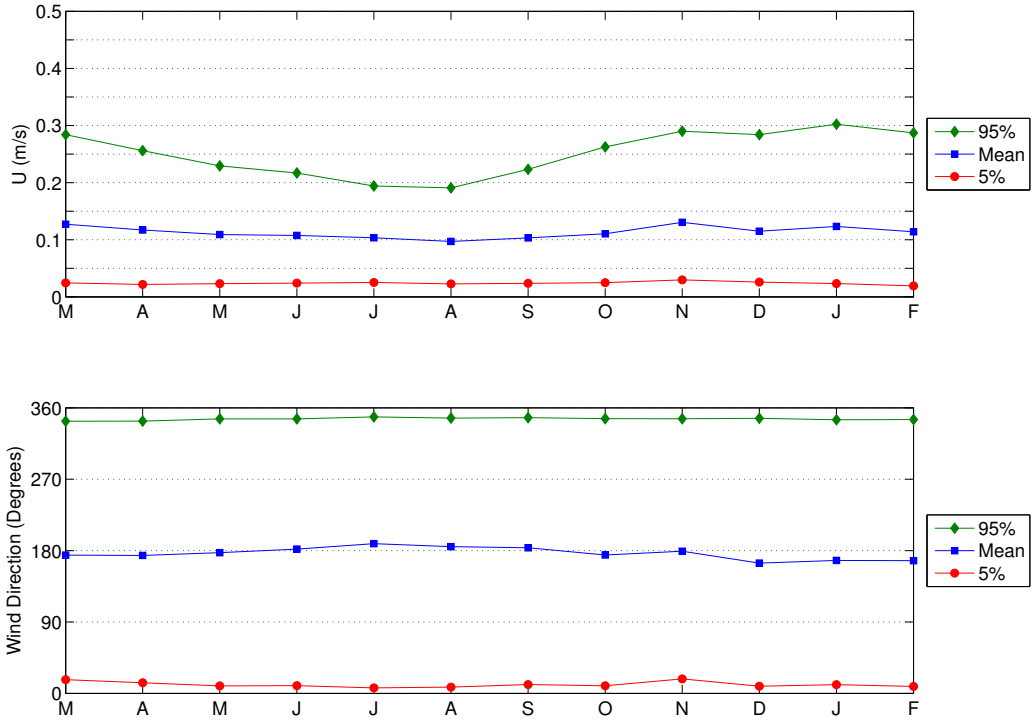

Figure 148: Monthly current velocity and direction estimated using the SR 520 bridge wind data on Lake Washington during the period 1/1/2005 to 12/31/2014.

(a)

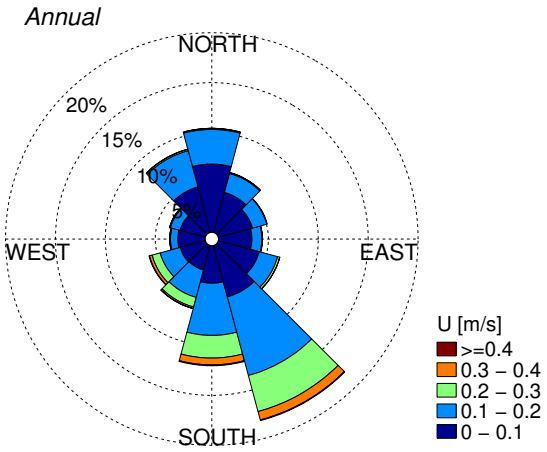

(b)

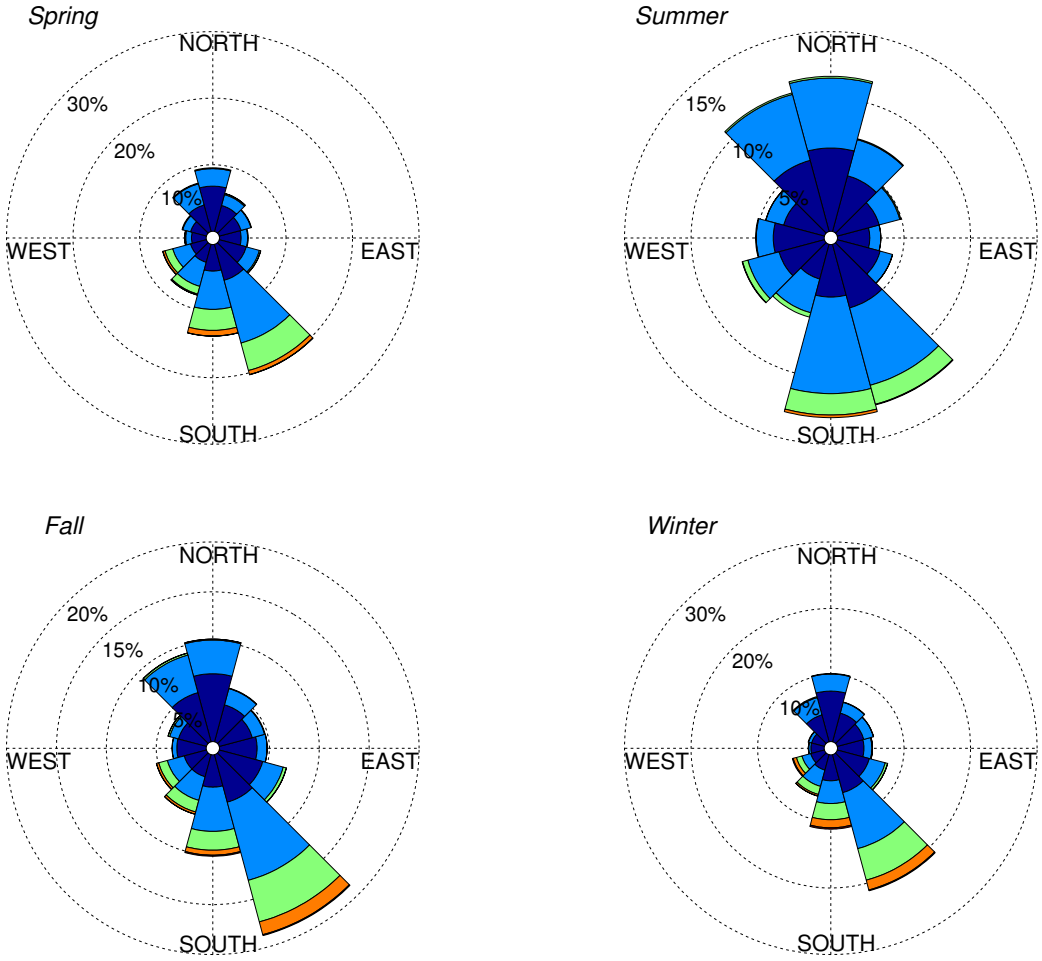

Figure 149: (a) Annual and (b) seasonal current roses of velocity and direction estimated using the SR 520 bridge wind data during the period 1/1/2005 to 12/31/14.

Table 32: Monthly surface current velocity and direction estimes using the SR 520 bridge wind data during the period 1/1/2005 to 12/31/14.

	$U[m/s]$			$Direction[^\circ]$		
	5%	**Mean**	**95%**	**5%**	**Mean**	**95%**
March	0.024	0.127	0.284	17	174	343
April	0.022	0.117	0.256	13	174	343
May	0.023	0.109	0.229	9	177	346
June	0.024	0.108	0.217	10	182	346
July	0.025	0.103	0.194	7	189	349
August	0.023	0.097	0.191	8	185	347
September	0.024	0.103	0.223	11	184	348
October	0.025	0.110	0.262	10	175	346
November	0.030	0.131	0.290	18	179	346
December	0.026	0.115	0.284	9	164	347
January	0.023	0.123	0.302	11	168	345
February	0.019	0.114	0.287	9	167	345

Appendix F: PACIFIC MARINE ENERGY TEST CENTER (PMEC): SOUTH ENERGY TEST SITE (SETS)

F.1. IEC TS Parameter Values

Table 33: The average, 5^{th} and 95^{th} percentiles of the six parameters at SETS (see Figure 78).

	$J[kW/m]$			$H_{m0}[m]$			$T_e[s]$		
	5%	**Mean**	**95%**	**5%**	**Mean**	**95%**	**5%**	**Mean**	**95%**
March	10.4	59.0	165.9	1.54	3.05	5.14	7.73	10.03	12.81
April	6.8	40.7	107.9	1.22	2.53	4.26	7.72	9.83	12.06
May	3.8	17.8	47.0	0.92	1.81	3.04	7.07	8.83	10.90
June	4.0	13.1	36.8	0.92	1.59	2.81	6.97	8.87	11.34
July	2.5	9.8	19.7	0.76	1.44	2.11	6.80	8.48	10.52
August	3.0	9.2	21.3	0.85	1.38	2.15	6.67	8.50	10.66
September	4.7	19.7	59.3	1.02	1.82	3.24	7.44	9.37	11.78
October	8.3	42.2	120.9	1.33	2.56	4.53	7.94	9.86	12.31
November	10.7	69.7	185.1	1.44	3.27	5.42	7.83	10.12	12.88
December	9.6	78.2	231.0	1.33	3.34	5.83	8.23	10.76	13.96
January	12.6	77.1	204.4	1.52	3.31	5.51	8.36	11.00	14.10
February	12.5	59.6	159.4	1.53	2.96	5.00	8.34	10.81	13.48

	ϵ_0			$\theta_j[^\circ]$			d_θ		
	5%	**Mean**	**95%**	**5%**	**Mean**	**95%**	**5%**	**Mean**	**95%**
March	0.23	0.30	0.40	242.5	274.9	297.5	0.81	0.91	0.96
April	0.24	0.32	0.47	252.5	279.0	297.5	0.76	0.90	0.96
May	0.25	0.35	0.48	242.5	273.2	302.5	0.76	0.88	0.95
June	0.27	0.38	0.51	237.5	269.6	302.5	0.74	0.85	0.93
July	0.29	0.40	0.53	242.5	276.5	307.5	0.70	0.82	0.92
August	0.27	0.40	0.53	247.5	276.6	307.5	0.72	0.82	0.92
September	0.24	0.35	0.49	242.5	278.9	302.5	0.76	0.87	0.94
October	0.22	0.29	0.41	247.5	280.1	302.5	0.82	0.90	0.95
November	0.22	0.29	0.36	242.5	279.5	302.5	0.82	0.91	0.96
December	0.19	0.28	0.36	237.5	276.4	302.5	0.82	0.91	0.96
January	0.20	0.29	0.38	247.5	274.0	297.5	0.85	0.92	0.97
February	0.19	0.28	0.38	237.5	275.3	302.5	0.82	0.92	0.97

F.2. Wave Roses

The annual wave rose of omnidirectional wave power, J, and direction of maximum directionally resolved wave power, θ_j, is shown in Figure 150, and essentially mirrors that for significant wave height, H_{m0}, and θ_j shown in Figure 151.

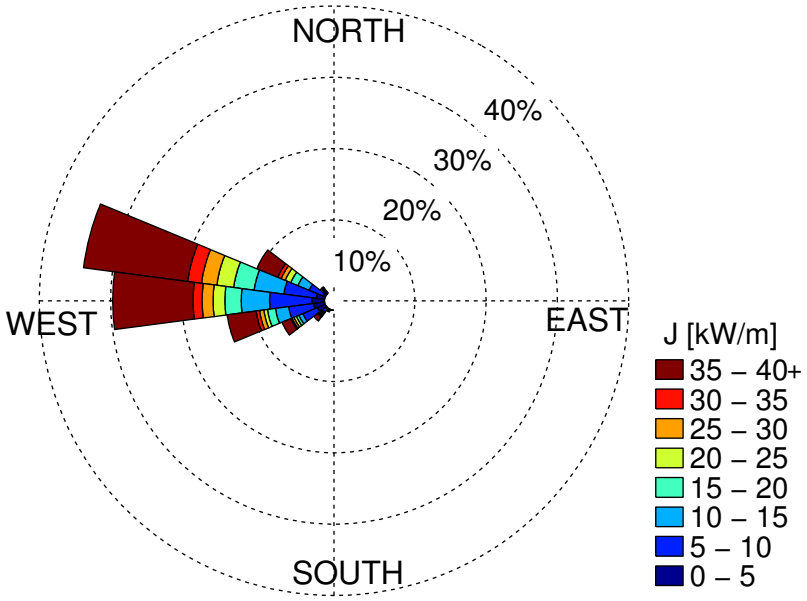

Figure 150: Annual wave rose of omnidirectional wave power and direction of maximally resolved wave power. Values of J greater than 40 kW/m are included in the top bin as shown in the legend.

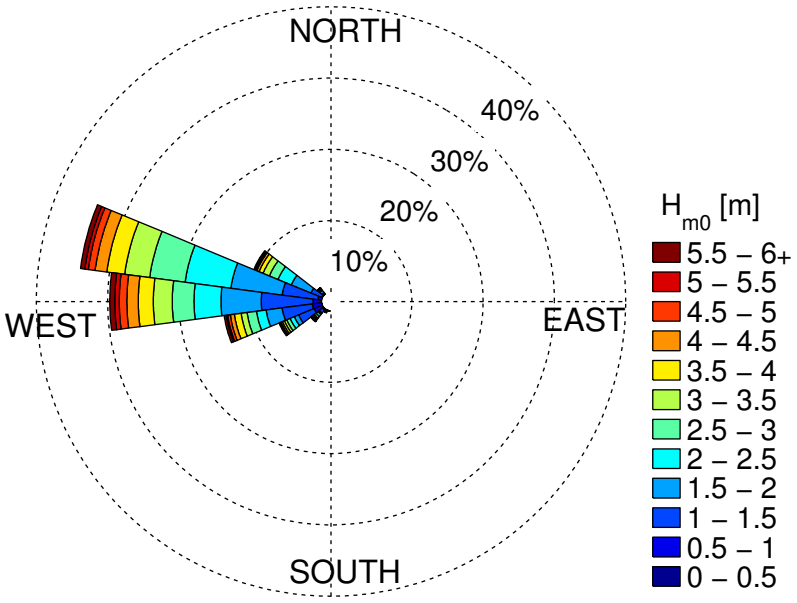

Figure 151: Annual wave rose of significant wave height and direction of maximally resolved wave power. Values of H_{m0} greater than 6 m are included in the top bin as shown in the legend.

F.3. Extreme Sea States

Table 34: Selected values along the 100-year contour for NDBC46050 (see Figure 84).

Significant wave height [m]	Energy period [s]
1	3.80
2	4.58
3	5.32
4	6.00
5	6.64
6	7.25
7	7.83
8	8.39
9	8.95
10	9.50
11	10.07
12	10.65
13	11.27
14	11.94
15	12.71
16	13.66
17	15.14
17.31	16.57
17	18.04
16	19.63
15	20.65
14	21.48
13	22.18
12	22.79
11	23.34
10	23.84
9	24.29
8	24.69
7	25.05
6	25.36
5	25.63
4	25.85
3	26.02
2	26.12
1	26.15

F.4. Wind Data

The wind data for this site (obtained from CFSR), is taken at 44.5 N, 124.5 W located approximately 23 km west/southwest of SETS (Figure 76), which is the nearest data point to the site. The average monthly values, along with the 5^{th} and 95^{th} percentiles, of wind are shown in Figure 152. The values are also tabulated in Table 35. The annual and seasonal wind roses are shown in Figure 153.

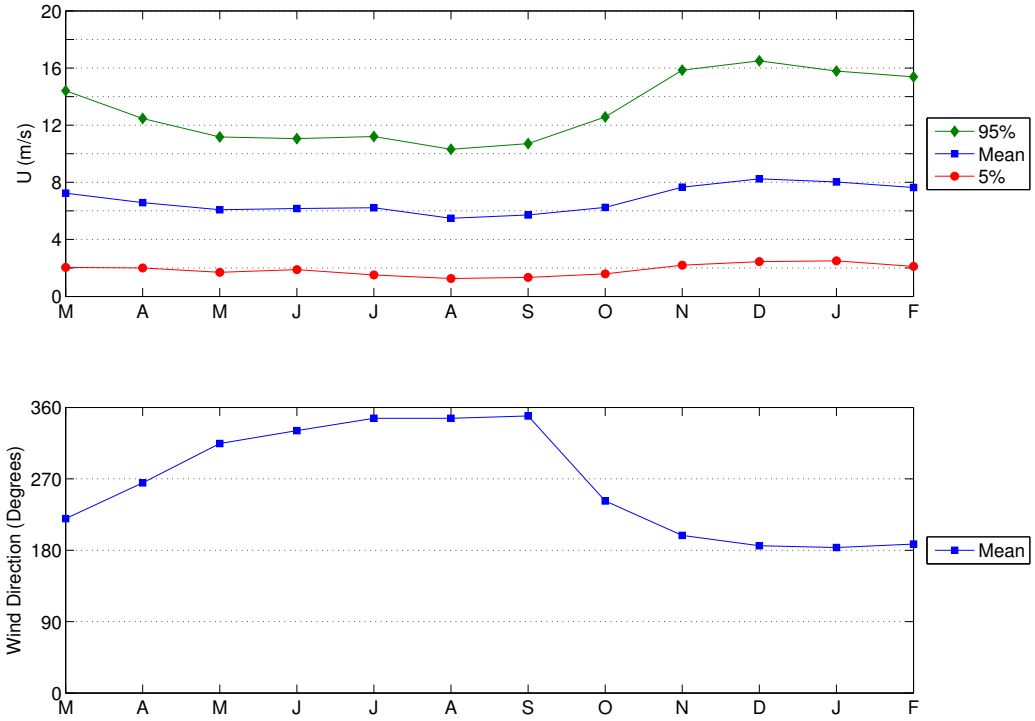

Figure 152: Monthly wind velocity and direction obtained from CSFR data during the period 1/1/1979 to 12/31/2014 at 44.5 N, 124.5 W, located 23 km west/southwest of SETS (Figure 76).

(a)

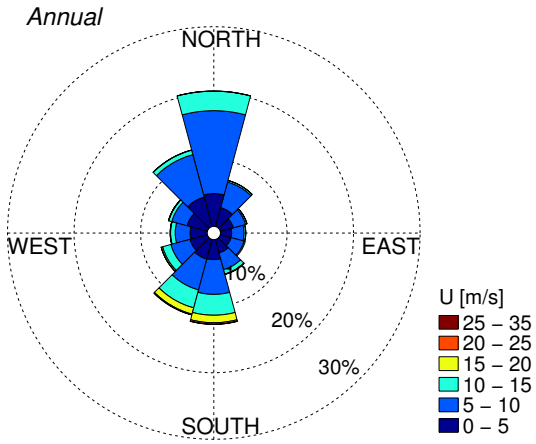

(b)

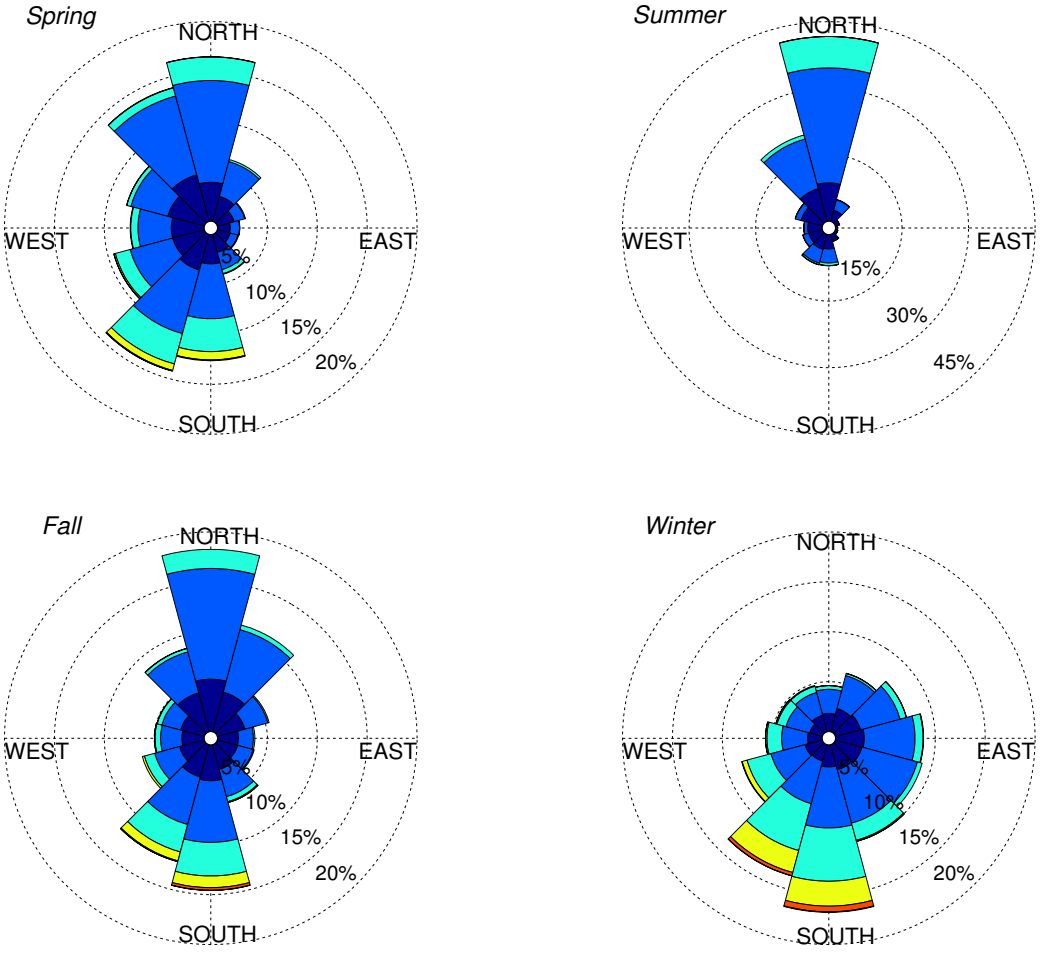

Figure 153: (a) Annual and (b) seasonal wind roses of velocity and direction obtained from CSFR data during the period 1/1/1979 to 12/31/2014.

Table 35: Monthly wind velocity and direction obtained from CSFR data during the period 1/1/1979 to 12/31/2014 at 44.5 N, 124.5 W, located approximately 23 km west/southwest of SETS.

	$U[m/s]$			$Direction[^\circ]$
	5%	**Mean**	**95%**	**Mean**
March	2.0	7.2	14.4	220
April	2.0	6.6	12.5	265
May	1.7	6.1	11.2	314
June	1.9	6.2	11.1	331
July	1.5	6.2	11.2	346
August	1.3	5.5	10.3	346
September	1.3	5.7	10.7	349
October	1.6	6.2	12.6	242
November	2.2	7.7	15.9	199
December	2.4	8.2	16.5	186
January	2.5	8.0	15.8	183
February	2.1	7.6	15.4	188

F.5. Ocean Surface Current Data

The surface current data (obtained from OSCAR) used for this site is located at 44.5 N, 125.5 W. There is data located closer to the site at 44.5 N, 124.5 W, however the period of record is short (about 2 years). Data from the two years available was compared at both locations. Surface current speeds at 124.5 W are slightly higher in the summer than at 125.5 W, however overall the patterns are similar. Therefore, the data point further out (125.5 W) with the longer period of record (about 20 years) was used for consistency with the other sites. The average monthly values, along with the 5^{th} and 95^{th} percentiles, of current are shown in Figure 154. These data points are listed in Table 36. The annual and seasonal current roses are shown in Figure 155.

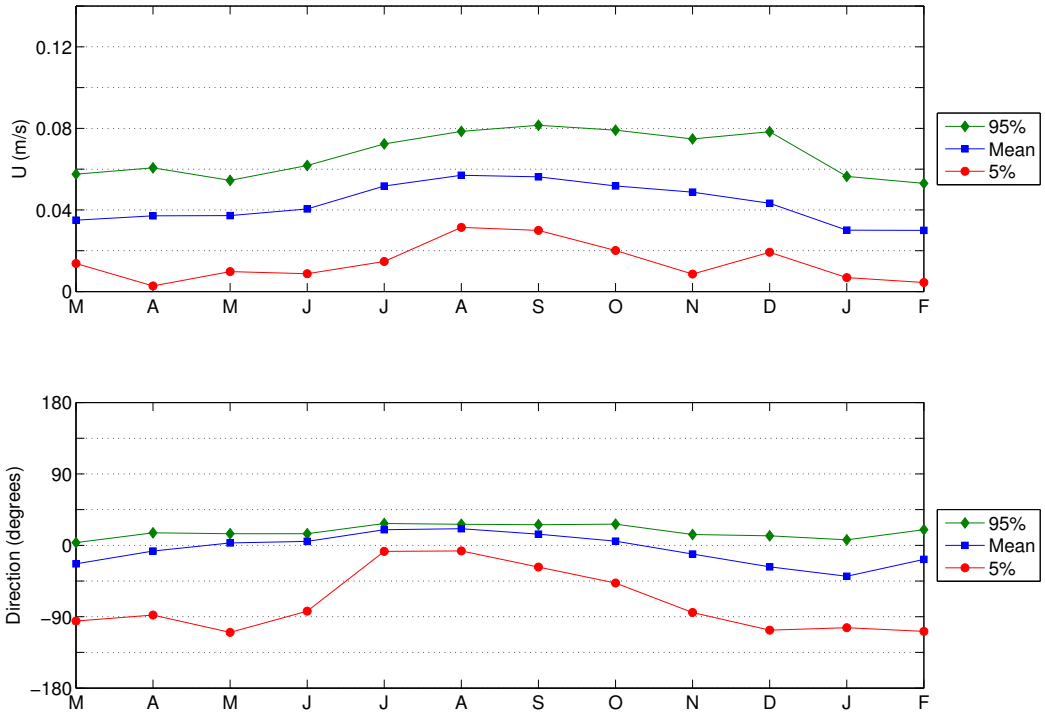

Figure 154: Monthly ocean surface current velocity and direction obtained from OSCAR at 44.5 N, 125.5 W. Data period 1/1/1993 to 12/30/2014.

(a)

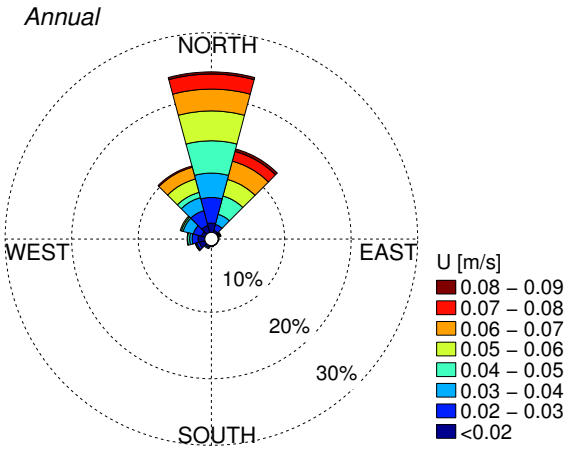

(b)

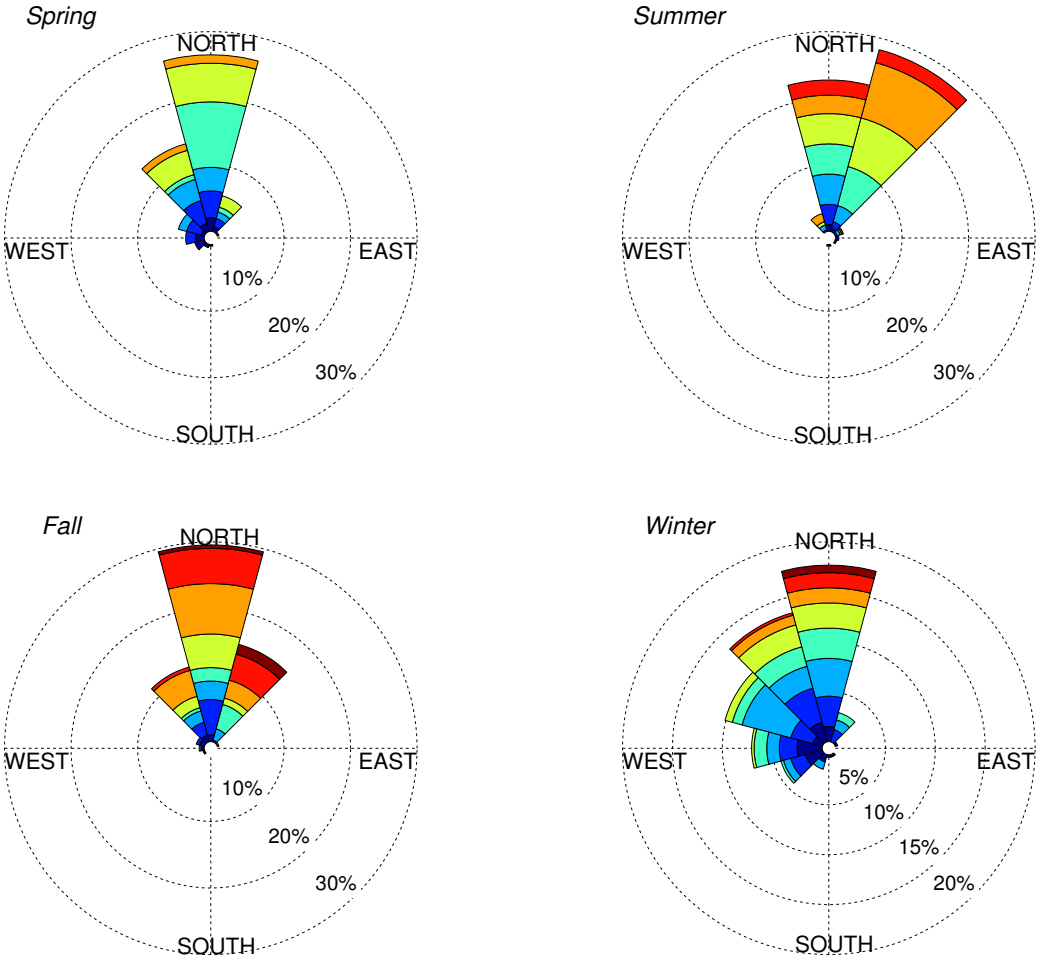

Figure 155: (a) Annual and (b) seasonal current roses of ocean surface current velocity and direction obtained from OSCAR at 44.5 N, 125.5 W. Data period 1/1/1993 to 12/30/2014.

Table 36: Monthly surface current velocity and direction obtained from OSCAR data during the period 1/1/1993 to 12/30/2014 at 44.5 N, 125.5 W.

	$U[m/s]$			$Direction[^\circ]$		
	5%	**Mean**	**95%**	**5%**	**Mean**	**95%**
March	0.014	0.035	0.058	-95	-23	3
April	0.003	0.037	0.061	-88	-7	16
May	0.010	0.037	0.055	-110	3	15
June	0.009	0.040	0.062	-83	5	15
July	0.015	0.052	0.072	-8	20	28
August	0.031	0.057	0.079	-7	21	27
September	0.030	0.056	0.082	-27	14	26
October	0.020	0.052	0.079	-48	5	27
November	0.009	0.049	0.075	-85	-11	14
December	0.019	0.043	0.078	-107	-27	12
January	0.007	0.030	0.056	-104	-39	7
February	0.004	0.030	0.053	-108	-18	20

Appendix G: CALWAVE PROPOSED CENTRAL COAST WEC TEST SITE AT VANDENBERG AIR FORCE BASE (VAFB)

G.1. IEC TS Parameter Values

Table 37: The average, 5^{th} and 95^{th} percentiles of the six parameters at the South Vandenberg site (see Figure 92).

	$J[kW/m]$			$H_{m0}[m]$			$T_e[s]$		
	5%	**Mean**	**95%**	**5%**	**Mean**	**95%**	**5%**	**Mean**	**95%**
March	9.5	55.0	143.9	1.33	2.75	4.43	9.19	11.98	15.54
April	9.2	38.3	91.3	1.39	2.50	3.89	7.35	10.75	14.24
May	6.2	27.3	62.1	1.18	2.19	3.35	6.13	10.17	15.63
June	6.9	24.9	54.2	1.18	2.21	3.29	6.18	9.47	14.87
July	5.3	16.0	32.0	1.07	1.82	2.60	5.76	9.13	14.79
August	3.4	16.6	33.6	0.95	1.81	2.57	5.76	9.48	14.92
September	5.2	20.0	45.8	1.08	1.84	2.83	5.98	10.36	14.82
October	7.1	31.0	81.7	1.20	2.20	3.63	7.96	10.88	14.72
November	10.7	46.1	128.1	1.42	2.56	4.26	8.73	11.58	14.70
December	11.9	65.8	166.7	1.43	2.94	4.68	9.59	12.29	15.68
January	12.4	67.9	173.1	1.56	2.95	4.84	9.13	12.47	15.99
February	15.4	74.6	202.2	1.61	3.09	5.19	9.62	12.53	15.97

	ϵ_0			$\theta_j[^\circ]$			d_θ		
	5%	**Mean**	**95%**	**5%**	**Mean**	**95%**	**5%**	**Mean**	**95%**
March	0.23	0.24	0.25	275.0	291.4	307.5	0.98	0.98	0.99
April	0.23	0.23	0.24	207.5	290.2	312.5	0.98	0.98	0.99
May	0.23	0.23	0.24	192.5	272.6	312.5	0.98	0.98	0.99
June	0.23	0.23	0.24	192.5	284.0	312.5	0.98	0.98	0.99
July	0.23	0.24	0.25	192.5	279.5	317.5	0.98	0.98	0.99
August	0.23	0.24	0.24	187.5	272.6	312.5	0.98	0.98	0.99
September	0.23	0.24	0.25	192.5	272.1	312.5	0.97	0.98	0.99
October	0.23	0.23	0.24	202.5	289.6	312.5	0.98	0.98	0.99
November	0.23	0.24	0.25	277.5	295.2	312.5	0.98	0.98	0.99
December	0.23	0.24	0.25	277.5	293.5	312.5	0.98	0.98	0.99
January	0.23	0.24	0.24	272.5	288.6	307.5	0.98	0.98	0.99
February	0.23	0.24	0.24	272.5	288.2	307.5	0.98	0.98	0.99

Table 38: The average, 5^{th} and 95^{th} percentiles of the six parameters at the South by Southeast Vandenberg site (see Figure 93).

	$J[kW/m]$			$H_{m0}[m]$			$T_e[s]$		
	5%	**Mean**	**95%**	**5%**	**Mean**	**95%**	**5%**	**Mean**	**95%**
March	7.9	42.4	105.8	1.22	2.44	3.94	8.96	11.70	15.21
April	8.0	30.0	68.3	1.26	2.24	3.42	7.21	10.50	13.99
May	4.9	22.6	50.6	1.07	2.01	3.03	6.11	10.02	15.51
June	5.9	20.5	42.9	1.10	2.02	2.96	6.12	9.31	14.81
July	4.2	13.6	28.1	0.99	1.68	2.39	5.74	9.01	14.69
August	2.3	13.9	28.4	0.81	1.66	2.35	5.73	9.32	14.79
September	3.6	16.3	36.8	0.87	1.67	2.50	5.97	10.22	14.72
October	5.8	23.6	58.4	1.08	1.94	3.07	7.74	10.64	14.56
November	8.2	34.2	91.3	1.26	2.23	3.69	8.50	11.27	14.37
December	9.4	49.2	125.8	1.30	2.56	4.14	9.32	11.98	15.35
January	10.3	54.8	140.8	1.41	2.66	4.42	8.89	12.22	15.78
February	12.5	59.0	165.2	1.45	2.75	4.60	9.36	12.26	15.72

	ϵ_0			$\theta_j[^\circ]$			d_θ		
	5%	**Mean**	**95%**	**5%**	**Mean**	**95%**	**5%**	**Mean**	**95%**
March	0.23	0.25	0.27	272.5	286.7	303.8	0.98	0.98	0.99
April	0.23	0.25	0.26	202.5	286.5	305.0	0.98	0.98	0.99
May	0.23	0.24	0.26	192.5	270.5	310.0	0.98	0.98	0.99
June	0.23	0.24	0.25	195.0	281.4	310.0	0.98	0.98	0.99
July	0.23	0.24	0.27	195.0	277.1	312.5	0.97	0.98	0.99
August	0.23	0.24	0.26	190.0	271.6	310.0	0.98	0.98	0.99
September	0.23	0.25	0.27	192.5	269.4	310.0	0.97	0.98	0.99
October	0.23	0.25	0.27	202.5	285.0	310.0	0.98	0.98	0.99
November	0.24	0.25	0.27	273.8	290.2	305.0	0.98	0.98	0.99
December	0.24	0.25	0.27	275.0	288.3	305.0	0.98	0.98	0.99
January	0.23	0.25	0.27	270.0	284.1	300.0	0.98	0.98	0.99
February	0.23	0.25	0.27	270.0	283.6	300.0	0.98	0.98	0.99

G.2. Wave Roses

The annual wave rose of omnidirectional wave power, J, and direction of maximum directionally resolved wave power, θ_j, is shown in Figures 156 and 157, and essentially mirrors that for significant wave height, H_{m0}, and θ_j shown in Figures 158 and 159 for the South and SSE sites.

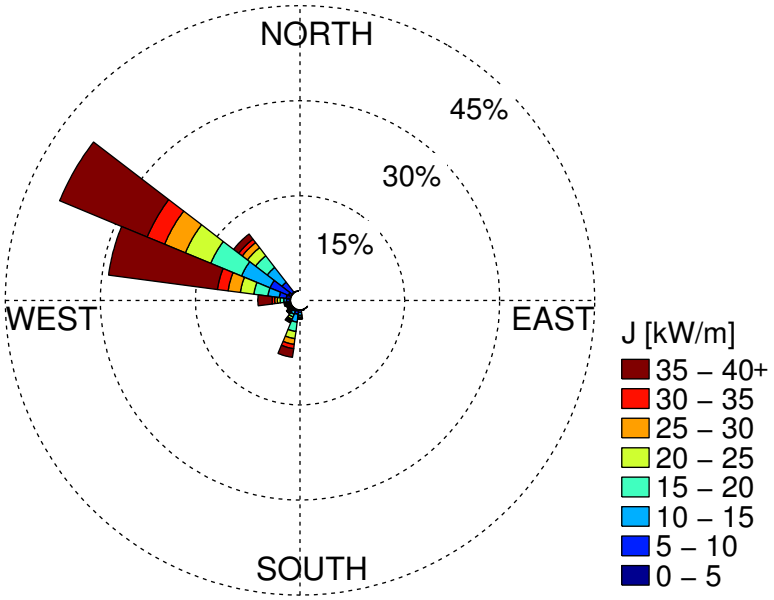

Figure 156: Annual wave rose of omnidirectional wave power and direction of maximally resolved wave power at the South location. Values of J greater than 40 kW/m are included in the top bin as shown in the legend.

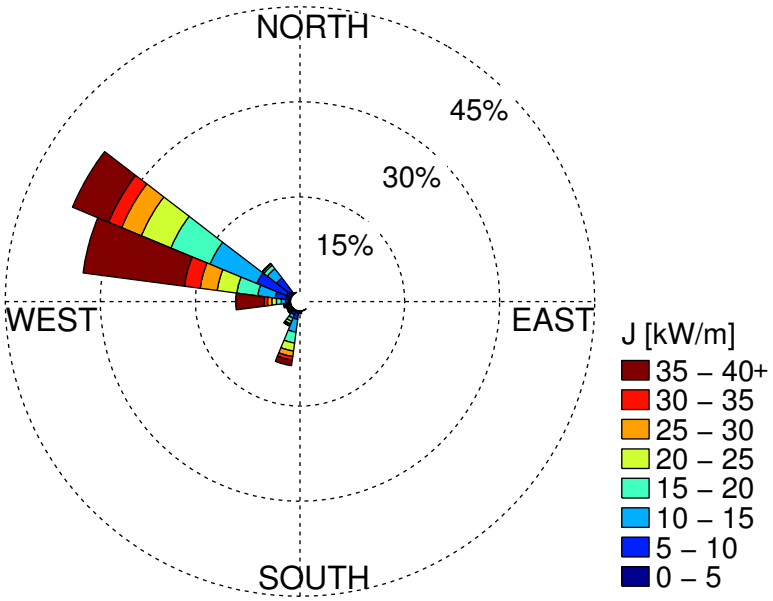

Figure 157: Annual wave rose of omnidirectional wave power and direction of maximally resolved wave power at the SSE location. Values of J greater than 40 kW/m are included in the top bin as shown in the legend.

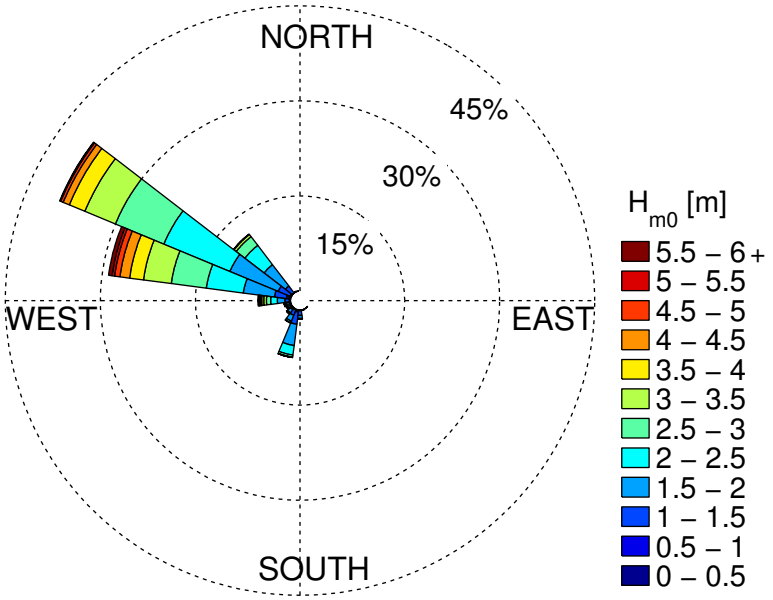

Figure 158: Annual wave rose of significant wave height and direction of maximally resolved wave power at the South location. Values of H_{m0} greater than 6 m are included in the top bin as shown in the legend.

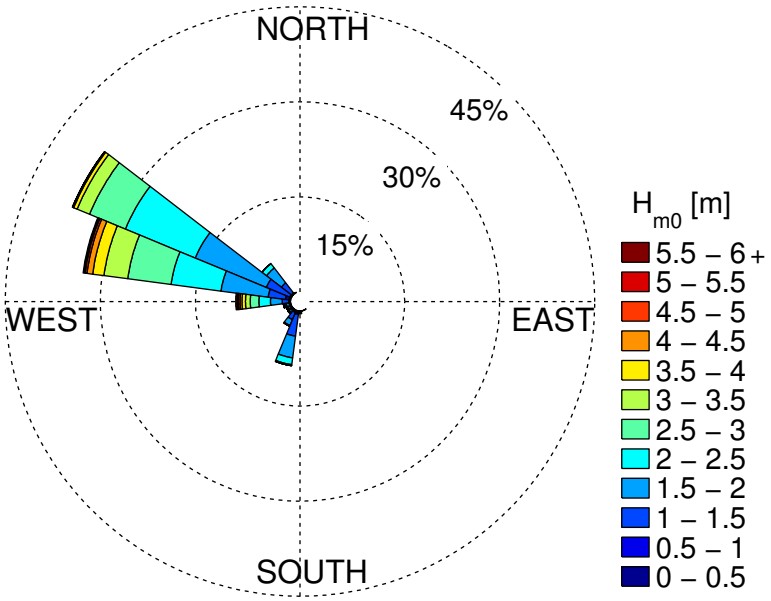

Figure 159: Annual wave rose of significant wave height and direction of maximally resolved wave power at the SSE location. Values of H_{m0} greater than 6 m are included in the top bin as shown in the legend.

G.3. Extreme Sea States

Table 39: Estimates of extreme significant wave height values using the generalized extreme value distribution (see Figure 104).

Return period [years]	Significant wave height [m]
10	8.17
25	8.90
50	9.44
100	9.98

Table 40: Estimates of extreme significant wave height values using the peak over thresholds method (see Figure 105).

Return period [years]	Significant wave height [m]
10	8.62
25	9.05
50	9.35
100	9.63

G.4. Wind Data

The wind data for this site (obtained from CFSR), is taken at 34.5 N, 121 W located approximately 30 km west of the site (Figure 89), which is the nearest data point to the site. The average monthly values, along with the 5^{th} and 95^{th} percentiles, of wind are shown in Figure 160. The values are also tabulated in Table 41. The annual and seasonal wind roses are shown in Figure 161.

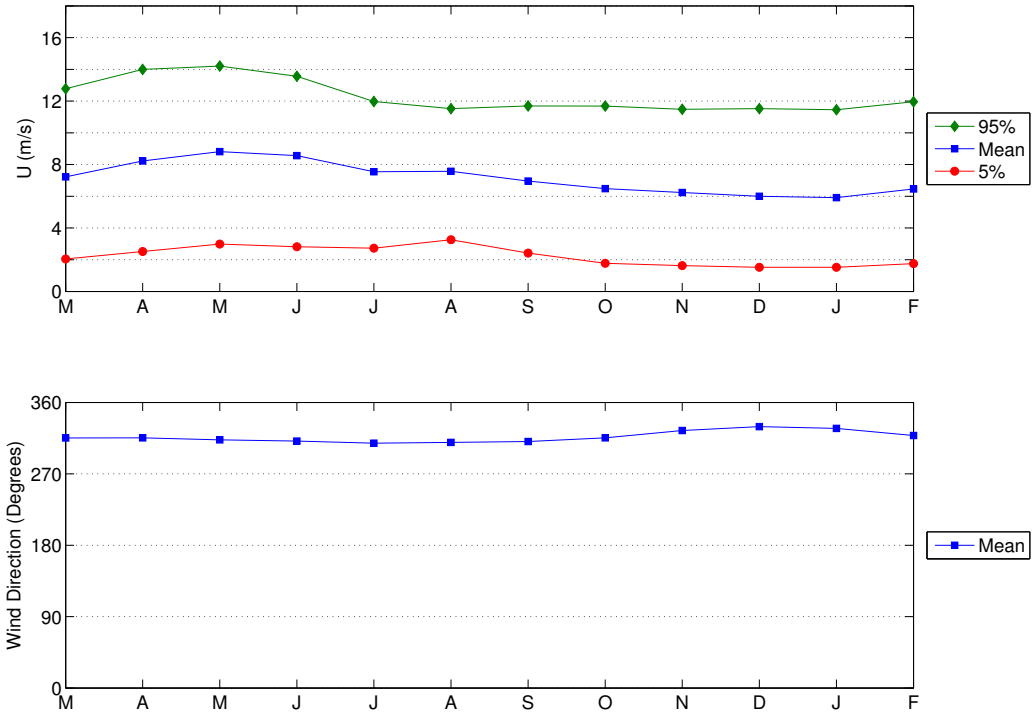

Figure 160: Monthly wind velocity and direction obtained from CSFR data during the period 1/1/1979 to 12/31/2014 at 34.5 N, 121 W, located approximately 30 km west of the test site.

(a)

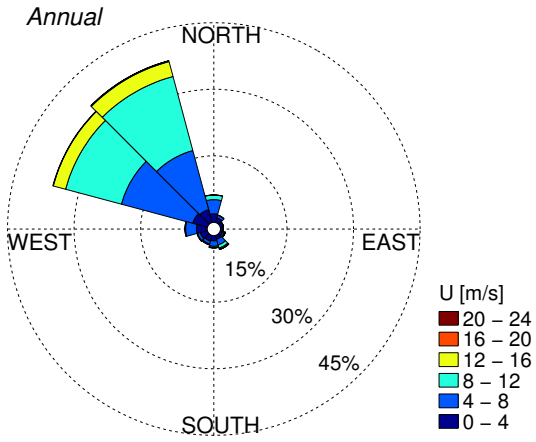

(b)

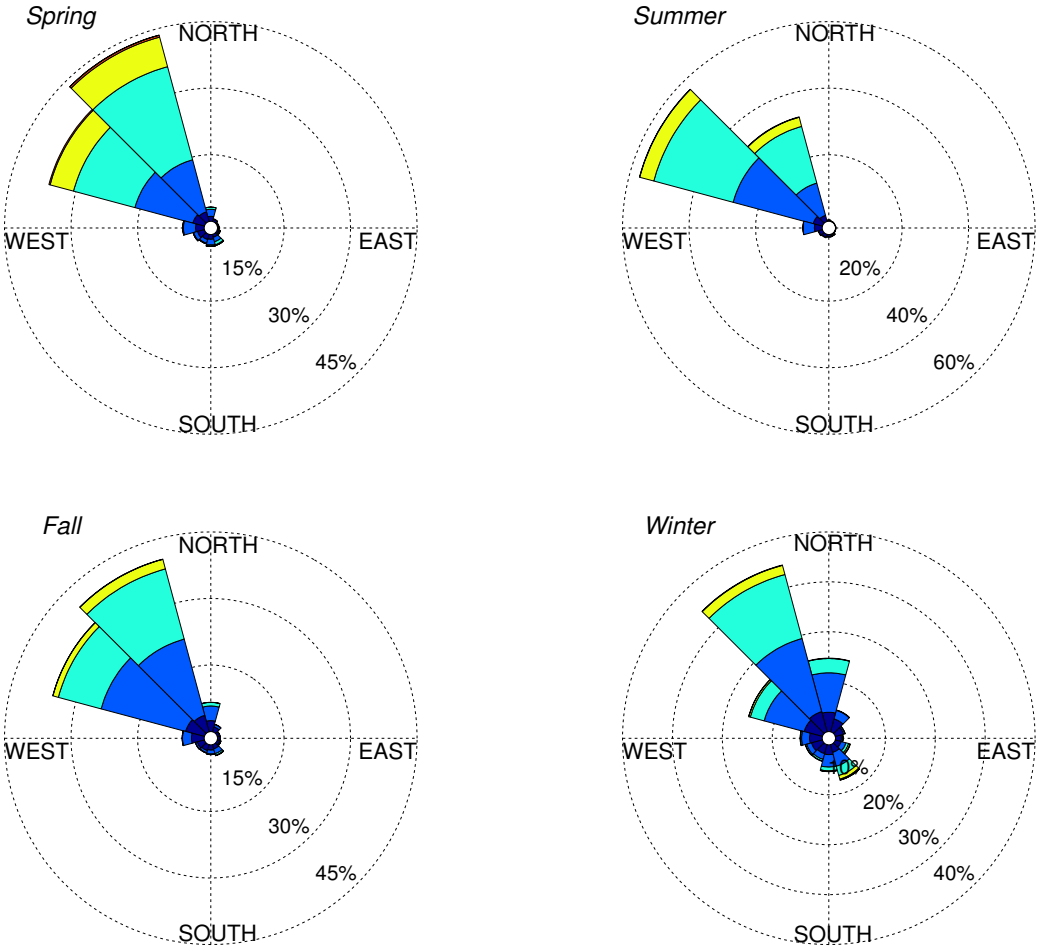

Figure 161: (a)Annual and (b) seasonal wind roses of velocity and direction obtained from CSFR data during the period 1/1/1979 to 12/31/14. Data taken at 34.5 N, 121 W, located approximately 30 km west of the test site.

Table 41: Monthly wind velocity and direction obtained from CSFR data during the period 1/1/1979 to 12/31/2014 at 34.5 N, 121 W, located approximately 30 km west of the Vandenberg AFB site.

	$U[m/s]$			$Direction[^\circ]$
	5%	**Mean**	**95%**	**Mean**
March	2.05	7.2	12.8	315
April	2.51	8.2	14.0	315
May	2.99	8.8	14.2	313
June	2.82	8.6	13.6	311
July	2.73	7.5	12.0	309
August	3.26	7.6	11.5	310
September	2.42	7.0	11.7	311
October	1.77	6.5	11.7	315
November	1.63	6.2	11.5	325
December	1.52	6.0	11.5	330
January	1.52	5.9	11.5	327
February	1.76	6.5	12.0	318

G.5. Ocean Surface Current Data

The surface current data (obtained from OSCAR), is located at 34.5 N, 121.5 W, the closest data point. The average monthly values, along with the 5^{th} and 95^{th} percentiles, of current are shown in Figure 162. These data points are listed in Table 42. The annual and seasonal current roses are shown in Figure 163.

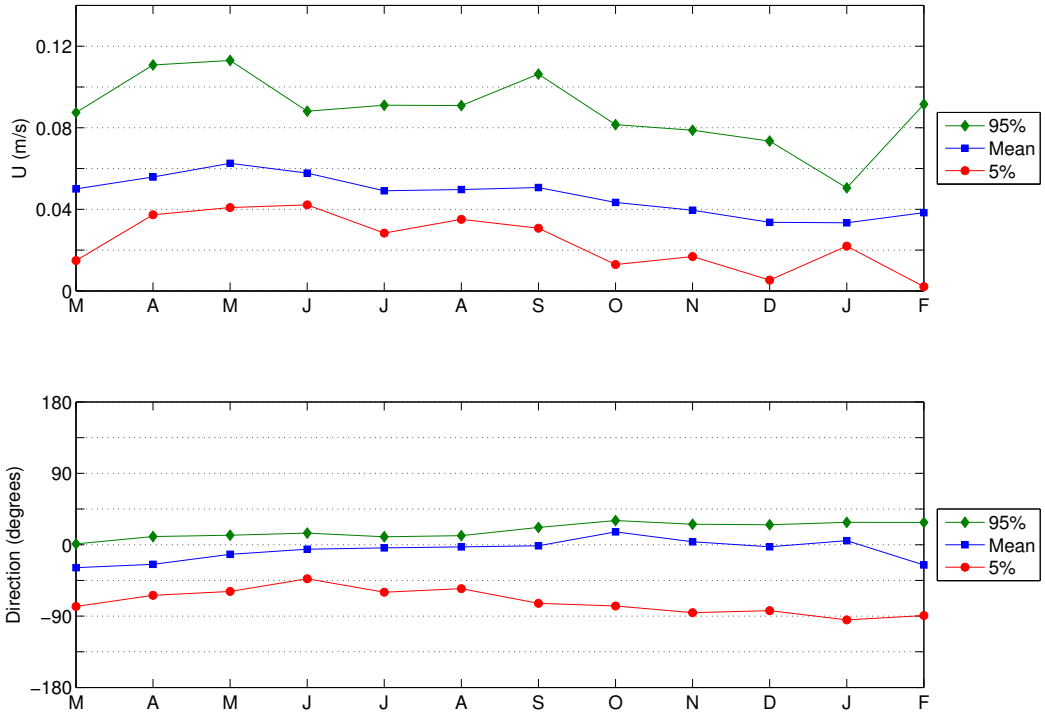

Figure 162: Monthly current velocity and direction obtained from CSFR data during the period 1/1/1993 to 12/31/2014 at 34.5 N, 121.5 W.

(a)

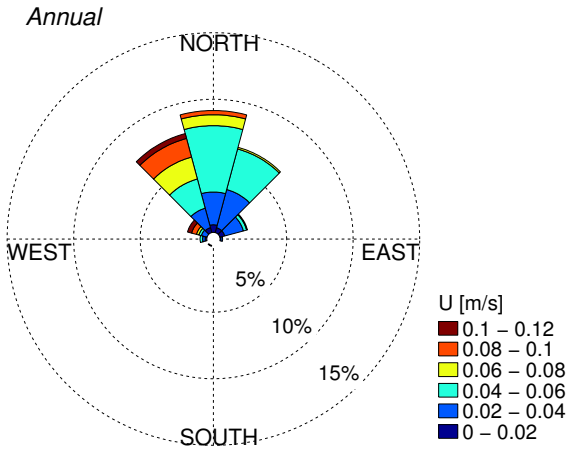

(b)

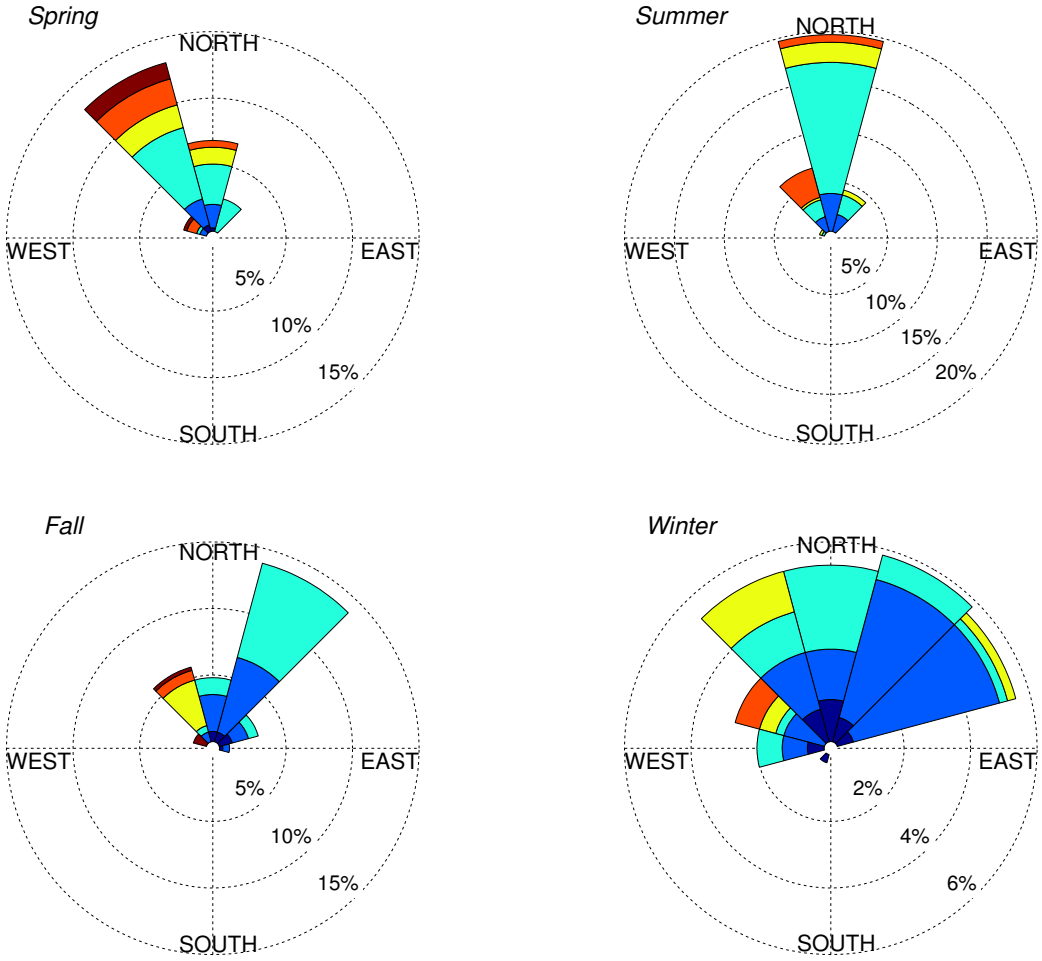

Figure 163: (a)Annual and (b) seasonal current roses of velocity and direction obtained from CSFR data during the period 1/1/1993 to 12/31/14. Data taken at 34.5 N, 121.5 W.

Table 42: Monthly surface current velocity and direction obtained from OSCAR data during the period 1/1/1993 to 12/31/2014 at 34.5 N, 121.5 W, located approximately 75 km from the site.

	$U[m/s]$			$Direction[^\circ]$		
	5%	**Mean**	**95%**	**5%**	**Mean**	**95%**
March	0.015	0.050	0.087	-78	-29	1
April	0.037	0.056	0.111	-64	-25	10
May	0.041	0.063	0.113	-59	-12	12
June	0.042	0.058	0.088	-43	-6	15
July	0.028	0.049	0.091	-60	-4	10
August	0.035	0.050	0.091	-55	-3	11
September	0.031	0.051	0.106	-74	-1	22
October	0.013	0.043	0.082	-77	16	30
November	0.017	0.040	0.079	-86	4	26
December	0.005	0.034	0.073	-83	-3	25
January	0.022	0.033	0.051	-95	5	28
February	0.002	0.038	0.092	-89	-26	28

Appendix H: HUMBOLDT BAY, CALIFORNIA: POTENTIAL WEC TEST SITE

H.1. IEC TS Parameter Values

Table 43: The average, 5^{th} and 95^{th} percentiles of the six parameters at Humboldt (see Figure 112).

	$J[kW/m]$			$H_{m0}[m]$			$T_e[s]$		
	5%	**Mean**	**95%**	**5%**	**Mean**	**95%**	**5%**	**Mean**	**95%**
March	8.3	44.5	113.0	1.34	2.60	4.16	7.66	10.07	12.91
April	5.6	27.7	72.4	1.16	2.16	3.48	6.81	9.21	11.61
May	2.9	14.9	40.4	0.89	1.74	2.84	6.18	7.81	10.21
June	2.6	12.7	32.6	0.81	1.70	2.77	5.89	7.35	9.19
July	2.3	10.7	24.7	0.79	1.64	2.54	5.66	6.95	8.36
August	2.3	10.1	24.6	0.80	1.57	2.46	5.72	7.03	8.83
September	2.9	14.0	34.9	0.83	1.71	2.67	6.32	7.95	10.19
October	5.2	30.3	89.6	1.10	2.20	3.79	6.81	9.28	11.95
November	5.9	47.9	125.2	1.11	2.61	4.37	7.96	10.28	13.41
December	10.1	66.8	181.2	1.39	3.02	5.13	8.47	11.00	14.03
January	8.3	58.0	148.9	1.31	2.82	4.67	8.33	10.99	13.87
February	10.4	50.1	134.9	1.43	2.66	4.45	8.15	10.93	13.63

	ϵ_0			$\theta_j[^\circ]$			d_θ		
	5%	**Mean**	**95%**	**5%**	**Mean**	**95%**	**5%**	**Mean**	**95%**
March	0.24	0.31	0.41	267.5	289.8	307.5	0.88	0.93	0.97
April	0.26	0.32	0.42	270.0	293.4	312.5	0.88	0.93	0.96
May	0.26	0.35	0.47	265.0	293.9	317.5	0.85	0.91	0.95
June	0.27	0.35	0.48	270.0	298.5	317.5	0.84	0.91	0.95
July	0.27	0.35	0.48	272.5	303.2	317.5	0.87	0.92	0.95
August	0.27	0.35	0.47	282.5	303.9	317.5	0.85	0.91	0.95
September	0.26	0.34	0.46	277.5	302.4	317.5	0.88	0.93	0.95
October	0.24	0.31	0.42	272.5	297.0	317.5	0.88	0.93	0.96
November	0.23	0.29	0.40	270.0	291.5	307.5	0.87	0.93	0.97
December	0.22	0.29	0.39	265.0	287.6	307.5	0.87	0.93	0.97
January	0.22	0.30	0.41	260.6	285.7	305.0	0.87	0.94	0.97
February	0.22	0.30	0.40	265.0	286.9	305.0	0.87	0.93	0.97

H.2. Wave Roses

The annual wave rose of omnidirectional wave power, J, and direction of maximum directionally resolved wave power, θ_j, is shown in Figure 164, and essentially mirrors that for significant wave height, H_{m0}, and θ_j shown in Figure 165.

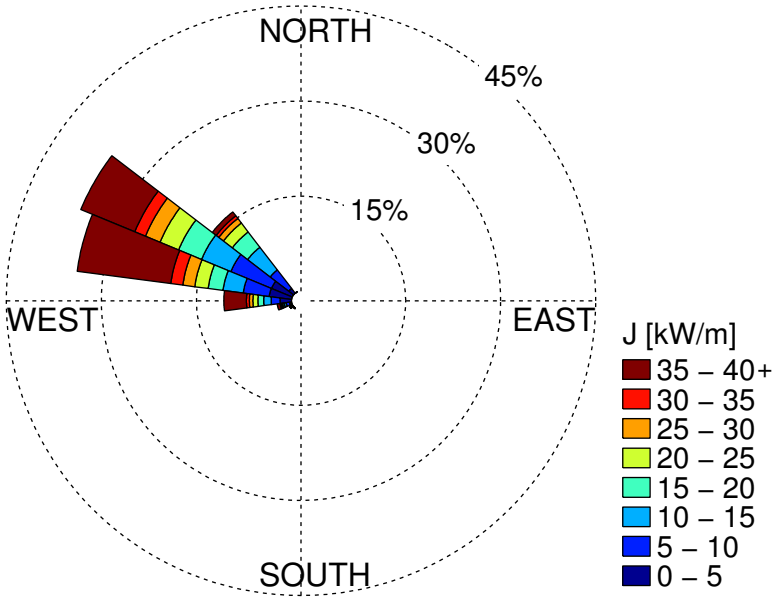

Figure 164: Annual wave rose of omnidirectional wave power and direction of maximum directionally resolved wave power. Values of J greater than 40 kW/m are included in the top bin as shown in the legend.

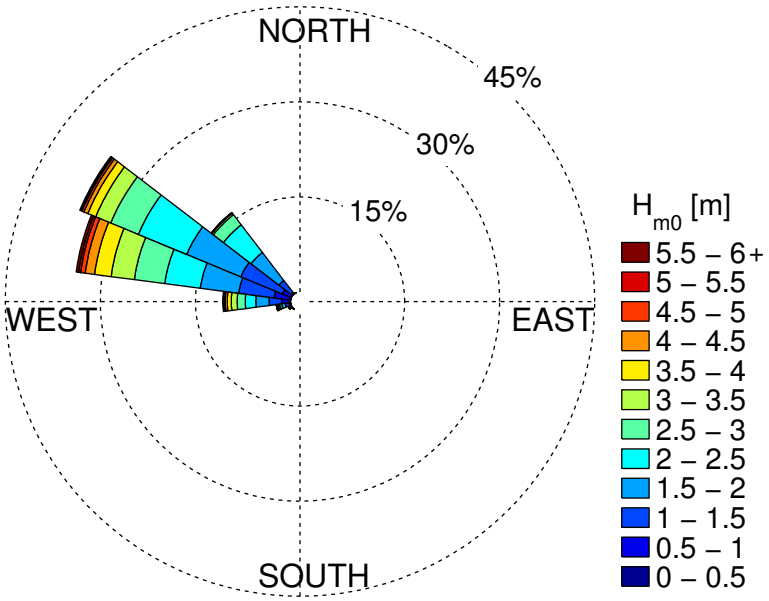

Figure 165: Annual wave rose of significant wave height and direction of maximum directionally resolved wave power. Values of H_{m0} greater than 6 m are included in the top bin as shown in the legend.

H.3. Extreme Sea States

Table 44: Selected values along the 100-year contour for CDIP128 (NDBC 46212) (see Figure 118).

Significant wave height [m]	Energy period [s]
1	3.66
2	4.43
3	5.46
4	6.56
5	7.69
6	8.84
7	10.04
8	11.31
9	12.71
10	14.43
10.91	17.78
10	20.63
9	21.70
8	22.39
7	22.87
6	23.19
5	23.38
4	23.44
3	23.35
2	23.09
1	22.60

H.4. Wind Data

The wind data for this site (obtained from CFSR), is the mean of magnitude and direction taken at 40.5 N, 124.5 W and 41 N, 124.5 W. Note that the central location between these two points is approximately 25 km southwest of the test site (Figure 110). The average monthly values, along with the 5^{th} and 95^{th} percentiles, of wind are shown in Figure 166. The values are also tabulated in Table 45. The annual and seasonal wind roses are shown in Figure 167. In the summer, the predominant direction of winds and waves correlate well. In the winter, the waves are dominated by distant swells, and the local winds have little effect.

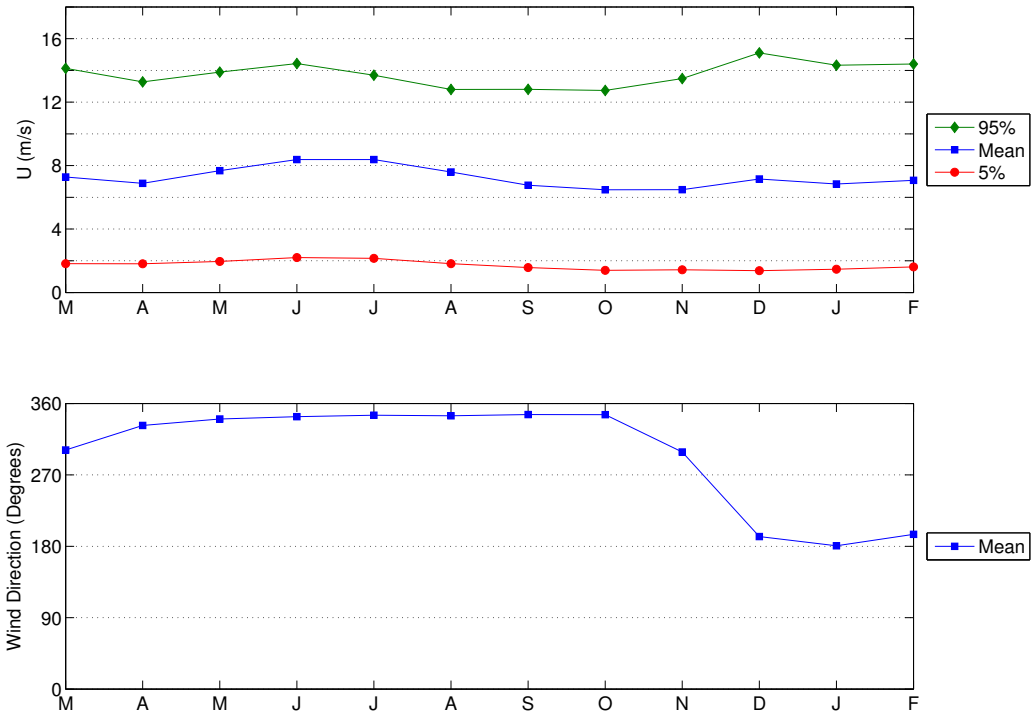

Figure 166: Monthly wind velocity and direction obtained from CSFR data during the period 1/1/1979 to 12/31/2014 at 40.75 N, 124.5 W, located approximately 25 km southwest of the test site (Figure 110).

(a)

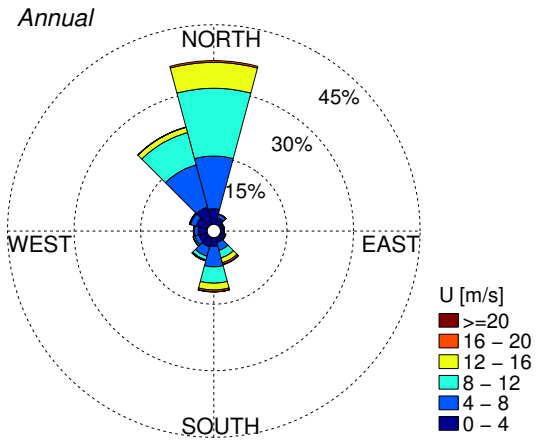

(b)

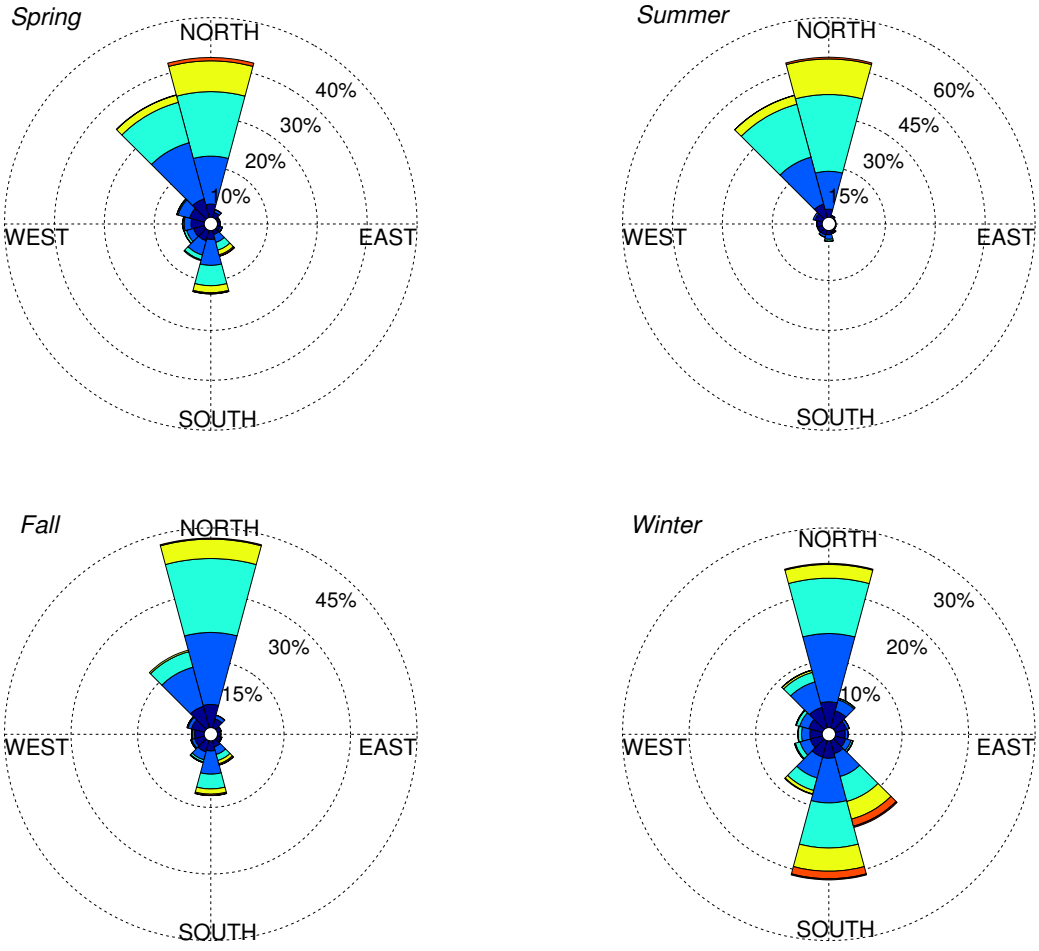

Figure 167: (a)Annual and (b) seasonal wind roses of velocity and direction obtained from CSFR data during the period 1/1/1979 to 12/31/14. Data taken at 40.75 N, 124.5 W, located approximately 25 km southwest of the test site.

Table 45: Monthly wind velocity and direction obtained from CSFR data during the period 1/1/1979 to 12/31/2014 at 40.75 N, 124.5 W, located approximately 25 km southwest of the Humboldt site.

	$U[m/s]$			$Direction[^\circ]$
	5%	**Mean**	**95%**	**Mean**
March	1.8	7.3	14.1	301
April	1.8	6.9	13.3	332
May	2.0	7.7	13.9	340
June	2.2	8.4	14.4	343
July	2.2	8.4	13.7	345
August	1.8	7.6	12.8	345
September	1.6	6.8	12.8	346
October	1.4	6.5	12.7	346
November	1.4	6.5	13.5	299
December	1.4	7.2	15.1	192
January	1.5	6.8	14.3	181
February	1.6	7.1	14.4	195

H.5. Ocean Surface Current Data

The current data (obtained from OSCAR), is located at 40.5 N, 125.5 W, the closest data point. The average monthly values, along with the 5^{th} and 95^{th} percentiles, of current are shown in Figure 168. These data points are listed in Table 46. The annual and seasonal current roses are shown in Figure 169.

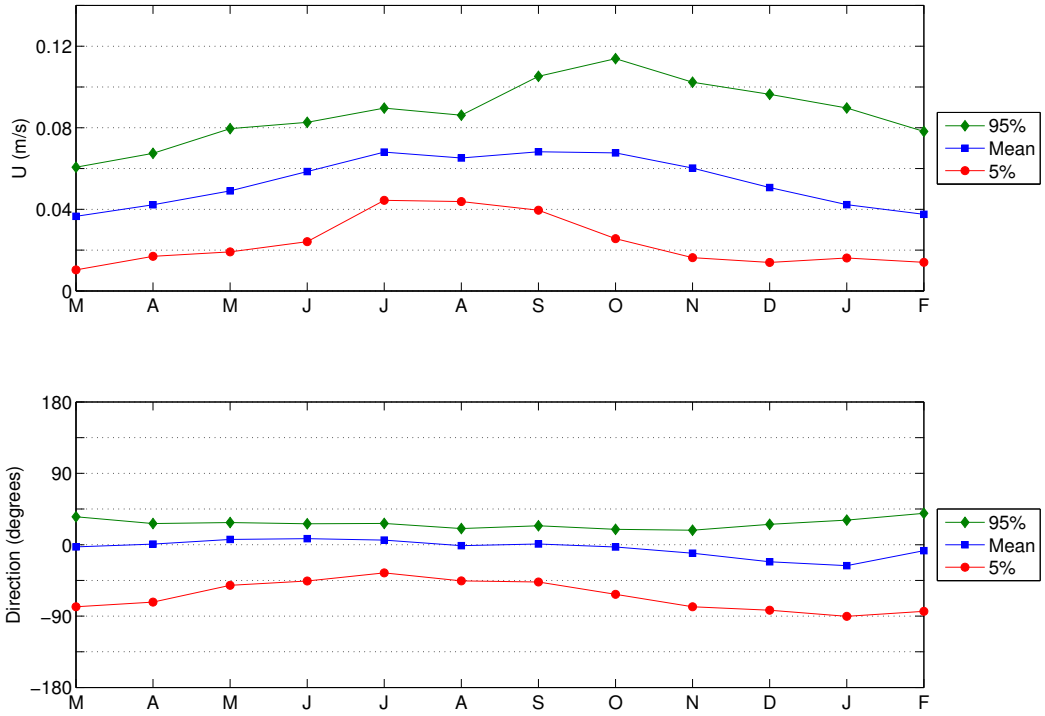

Figure 168: Monthly ocean surface current velocity and direction obtained from OSCAR at 40.5 N, 125.5 W, located approximately 110 km southwest of the Humboldt Site. Data period 1/1/1993 to 12/30/2014.

(a)

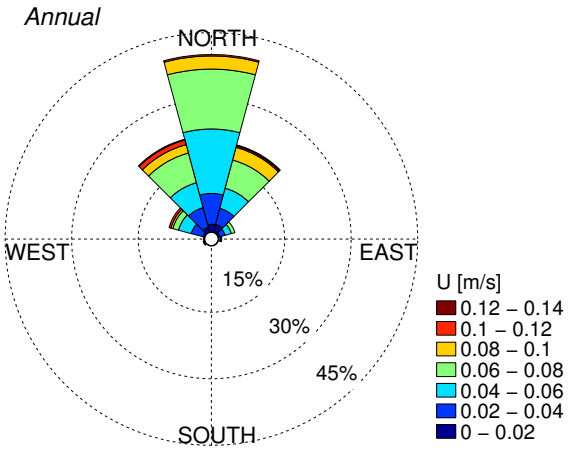

(b)

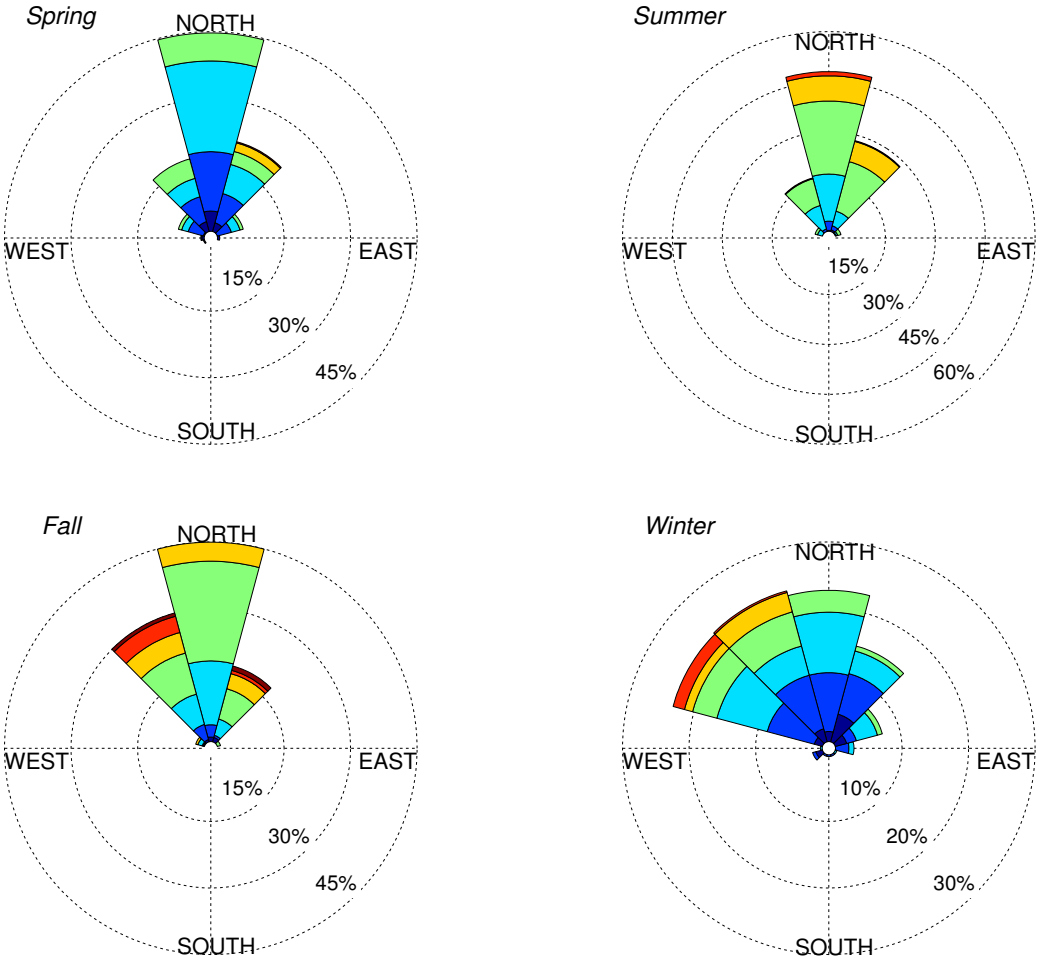

Figure 169: (a)Annual and (b) seasonal current roses of ocean surface current velocity and direction obtained from OSCAR at 40.5 N, 125.5 W, located approximately 110 km southwest of the Humboldt Site. Data period 1/1/1993 to 12/30/2014.

Table 46: Monthly surface current velocity and direction obtained from OSCAR data during the period 1/1/1993 to 12/30/2014 at 40.5 N, 125.5 W, located approximately 110 km from Humboldt test site.

	$U[m/s]$			$Direction[^\circ]$		
	5%	**Mean**	**95%**	**5%**	**Mean**	**95%**
March	0.010	0.037	0.061	-78	-3	35
April	0.017	0.042	0.067	-72	1	27
May	0.019	0.049	0.080	-51	7	28
June	0.024	0.059	0.083	-46	8	26
July	0.044	0.068	0.090	-36	6	27
August	0.044	0.065	0.086	-46	-1	20
September	0.040	0.068	0.105	-47	1	24
October	0.026	0.068	0.114	-62	-3	19
November	0.017	0.061	0.101	-78	-11	18
December	0.014	0.051	0.093	-82	-20	25
January	0.016	0.042	0.090	-90	-26	31
February	0.014	0.038	0.078	-84	-7	40


Sandia National Laboratories